Role of DDK kinase in DNA double-strand break repair and insights into the DDK-Cdc5/PLK1 kinase complex

Dissertation der Fakultät für Biologie
der Ludwig-Maximilians-Universität München

Vorgelegt von

Lorenzo Galanti

aus Asolo, Italien

September 2021

Eidesstattliche Erklärung

Hiermit erkläre ich an Eides statt, dass ich die vorliegende Dissertation selbstständig und ohne unerlaubte Hilfe angefertigt habe. Ich habe weder anderweitig versucht, eine Dissertation einzureichen oder eine Doktorprüfung durchzuführen, noch habe ich diese Dissertation oder Teile derselben einer anderen Prüfungskommision vorgelegt.

……..

Lorenzo Galanti
München, den 27/09/2021

Tag der Einreichung: 27/09/2021

Tag der mündlichen Prüfung: 11/01/2022

Erstgutachter: Prof. Dr. Peter Becker

Zweitgutachter: Prof. Dr. Heinrich Leonhardt

The data presented in this doctoral thesis were acquired from September 2015 until July 2021 in the laboratory of Dr. Boris Pfander (Max Planck Institute of Biochemistry, Martinsried, Munich). Data obtained in collaboration are listed in the "Results obtained in collaboration" section at page 75.

Table of Contents

Summary

The eukaryotic cell cycle consists of an ordered sequence of tightly regulated events to restrict specific activities within specific cycle phases. Key regulators are cell cycle kinases. Budding yeast harbor three essential cell cycle kinases conserved in humans: Dbf4-dependent kinase Cdc7 (DDK), Cyclin-dependent kinase (CDK) and the single yeast Polo-like kinase, Cdc5 (PLK1 in human).

DNA double-strand breaks (DSBs) are a severe form of DNA damage. Two main pathways evolved for the repair of such toxic lesions are homologous recombination (HR) and non-homologous end joining (NHEJ). HR often uses the homologous sequence of the sister chromatid as template for error-free DSB repair. Therefore, HR is upregulated in S, G2 and M phase when a sister chromatid is present, while NHEJ is the preferred repair pathway in G1. The crucial switch from repair via NHEJ to HR is considered to be the processing of the broken ends during DNA end resection, which primes for repair by HR and inhibits repair by NHEJ. Part of this regulation comes from CDK phosphorylation of Sae2-MRX (CtIP-MRN in human), which initiates DNA end resection. However, it is increasingly clear that additional cell cycle regulated mechanism might be involved in the regulation of DNA end resection initiation.

To identify novel functions of DDK, we performed phosphoproteomic experiments and discovered that DDK phosphorylates several proteins involved in DSB repair via HR, among which also factors involved in DNA end resection. We therefore followed a first line of research focused on the possible role of DDK in regulating DNA end resection. We showed that DDK is required for resection and HR, unveiling a previously unknown role of DDK in the cell cycle regulation of DSB repair. Mechanistically, we focused on phosphorylation of Sae2. We showed DDK-dependent phosphorylation of Sae2 *in vivo* and *in vitro,* and found that via phosphorylation of Sae2, DDK can stimulate the nucleolytic activity of the Sae2-MRX complex. Given the importance of DDK as regulator of resection, we tested if we could bypass the cell cycle regulation of DNA end resection and HR by forcing DDK expression in G1 cells. We observed that DDK expression in G1 cells lead to premature phosphorylation of Sae2, and by performing DNA end resection and HR assays we observed that synthetic activation of DDK in G1 leads to a moderate activation of HR, highlighting the central role of DDK in DSB repair pathway choice.

Cell cycle kinases also regulate the resolution of recombination structures by the Mus81-Mms4 nuclease during late steps of HR. DDK and Cdc5 can physically interact with each other and it was previously shown that this two-kinase complex is required for phosphorylation and activation of Mus81-Mms4. In a second project we therefore focused on the DDK-Cdc5 kinase complex and how it works as two-kinase complex to phosphorylate Mus81-Mms4 and other proteins. In a candidate approach, we identified a novel phosphorylation substrate of the kinase complex, the DNA replication factor Sld2, suggesting the DDK-Cdc5 complex might be a more general regulator of M phase. We developed protocols to purify to homogeneity from yeast cells the DDK-Cdc5 complex and the single kinases. Through a series of *in vitro* experiments, we showed that the DDK-Cdc5 complex was overall active as well as the single kinases. Different phosphorylation substrates were specifically phosphorylated by either one of the two kinases, either when on their own or as part of the complex, suggesting that within the complex each of the kinases could act as scaffold or adaptor for substrates. Lastly, we showed that also the human proteins DDK and PLK1 (human ortholog of Cdc5) physically interact, indicating that the DDK-Cdc5/DDK-PLK1 complex is an evolutionary conserved composite cell cycle regulator.

Taken together, the work presented in this thesis uncover a novel role of DDK in regulating DSB repair and offer insights into the evolutionary conserved DDK-Cdc5 kinase complex.

Introduction

Several pathways need to be strictly coordinated with the cell cycle equipping cells at each cell cycle phase with their specific needs. A key modulation is achieved via phosphorylation through a series of specific cell cycle kinases. The Dbf4-dependent kinase Cdc7 (DDK), subject of this PhD thesis, is a fundamental cell cycle kinase conserved across eukaryotes.

1. Cell cycle kinases

Every cell cycle is subdivided in different phases, each with its specific requirements and pathways, that need to be activated or inactivated precisely ensuring cell viability. Among others, one frequent system that cells use to regulate specific substrates is via post translational modifications (PTMs), which allow to quickly modify a given substrate to modulate its activity, localization or stability, to transmit signals or several other aspects. Phosphorylation, the addition of a phosphate group to a serine, threonine or tyrosine, is one of the most common PTMs used for regulation of cellular processes and is accomplished by a specific set of proteins known as kinases [1]. Specifically, several cell cycle regulated processes are under control of specific phosphorylation events, which allow to activate/inactivate them within specific phases. Three essential cell cycle kinases in budding yeast, conserved also in higher eukaryotes, are the Cyclin-dependent kinase (CDK), the Dbf4-dependent kinase Cdc7 (DDK) and the Polo-like kinase (Cdc5)

1.1 Cyclin-dependent kinase (CDK)

Cyclin-dependent kinase (CDK) is a well-studied master regulator of the cell cycle. Budding yeast cells have a single CDK gene, *CDC28,* while in higher eukaryotes multiple CDKs are present [2]. A key feature of CDK is that it acquires substrate specificity and activation via its binding to different cyclins throughout the cell cycle [3]. Different sets of cyclins are therefore involved in engaging with CDK in different phases of the cell cycle to target its activity to specific substrates of interest. Budding yeast carry three groups of cyclins, regulating G1, S and mitotic processes. Cyclins are on their own cell cycle regulated via transcription, degradation, localization, or inhibition ensuring specificity of CDK-mediated phosphorylation for the regulation of several pathways [3]. DNA replication

initiation requires CDK to activate the replicative helicase via recruitment of essential subunits of the replicative helicase [4-6]. CDK is also important to avoid more than one per cycle round of replication as it is not only required to initiate DNA replication but also to inhibit additional initiation events once DNA replication is started [6,7]. Moreover, CDK regulates DNA replication, being involved in the degradation of the replication factor Sld2 in mitosis [8]. CDK was also shown to be important to regulate repair of DSBs via homologous recombination (HR) at different steps, from the beginning to the end of the repair process [9-13]. Additional CDK related functions list spindle pole body duplication, mitotic spindle assembly and mitosis exit via a feedback loop leading to activation and accumulation of the phosphatase Cdc14 [3]. CDK is also important during meiosis as it is required to initiate meiotic recombination and to regulate chromosome segregation [14].

1.2 Dbf4-dependent kinase Cdc7 (DDK)

Dbf4-dependent kinase Cdc7 (DDK) is a two-subunit complex, consisting of the regulatory subunit Dbf4 and the kinase Cdc7 [15]. The levels of Cdc7 are constant throughout the cell cycle, but Dbf4 is downregulated via degradation during late M and G1 phases [16-18]. Since Cdc7 requires Dbf4 for its functionality, DDK is active during the S, G2 and M phases. The essential function of DDK is the activation of the replicative helicase for the initiation of DNA replication in S phase [19,20]. In particular, DDK phosphorylation of the Mcm2-7 replicative helicase is required to remove an autoinhibitory mechanism within the Mcm4 subunit of the inactive replicative helicase [21]. DDK's essential function is during the initiation of DNA replication, but other important functions have been uncovered as well. DDK is required to downregulate the replication capacity of cells, contributing to the phospho-dependent degradation of the essential replication factor Sld2 [8], and was also suggested to regulate the Rif1-mediated replication repression via Rif1 phosphorylation [22]. Additionally, it was observed that DDK is important for the activation of the endonuclease complex Mus81-Mms4, required for resolution of recombination intermediates formed during the repair of DSBs [13]. Sister chromatid cohesion was also shown to be regulated by DDK [23]. DDK activity was not only shown to be important during mitosis, but also during meiosis. For example, it was shown that DDK is required to regulate meiotic recombination and the segregation of chromosomes [14,24-27].

1.3 Yeast Polo-like kinase (Cdc5)

The yeast Polo-like kinase (Cdc5), ortholog of the human PLK1, is another essential cell cycle kinase, conserved from yeast to human. In human additional Polo-like kinases are present, all important regulators of the cell cycle [28]. A key feature of Polo like kinases is the presence of the kinase domain within their N-terminus, and the phospho-binding module known as Polo Box Domain (PBD) towards the C-terminus [28-30]. Differently from CDK and DDK that are already active in S phase and through the G2 and M phases, Cdc5 becomes active during the S phase and stays active through G2 and M to coordinate several mitotic functions [31]. Cdc5 is important to regulate mitotic entry by promoting expression of Clb2 cyclin [32] and by acting as negative regulator of mitotic inhibitors [33]. It was also shown to be important in regulating sister chromatid segregation favouring cleavage of cohesin rings [34] and in regulating Cdc14, a phosphatase crucial to promote exit from mitosis [35]. Cdc5 is also important for cytokinesis [36] and together with CDK and DDK, for the regulation of DNA replication by means of degradation of the firing factors Sld2 [8] and regulation of DSB repair via activation of the endonuclease complex Mus81-Mms4 [12,13,37]. Cdc5 is also important to regulate chromosome segregation in meiosis [24]. A role of Cdc5 in promoting cohesin cleavege in meiosis was also suggested [38], even though another study proposed other kinases to be important for this function rather than Cdc5 [27].

1.4 Multiple kinase regulation

Phosphorylation-mediated regulation allows tight control over several pathways, with complex modification patterns that can be generated. Substrate regulation can indeed be achieved with several sites being phosphorylated by the same kinase, or with different kinases phosphorylating the same substrate. This generates a more complex multi-site/kinase regulation. Several events were discovered to be under control of double (or even triple) kinase regulation. CDK and DDK act together in the regulation of several pathways. A very well-known example is the initiation of DNA replication, where activation of the replicative helicase relies on essential phosphorylation events mediated by both CDK and DDK. CDK-phosphorylated Sld2 and Sld3 promote the recruitment of

Cdc45 and GINS, respectively, to the replicative helicase Mcm2-7, while DDK phosphorylation of the replicative helicase alleviate an autoinhibitory mechanism and promote the binding of Sld3 to Mcm2-7 [4-6,21,39]. Regulation of DNA replication or completion of homologous recombination are also regulated by both DDK and CDK [8 13] as well as initiation of meiotic recombination via phosphorylation of Mer2 [14]. In some cases, double kinase regulation via DDK and CDK is mechanistically intertwined. DDK preferentially phosphorylates serine or threonine when there is a negative charge in position +1 [40-42]. The negative charge in position +1 can either come from aspartate or glutamate, but importantly also by a phosphorylated serine or threonine. There are therefore examples where the priming phosphorylation by CDK is followed by phosphorylation of DDK using the CDK targeted serine or threonine as the negative charge in position +1 [8,14]. Multiple kinase regulation can therefore be even more intricate, with one kinase performing a priming phosphorylation event required by a second kinase.

1.5 Cell cycle kinases-the DDK-Cdc5 kinase complex

Several years ago, by performing yeast-two hybrid and copurification experiments, it was suggested that DDK (via the Dbf4 subunit) and Cdc5 can physically interact with each other [43]. More recently, a series of studies confirmed and analysed more in detail the physical interaction between DDK and Cdc5 [24,44,45]. The interaction was mapped to the N terminus of Db4, requiring a short stretch of amino acids (83-RSIEGA-88) and the Polo Box Domain (PBD) of Cdc5 [45]. DDK and Cdc5 physically interact both in mitosis and meiosis [13,24,25,44,45]. The interdependent activity of DDK and Cdc5 was shown to be important for chromosome segregation in meiosis [24] and for regulation of synaptonemal complex degradation [25], suggesting the two-kinase complex to be a requirement for phosphorylation of specific substrates in meiosis. A different working model for the two-kinase complex was however hypothesised for the mitotic M phase. It was initially proposed that the binding of Dbf4 to the PBD of Cdc5 would lead to inhibition of Cdc5, not by inhibiting its kinase activity but titrating it away from its substrates [44]. The mitotic M phase-inhibition model was recently challenged. It was discovered that the Mus81-Mms4 complex, important for DSB repair, is not only phosphorylated by both DDK and Cdc5 (and CDK), but that this phosphorylation requires the physical interaction of DDK

and Cdc5 [12,13,37]. The Mus81-Mms4 nuclease thereby represents the first example of a mitotic protein specifically targeted by the DDK-Cdc5 kinase complex, raising interesting question on the two-kinase complex. The interdependency between DDK and Cdc5 indeed suggests that the two kinases could, via some unknown mechanism, regulate each other. The two kinases could interdependently modulate their kinase activity or one kinase might be important for tethering/recruiting the other kinase to the substrate.

2. Double Strand break (DSB) repair

DNA Double Strand Breaks (DSBs) represent a highly toxic form of DNA damage [46,47]. A single DSB can potentially be lethal for a cell. In order to respond to such deleterious lesions, cells have evolved different mechanisms to repair DSBs. The two most well-known pathways for repair of a DSB are hon-homologous end joining (NHEJ) and homologous recombination (HR), but additional sub-pathways exist.

NHEJ is the direct ligation of the broken end, and as such it requires little or no processing of the broken ends [48-50]. The ligation of the broken ends via NHEJ is generally considered to be an error-prone mechanism as it can induce short insertions or deletions, if sequence has been lost from DNA ends, or even large deletions and chromosomal rearrangements if broken ends from different DSBs are ligated with each other [48]. In the initial steps of NHEJ the Yku70-Yku80 heterodimers encircle the broken ends, which are subsequently tethered by other factors [51,52]. The subsequent recruitment of the DNA ligase complex at the DSB allows then to perform the ligation of the broken ends [53]. A sub-pathway of end-joining based repair is known as microhomology-mediated end joining (MMEJ), also referred to as Alternative-end joining (Alt-EJ). Despite being an end-joining mechanisms, MMEJ does not require the canonical NHEJ factors but requires short stretches of homology (up to 20 nucleotides) between the broken strands [48,54]. Mechanistically, limited resection of the broken ends is required to expose the homology, allowing the two strands to anneal. Annealing of the micro-homologous sequences generates non-homologous flaps/tails. After flaps/tails removal, gap-filling DNA synthesis and ligation, the repair is completed [48,54,55]. Among the factors involved, Sae2/CtIP and the MRX/MRN complex have a role in the initiation of end resection [55]. Pol32 in yeast and Polθ (theta) in humans are important for the DNA synthesis step, Rad1-Rad10 (XPF-ERCC1) is required for flap removal, while the ligation step was shown to rely on DNA ligase III [55-

[60]. Interestingly, despite being an end-joining based pathway, MMEJ shares some similarities with Homology-based pathways, due to the requirement of short stretches of homology. Indeed, low amounts of DNA end resection will promote MMEJ, and the Yku complex is therefore inhibitory towards MMEJ as it is to HR [48,58,61]. The role DNA polymerase Theta in higher eukaryotes is of high interest, also considering that homology-mediated end joining pathways seem to be more frequent; the pathway is therefore also referred to as Theta-mediated end joining (TMEJ) [55,62,63].

Different from joining based pathways, HR relies on a homologous sequence, generally from the sister chromatid, to be used as a template to direct the error-free repair of DSBs and relies on DNA end resection, the nucleolytic degradation of the 5'-terminated broken strand [64-67].

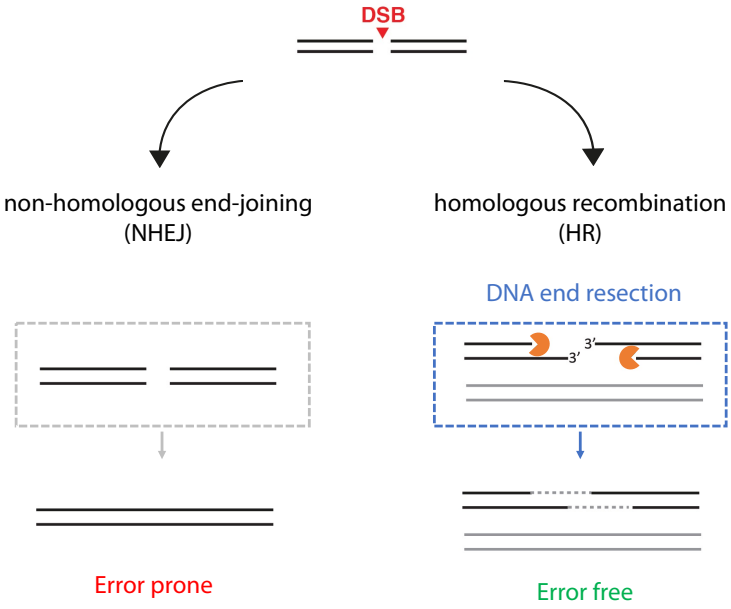

Figure 1- **Eukaryotic DSB repair pathways**

NHEJ and HR are the two main pathways for repair of DSBs. NHEJ is generally error prone, while HR is generally error free.

DNA end resection is initiated by the Mre11-Rad50-Xrs2 (MRX) complex together with Sae2 in yeast (MRE11-RAD50-NBS1 (MRN) complex together with CtIP in human) [68-71]. Mechanistically, Sae2-MRX first perform an endonucleolytic cut downstream the DSB catalyzed by Mre11, followed by resection towards the break ends using Mre11

exonucleolytic activity [71-76]. The endonucleolytic activity requires Sae2/CtIP [71,73] and the ATPase activity of Rad50/RAD50, in both yeast and humans [77]. The role of Xrs2 in yeast is not entirely clear, as it was suggested that it might be mainly important to induce nuclear localization of Mre11 rather than regulating its activity [78], while human NBS1 was shown to be critical also for regulation of the nucleolytic activity of MRE11 [79]. *In vitro* experiment however also suggested a role for yeast Xrs2 in stimulating the nucleolytic activity of the MRX complex [80]. The nucleolytic degradation of the 5'-terminated strands mediated by the Sae2-MRX/CtIP-MRN complex is particularly important for removal of blocks at broken ends such as the Yku complex or during the initiation of meiotic recombination to remove Spo11 bound to meiotic DSBs [69,72,74,80-85]. The nucleolytic degradation mediated by the Sae2-MRX complex is limited to the proximity of the DSB and is called short-range resection. Thereby, short-range resection generates the entry sites for additional nuclease, such as Exo1 or the Sgs1-Dna2 complex which can extend the length of the resected tract during what is defined as long-range resection [86]. Exo1 is a dsDNA-specific exonuclease which degrades the 5'-terminated strands within the dsDNA [87]. Dna2 is a ssDNA specific nuclease which cannot cut dsDNA and therefore relies on the contemporary melting of DNA mediated by the STR (Sgs1-Top3-Rmi1) helicase [88-92]. During this stage up to kilobases of DNA can be resected [86]. It is worth to mention that to date it is not entirely clear how much DNA needs to be resected in order to activate the subsequent steps. It was proposed that as little as 2 Kb of resected DNA could be enough to promote the downstream steps of HR [93].

The single stranded DNA (ssDNA) overhangs generated by resection are immediately coated by the ssDNA binding protein RPA, to avoid degradation of the ssDNA or formation of secondary structures [94]. The RPA coated ssDNA represents an essential platform for the subsequent recruitment of Rad51, leading to the formation of the Rad51 nucleoprotein filament, also known as the presynaptic filament. Crucial for the loading of Rad51 and for the subsequent strand invasion of the Rad51 nucleofilament are mediator proteins among which Rad52 is central to HR in yeast, and BRCA2 has a key role in human resection [95-97]. Strand invasion generates so called D-loop structures, in which the invading strand pairs with one strand of the homologous dsDNA template, displacing the other strand [98]. Once the D-loop is stabilized it can anneal to the second resected DNA, generating a double D-loop. The 3' terminated strand within the D-loop will then serve as a primer to initiate DNA synthesis [99,100]. Upon synthesis and ligation, structures known

as Double Holliday junctions (dHJs) are formed [101]. In order to complete the homology directed repair of the DSB, the dHJs needs to be removed by one of two mechanisms called dissolution or resolution. During dissolution, the Sgs1-Top3-Rmi1 (STR) complex uses the helicase activity of Sgs1 and the topoisomerase Top3 to induce migration of the two holliday junctions towards each other first, followed by cleavage of the catenated structure [102-104]. On the other hand, HJ resolution relies on the activity of Structure Selective Nucleases (SSEs). The main SSEs in yeast are the Mus81-Mms4 complex and Yen1 [105,106]. SSEs can directly cut the HJ to resolve it and are effective against a variety of branched structures [107-112]. A scheme of HR with a focus on DNA end resection is summarised in figure 2.

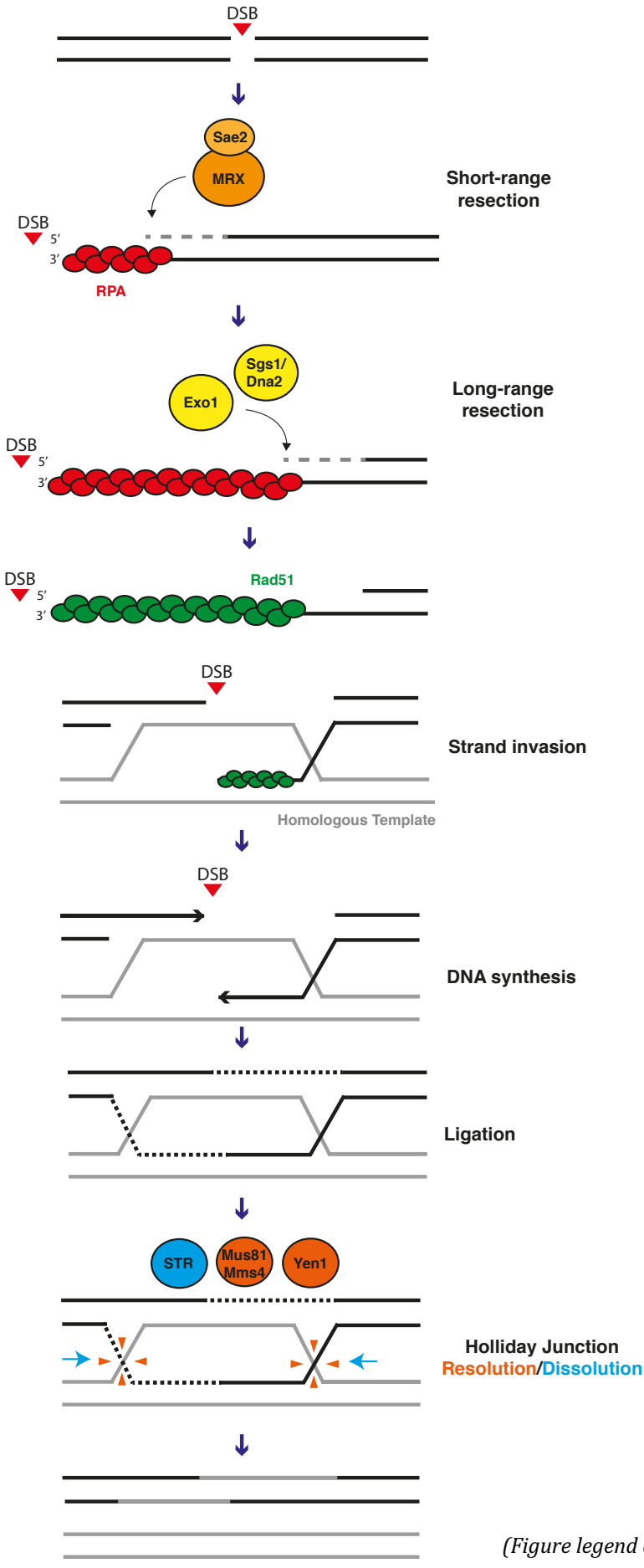

(Figure legend on the following page)

Figure 2- ***S.cerevisiae*** **DNA end resection and HR**

DNA end resection is initiated by the Sae2-MRX complex which complete the so-called short-range resection. Additional nucleases, Exo1 and/or Sgs1-Dna2, are then recruited to extend the length of the resected tract during long-range resection. RPA coated ssDNA is the platform for recruitment of Rad51, which performs the homology search and strand invasion. D-loop structures are formed. DNA synthesis and the recombination structures that are generated are resolved or dissolved to complete the homology-directed repair.

Next to canonical HR (presented here) additional sub pathways exist. As previously introduced, once a resected broken end invades the dsDNA homologous template, a joint molecule is formed and DNA synthesis initiates. During synthesis-dependent Strand Annealing (SDSA), the joint molecule is destabilized after DNA synthesis and the newly synthetized DNA strand anneals back to the other end of broken DNA [61,113]. Single Strand Annealing (SSA) requires resection to expose repetitive sequences which can then anneal with each other and lead, after removal of resulting DNA flaps, to repair by ligation [114]. Due to the loss of the DNA located between the repetitive sequences, SSA is highly mutagenic, and is effective only when the repetitive sequences are in proximity to the DSB. SSA requires resection but as it relies on annealing of repetitive sequences, does not require invasion of a homologous template [114]. Another sub-pathway is Break-induced replication (BIR). BIR is the pathway of choice for repair of single-ended DSBs that can arise during DNA replication. After invasion of the homologous template, the joint molecule is stabilized, and DNA synthesis proceeds for the whole length of the template DNA, eventually until the chromosome ends [115,116].

2.1 Cell cycle regulation of DSB repair pathway choice

Repair via HR per definition requires to have a homologous template whose sequence can be used to direct the error free repair of the DSB. The homologous template is generally provided by the sister chromatid, which is therefore available only during the S, G2 and M phases of the cycle. This imposes a rather simple, but fundamental basis for the DSB repair pathway choice as it strictly connects the pathway choice with the cell cycle phase in which cells are [117]. G1 cells will preferentially repair the DSB by using NHEJ,

while S, G2 and M cells, having the sister chromatid available will repair the DSB by using the error free HR-based repair.

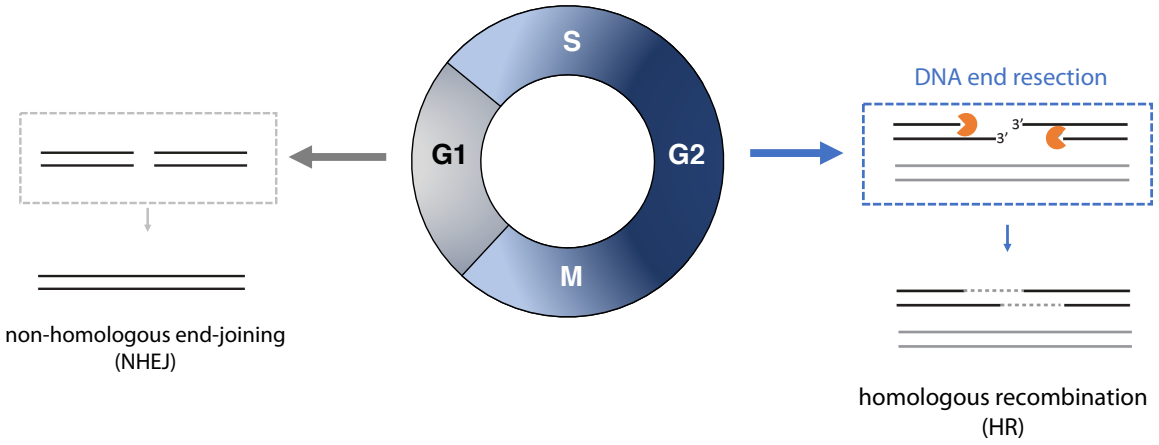

Figure 3-**Cell cycle regulation of DSB repair pathway choice**

HR and NEHJ are strictly regulated via the cell cycle. NHEJ is the preferred pathway during the G1 phase, as it relies on the direct ligation of the broken ends; HR is activated when the sister chromatid is available as repair template during the S, G2 and M phases.

Cell cycle kinases play a key role in regulating DSB repair pathway choice during the cell cycle [117]. CDK activity is low in G1 and high in the S, G2 and M phases. The spectrum of CDK activity therefore mirror those cell cycle phases that are permissive for repair of DSBs via HR. And it was indeed shown that CDK is required for HR, since CDK inhibition in G2 and M inhibits HR and DNA end resection [118,119]. To date different proteins involved in HR and DNA end resection have been discovered to be regulated via CDK phosphorylation. CDK-mediated phosphorylation of Sae2 on serine 267 is essential for activation of the Sae2-MRX complex and hence for initiation of DNA end resection [9,120]. This regulation is conserved also in humans, where CtIP (human ortholog of Sae2) is phosphorylated in a cell cycle dependent manner by CDK on threonine 847. Again, CDK-mediated phosphorylation is essential for the activation of the CtIP-MRN complex [121]. In case of long-range resection CDK phosphorylation of yeast Dna2 was shown to be important for the recruitment of Dna2 to DSBs and for extensive resection [10]. In humans, a role for CDK phosphorylation of EXO1 was also observed [122]. The chromatin remodeler

Fun30 (SMARCAD1 in human) is phosphorylated by CDK in both yeast and human with the phosphorylation being important for its recruitment to DSBs to promote long-range resection [11,123].

2.2 Cell cycle regulation of DSB repair pathway choice-focus on the phosphorylation of Sae2/CtIP

Phosphorylation of Sae2/CtIP is known to be a crucial regulatory mechanism for DNA end resection [9,71,73,120,121], and despite increasing mechanistic details have been uncovered, the picture is still quite complex. One first thing to consider, is that Sae2 is targeted by different kinases. Not only the essential cell cycle phosphorylation by CDK, but also the DNA damage checkpoint kinases Mec1/Tel1 can phosphorylate Sae2 [9,124]. There are two main aspects about the Sae2-MRX (or human CtIP-MRN or fission yeast Ctp1-MRN) that are known to be regulated by phosphorylation. One is the oligomeric state of Sae2/CtIP/Ctp1 and the other is the regulation of the interactions between the different components of the complex.

First, it was observed that Sae2 can self-interact and was suggested this could lead to multimerization of Sae2 [125]. It was later shown that phosphorylation of Sae2 can induce changes in the size distribution of Sae2 oligomers, upon induction of DNA damage [126]. More recently, a detailed mechanistic analysis of the role of phosphorylation in regulating Sae2-MRX activity discovered that Sae2 phosphorylation leads to a shift from a high order multimer to an active-phosphorylated tetramer [120]. Interestingly, the authors also observed that CDK mediated phosphorylation of Sae2 is not sufficient for full activation of the Sae2-MRX complex mediated initiation of DNA end resection, and also observed that Mec1/Tel1 mediated phosphorylation of Sae2 has a minor role in resection [120]. This was later confirmed by a genetic analysis showing that CDK and Mec1/Tel1 phosphorylation of Sae2 have different functions in resection, with the cell cycle phosphorylation being important to initiate resection and the DNA damage-induced phosphorylation being important to attenuate the checkpoint response [127]. Despite being clear that Sae2 exist in a multimeric form and that upon phosphorylation its size distribution is shifted towards the active tetrameric form, it is currently not known what is the role of specific kinases to these changes.

Second, it is not entirely clear how the different components of the MRX complex interact with Sae2. *In vivo* and *in vitro* experiments analysing the phospho-regulation of Sae2-MRX

interaction have been performed also in human (CtIP-MRN complex) or in fission yeast (Ctp1-MRN complex). To note, unless otherwise stated, phosphorylated Sae2/CtIP/Ctp1 means that it is not a kinase-specific phosphorylation. In case of budding yeast, it was shown that Sae2 can bind the full MRX complex *in vitro* independently of its phosphorylation status [71,120]. It was later shown that a C-terminal construct of Sae2 (Sae2ΔN109) could bind to Rad50 in a phosphorylation-dependent manner *in vitro* [120]. Another phosphorylation dependent binding was observed between the Forkhead-associated (FHA) domain of Xrs2 and Sae2 via pulldowns from cell extracts. In this case, the binding of Sae2 to the FHA domain of Xrs2 was lost upon treatment of extracts with λ phosphatase [128].

For the human CtIP-MRN complex it was shown that *in vitro,* CtIP (ortholog of Sae2) can bind to the NBS1 (ortholog of Xrs2) subunit in a phosphorylation-dependent manner, and the interaction was shown to be dependent on the FHA domain of NBS1 [79]. Binding of CtIP to MRE11 or RAD50 subunits was however shown to happen independently of the phosphorylation status of CtIP. The authors also observed a phosphospecific interaction of CtIP with the fully assembled MRN complex [79]. *In vivo* immunoprecipitation experiments showed that CtIP can interact with NBS1, both at the N and C terminus, suggesting that CtIP could make contacts with NBS1 (and eventually the MRN complex) via multiple surfaces. The observed binding was lost when CDK consensus sites in CtIP where mutated to non-phosphorylatable alanine, suggesting a possible phosphorylation-dependent interaction *in vivo* [129].

In *S. pombe* it was discovered a phospho-dependent binding of Ctp1 and the MRN complex. It was observed that the incorporation of Ctp1 in the MRN complex is phosphorylation-dependent and relies on the phosphorylation-dependent interaction between Ctp1 and Nbs1 [130]. Consistent with what previously described the observed interaction was shown to be important also for the stimulation of the nuclease activity of the MRN complex. It also appears that multiple surfaces might be important for the overall stimulation of the nuclease activity of the MRN complex. Indeed, it was observed that the interaction between Ctp1 and Nbs1 requires phosphorylation of the N terminus of Ctp1 and it was shown that Casein Kinase II (CKII) is responsible for this phosphorylation, which is interesting, considering that CKII is related to DDK [130]. It was also shown that a crucial function for the stimulation of the nucleolytic activity of the MRN complex resides in a 15 amino acids peptide in the C-terminus of Ctp1 [130]. It seems

that different surfaces and possible structural changes might be overall involved in the regulation of the nucleolytic activity of the MRX/MRN complex via Sae2/CtIP/Ctp1. As summarized in this section, it is clear that there are several aspects that relies on phosphorylation, but it is still not entirely clear how single kinases can regulate these different phospho-specific events. It is generally clear that at least in humans and in *S. pombe* there is a phospho-dependent interaction between NBS1/Nbs1 and CtIP/Ctp1 which involves the FHA domain of NBS1/Nbs1 [79,130]. It was also observed in *S. cerevisiae* [128], but was not further analysed in detail, as the overall role of Xrs2 in regulating the activity of the MRX complex is unclear. It was suggested that Xrs2 is only required to induce the nuclear localization of Mre11 *in vivo*, and lack of Xrs2 was shown to not have an impact on the *in vitro* nucleolytic activity of the MR complex [78]. Other experiments with a similar *in vitro* setup however observed a Xrs2-dependent stimulation of the nucleolytic activity of the MR complex [80]. Despite having information on how Sae2/CtIP/Ctp1 phosphorylation can regulate its activity and interactions, there is not yet a uniform model. Additionally, there is general lack of information on how kinase-specific events can regulate Sae2/CtIP/Ctp1.

Aim of the study

Dbf4-dependent kinase Cdc7 (DDK) is an essential cell cycle kinase conserved from yeast to humans. DDK is known to be an important regulator of the cell cycle together with other essential, evolutionary conserved kinases such as CDK and Cdc5/PLK1. DDK is well studied for its essential function in the activation of the replicative helicase during DNA replication initiation, but other functions have been discovered.

In an effort to identify novel pathways regulated by DDK we performed phosphoproteomics experiments, in which we discovered that DDK phosphorylates proteins involved in the repair of double strand breaks (DSBs) via homologous recombination (HR). Interestingly, our analysis suggests that DDK might act already in the very first steps of HR already during DNA end resection. This novel role of DDK in the regulation of HR was therefore a main topic of research: we aimed to identify which substrates might be critical for the DDK-mediated regulation of resection and by which mechanism DDK promotes resection. Additionally, we decided to investigate whether activation of DDK is sufficient for cell-cycle independent activation of DNA end resection and repair via HR.

It was discovered that in yeast DDK and Cdc5 can physically interact with each other. As part of the kinase complex with Cdc5, DDK was shown to be important in the final steps of HR during the repair of DSBs for activation of the nucleases involved in the resolution of recombination intermediates. We therefore reasoned that the DDK-Cdc5 kinase complex should be viewed as a new cell cycle regulator with its own set of substrates and functions. In this PhD project, we tested for new substrates regulated by the double kinase complex. We also aimed to get insights into the catalytic mechanism of this peculiar enzyme, which harbors two catalytic sites, as well as to obtain information on the complex structure. Lastly, another goal of this project was to investigate the conservation of the double kinase complex in higher eukaryotes.

In summary, the research presented in this PhD thesis aimed to investigate novel functions of the essential kinase DDK, a clinically relevant protein known to be overexpressed in several cancers, with a focus on its role in regulating DSB repair and its functions as part of the DDK-Cdc5 kinase complex.

Results

1. Dbf4 dependent kinase Cdc7 (DDK) targets homologous recombination proteins

1.1 Identification of DDK substrates by mass spectrometry

To identify novel potential substrates of DDK we decided to measure the phosphoproteome of Wild Type cells, and compare it to the phosphoproteome of cells lacking DDK. This approach is expected to reveal not only the identity of substrate proteins, but also of DDK-dependent phosphosites. DDK is an essential kinase so it is not possible to simply delete it. The essential function of DDK in an unperturbed cell cycle is during the initiation of DNA replication, where DDK together with CDK (a second essential cell cycle kinase) mediates activation of the replicative helicase. A point mutation in one of the subunits of the replicative helicase (Mcm5 P83L; known as *bob1-1*) allows to bypass the essential function of DDK in replication initiation [131]. It is therefore possible to delete DDK in cells harboring the *bob1-1* allele. This can be done either by deleting the regulatory subunit *DBF4* or the actual kinase *CDC7* (note that deletion of *DBF4* or *CDC7* abolishes DDK activity in the same way). We performed an experiment to measure the phosphoproteome of Wild Type, *bob1-1,* and *bob1-1dbf4Δ* cells. Cells depleted of *DBF4* or *CDC7* in the *bob1-1* background are viable, but have a proliferation defect. In order to avoid differences that could rise due to cells being in different stages of the cell cycle, we measured the phosphoproteome of cells arrested in the M-phase of the cell cycle via nocodazole. We therefore collected four replicates of M arrested cells for each strain of interest. As shown in figure 4 we can confirm that cells were arrested in M by measuring DNA content of our samples via fluorescence-activated cell sorting (FACS).

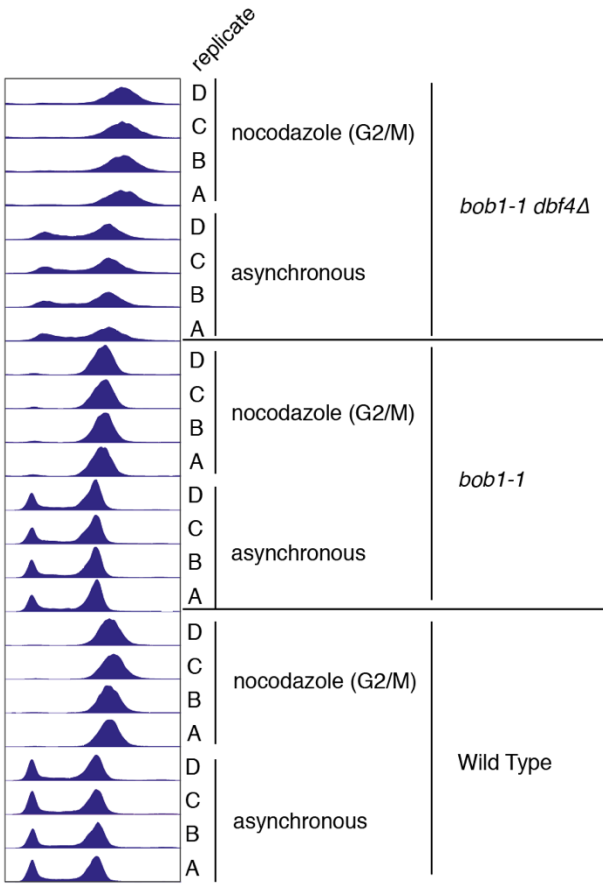

Figure 4-**DNA content measurement via FACS**

Four biological replicates (n=4) were collected for each strain to measure the phosphoproteome. FACS measurement of the DNA content revealed the proper arrest of cells in the M-phase.

1.2 Phosphoproteome data analysis

By using the system described in section 1.1, we collected four replicates for each strain, and measured the phosphoproteome of each (for a total of 12 samples). Note that as a control, also the total proteome of each sample was measured. We analyzed our data using the Perseus/MaxQuant software (version 1.6.15.0) [132]. We first removed from our datasets all the phosphorylation sites that had a localization probability lower that 0.75 and maintained only so-called class I phosphopeptides. Next, we focused on the differences between our different conditions (in order to identify sites that are lost in cells depleted of DDK). To this end we performed an ANOVA (analysis of variance) test, with a permutation-based FDR (false discovery rate) of 0.05, to identify sites that are significantly changed within the different replicates. After filtering sites that are not

changed between the different conditions, we get a list of class I peptides that significantly change between the different measurements. In order to have a closer look into how the replicates of the same background look compared to each other, and to compare to the other backgrounds, we performed hierarchical clustering (figure 5). Sites are collected in different clusters as reported. Our main interest was in Cluster 3974 (hereafter referred as DDK cluster), since it contains phosphosites that were found to be specifically downregulated in *bob1-1dbf4Δ* cells, but that were enriched in *bob1-1* and Wild Type cells.

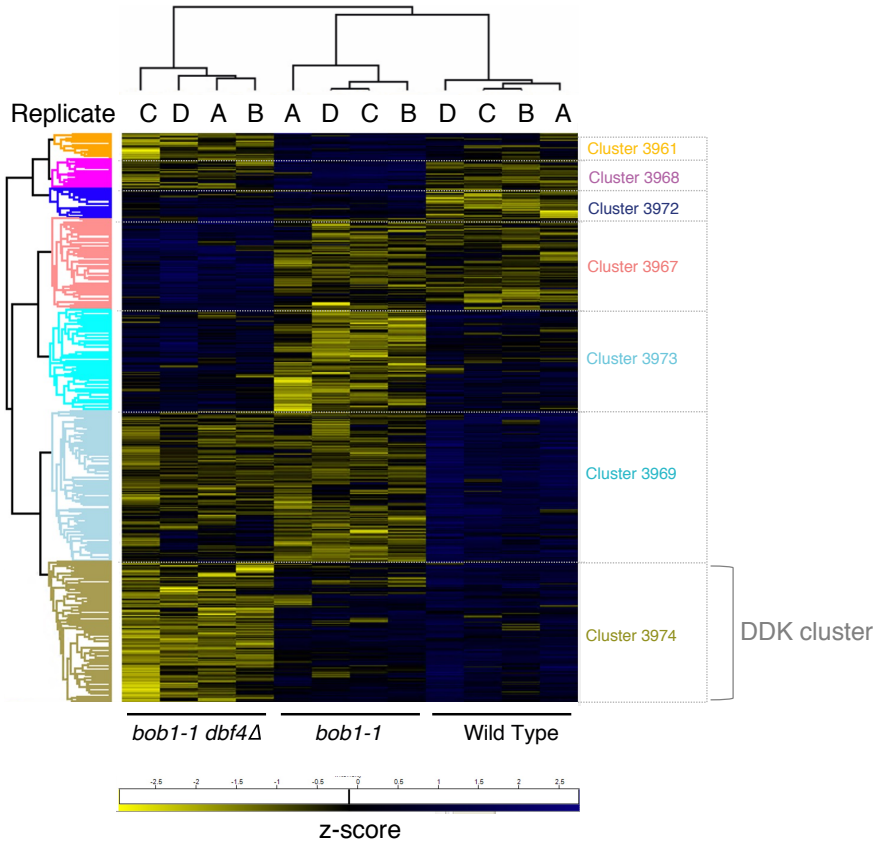

Figure 5-**Heat Map of ANOVA significant phosphopeptides**

Analysis of the phosphoproteomic experiment using Persues (version 1.6.15.0). For each strain, four biological replicates (n=4, A-D) were measured and analyzed. Class-I phosphopeptides were subjected to ANOVA (analysis of variance) test with a permutation-based FDR (false discovery rate) of 0.05. The phosphopeptides significantly changing between the different groups (strains) in at least 3 out of 4 replicates where subjected to hierarchical clustering. Phosphopetides were clustered in seven different clusters based on their changes in the different groups (strains). Heat map shows the calculated z-score. Highlighted as "DDK cluster" is the cluster containing phosphopetides that were reproducibly enriched in Wild Type and *bob1-1,* but not in *bob1-1dbf4Δ* cells.

The DDK cluster provided us with a list of phosphopeptides that were specifically lost in cells depleted of DDK and we decided to further analyze it (note that also other clusters were further analyzed as control). We decided to also apply filtering which takes into account changes in total proteome in *bob1-1dbf4Δ* cells. The rationale is that if a phosphopeptide from a protein of interest is found less, this is not due to a reduction of that protein in the total proteome itself. We therefore compared the total proteome of: I) Wild Type and *bob1-1* II) Wild Type and *bob1-1dbf4Δ* and III) *bob1-1* and *bob1-1dbf4Δ*. Proteins that were significantly different in the total proteome of any of these comparisons, were filtered out.

We also included filtering based on the DDK consensus site. DDK is a kinase that preferentially phosphorylates sites (S or T) that have a negative charge in the residue in position +1 [40-42]. This can come from an aspartate or glutamate residue, or from a phosphorylated serine or threonine. A general consensus for DDK is therefore S/T-(D/E/S/T)$_{+1}$. There are also several cases of proteins known to be primed for DDK phosphorylation by CDK-mediated phosphorylation, leading to a specific consensus of S/T-S/T$_{(+1)}$-P$_{(+2)}$ given that CDK preferentially phosphorylate S/T sites followed by a Proline. We decided to look into the DDK cluster for sites that mimic the general consensus S/T-(D/E/S/T)$_{+1}$ and found 159 sites matching the consensus (figure 6).

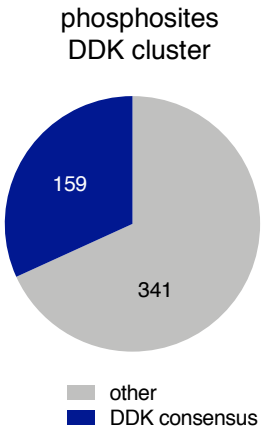

(Figure legend on the following page)

Figure 6-**DDK consensus-based filtering of phosphopeptides part of the "DDK cluster"**

Analysis of the "DDK cluster" (see figure 5) using Perseus (version 1.6.15.0). The phosphopeptides part of the "DDK-cluster" (cluster 3974) were filtered for the DDK consensus motif (S/T-(D/E/S/T)$_{+1}$) revealing that among the 500 phosphopeptides that were part of the cluster (after filtering for the total proteome), 159 were found to be phosphorylated on serines or threonines matching the DDK consensus motif (details of the analysis in the text).

1.3 DDK targets proteins involved in double-strand break repair, homologous recombination and DNA end resection

Among the 159 phosphopeptides mimicking the general DDK consensus motif, 124 were reported to be phosphorylated in a database reporting phosphoproteomics data for yeast (Superphos) developed by the Smolka lab [133]. As further positive control we identify known DDK substrates, such as for example the endonuclease complex Mus81-Mms4 or Rif1 [13,22].

For the putative DDK substrates, part of the DDK cluster, whose phosphopeptides were identified in our analysis, we performed GO analysis for biological processes to obtain insights into overall pathways possibly regulated by DDK. Interestingly, among the significantly enriched pathways we identified double strand break repair (GO:0006302), DNA repair (GO:0006281) and chromatin organization (GO:0006325). Highlighted in figure7 are the proteins of the cluster part of these GO terms.

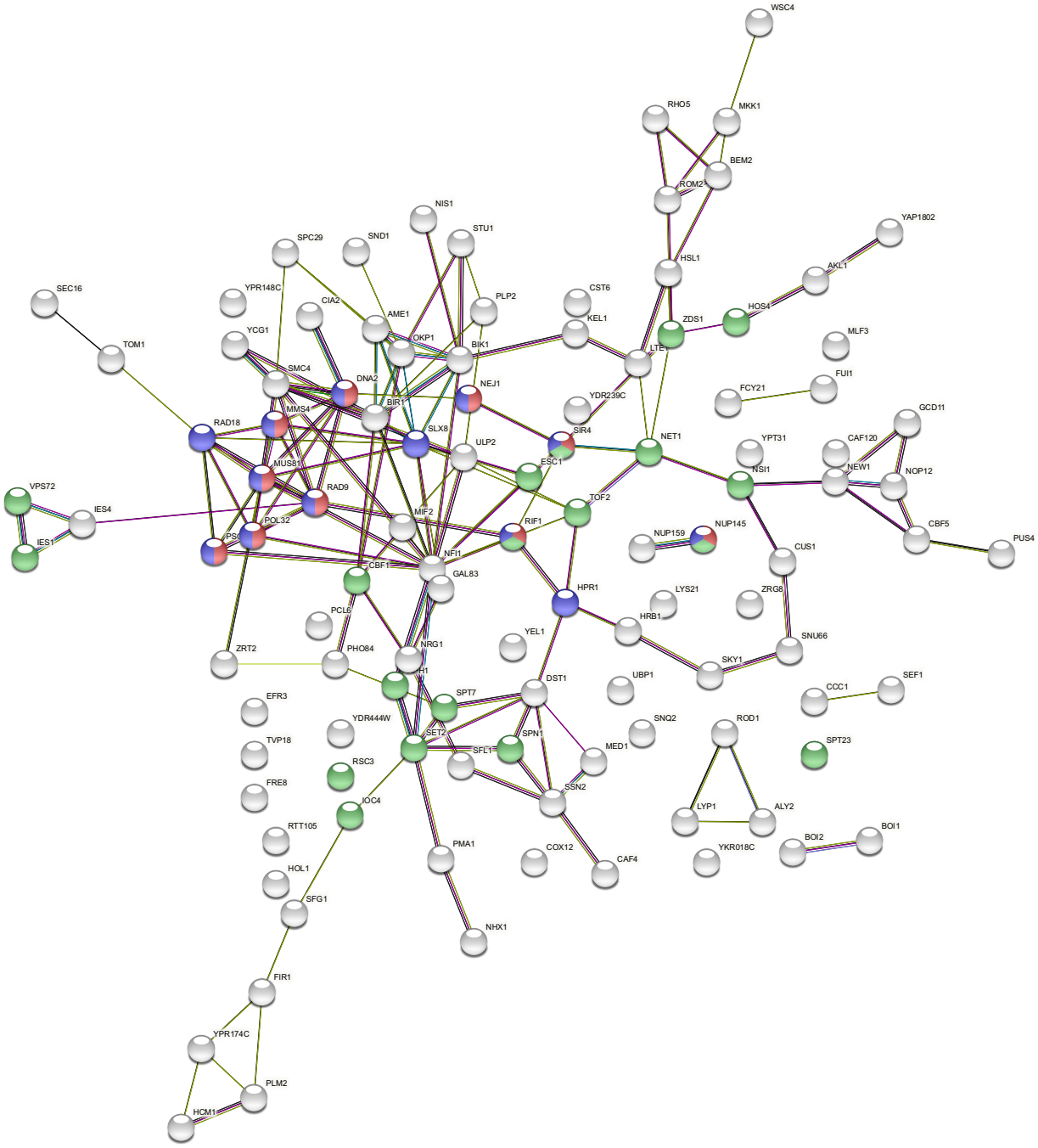

(Figure legend on the following page)

Figure 7-**Gene onthology (GO)-biological processes analysis reveals an enrichment for DSB repair related processes**

Proteins of the "DDK cluster" with enriched phosphopeptides in the presence of functional DDK (figure 5) and matching the DDK consensus motif (figure 6) were subjected to a GO-biological processes analysis using String [193]. Highlighted are proteins for the following enriched biological processes: DNA repair (GO:0006281, in blue; strength=0.42 and FDR=0.0185), double-strand break repair (GO:0006302, in red; strength=0.66 and FDR=0.0024) and chromatin organization (GO:0006325 in green; strength=0.54 and FDR=0.00013). The FDR (false discovery rate) and strength calculated by String [193] are reported. Strength (Log10(observed/expected)) is a measure describing how large is the enrichment effect for a certain GO-term. It is the ratio between the number of proteins in the submitted network annotated with a certain term, and the number of proteins that String [193] expects to be annotated with the same term in a random network of the same size.

An involvement of DDK in late steps of DSB repair via HR was previously shown, as DDK is required to activate via phosphorylation the endonuclease complex Mus81-Mms4 (which we also identified in our analysis) [13]. In addition to Mus81-Mms4 we found several putative DDK substrates involved in earlier steps of HR. In particular, the initiation of HR relies on the processing of the broken ends in a process known as DNA end resection. During resection, nucleolytic degradation of the 5' broken ends occur, leaving 3' ssDNA overhangs, immediately coated by the ssDNA binding protein RPA. Different chromatin remodelers were shown to be important for the remodeling of chromatin around the breaks, making It accessible for the nucleolytic degradation of the broken ends [66]. Different proteins identified in our analysis (and part of the enriched biological processes), are known to be important for DNA end resection. The endonuclease Dna2 [88-92], or subunits of the RSC and INO80 complex, chromatin remodelers associated to DSB repair and DNA end resection [134-138]. We can therefore conclude from our analysis, that DDK phosphorylates proteins involved in the repair of DSBs via HR, such as Mus81-Mms4, as previously shown [13], but also proteins that are important for the activation of HR via DNA end resection, therefore suggesting that DDK might have a more prominent role than previously expected in the cellular response to DSBs and possibly in the repair of DSBs via HR.

2. DDK is required for DNA end resection and homologous recombination

2.1 DDK is required for viability in the presence of DNA damage

In order to investigate if DDK is required for the cellular response to DSBs, we monitored the ability of cells depleted of *DBF4* or *CDC7* to grow in the presence of chronic exposure to DNA damage. In particular, we used camptothecin (CPT) as a source of DNA damage. CPT is a topoisomerase I inhibitor, that by inhibiting the topoisomerase I re-ligation step leads to accumulation of DSBs in cycling cells [139,140]. As shown in figure 8, *bob1-1* cells that are depleted of *DBF4* or *CDC7* are highly sensitive to CPT, providing evidence that DDK is required for the cellular response to DSBs.

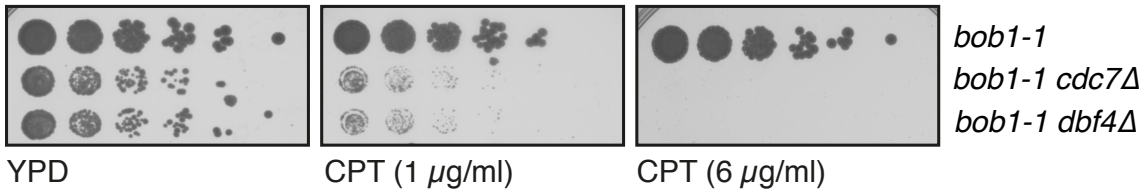

Figure 8-**DDK is essential for viability in the presence of CPT**

Serial dilutions of *bob1-1*, *bob1-1 dbf4Δ* or *bob1-1cdc7Δ* were spotted on YPD plates containing increasing concentrations of CPT (and YPD without any drug as control), showing that DDK is required for viability when cells experience CPT-induced DNA damage. The experiment was performed in two biological replicates (n=2). Representative images are shown.

2.2 DDK is required for homologous recombination

HR is upregulated during S, G2 and M phases of the cell cycle, and we therefore investigated if DDK is important for HR.

To measure HR in cells we used a gene conversion assay [137]. Briefly, a single HO endonuclease cut site is inserted withing a GFP reading frame and integrated in the genome in a certain position (chromosome IV, 491 kb). A homologous sequence harboring a second, mutated, HO cut site as well as a unique sequence, is integrated in another position in the genome (chromosome IV, 795 kb). In a background with the HO

endonuclease under control of the GAL promoter, it is then possible to induce a single DSB via addition of galactose. Upon DSB induction, the homology of the two GFP reading frames allow for repair via HR, which can be monitored by formation of a specific qPCR product using a primer annealing specifically to the GFP reading frame construct with the cleavable HO cut site, and one primer annealing to the unique sequence present in the second GFP reading frame construct, which serve as donor template. In figure 9 a scheme of the conversion assay is presented.

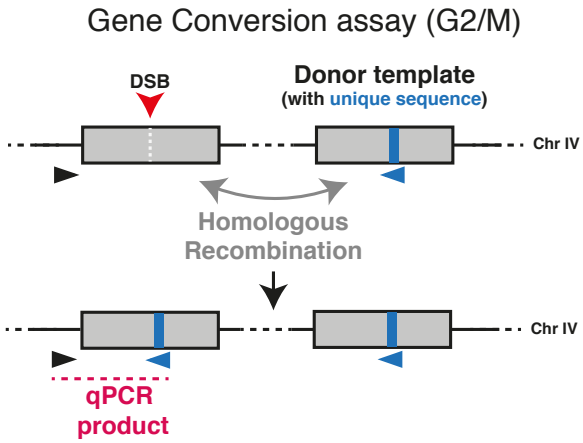

Figure 9-**Gene conversion assay scheme**

Scheme of the gene conversion assay used to measure HR. A DSB is generated via galactose-mediated induction of the HO-endonuclease. Homology between the flaking regions of the HO cut site (DSB; integrated on chromosome IV, 491 kb)) and the donor sequence (integrated on chromosome IV, 795 kb) allow for repair of the DSB by HR. The presence of a 23 bp unique sequence in the donor sequence can be used to quantify the homology directed repair via qPCR.

Survival of cells to chronic DSB induction (e.g. growth on galactose containing medium) relies on the loss of the HO cut site. This can happen either via mutagenic NHEJ, or through gene conversion, given that the donor template harbors a mutated HO cut site. As shown in figure 10, by analyzing the ability of cells to grow in the presence or absence of DSB induction (growth on glucose containing medium i.e. no DSB or galactose containing medium i.e. DSB induction), we could observe that cells lacking a donor template are not able to survive chronic DSB induction. This suggests that lack of the

donor template renders such a DSB irreparable via HR due to lack of homology and that mutagenic NHEJ-mediated repair does not occur at sufficient rates. On the other hand, cells harboring a donor template (which contains a mutated HO cut site), are able to survive chronic induction of the DSB via HR mediated repair. Importantly, in the absence of DDK, cells are not able to survive DSB induction showing that DDK is required for HR.

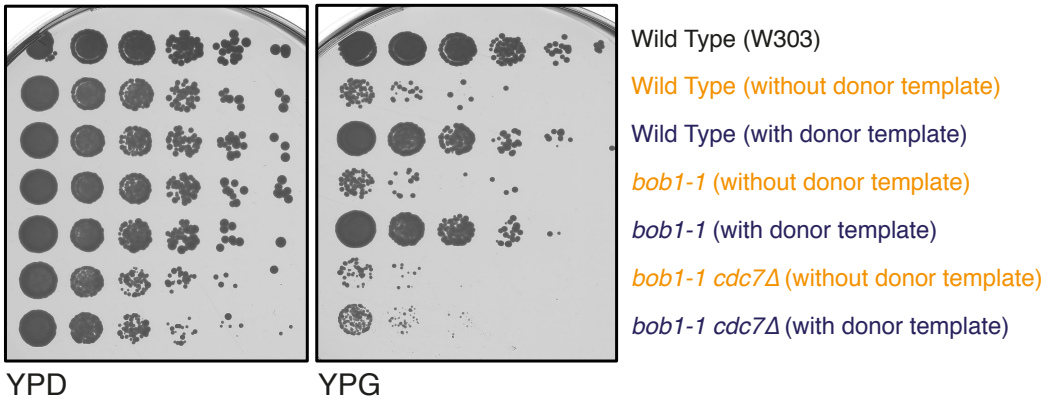

Figure 10-**DDK is required for HR-dependent survival**

Serial dilutions of Wild Type, *bob1-1* or *bob1-1cdc7Δ* carrying the gene conversion system either with or without a donor template were spotted on plates containing glucose (YPD) or galactose (YPG). Wild Type (W303) cells not harboring the gene conversion system were used as control. With this system, a DSB is generated via galactose-mediated induction of the HO-endonuclease. Cell survival on YPG relies on mutagenesis of the HO cut site, which can be achieved after HR. Wild Type and *bob1-1* cells carrying a donor template can repair the DSB via HR and can grow on YPG. *bob1-1cdc7Δ* cells, despite carrying a donor template, are not able to survive on YPG, suggesting a defect in HR in cells lacking DDK. The experiment was performed in two biological replicates (n=2). Representative images are shown.

To directly measure DSB repair by HR, we quantified the repair product by qPCR. Again, to avoid any secondary effect coming from intrinsic cell cycle differences between cells with or without DDK, we arrested cells in M phase by nocodazole. Cells were grown in raffinose containing medium until the arrest. After arrest, we induced the DSB by galactose addition, and collected different time points up to 9 hours after-induction. As

shown in figure 11, we do not observe any product in cells lacking the donor template. *bob1-1* cells harboring the donor template are proficient in HR, and we can indeed measure the repair via HR as an increasing signal in the qPCR. Consistent with our survival assay, cells that are depleted of DDK (*bob1-1cdc7Δ)* have a strong defect in HR as shown by the lack of qPCR product. We therefore conclude that DDK is required for repair of DSBs via HR in yeast.

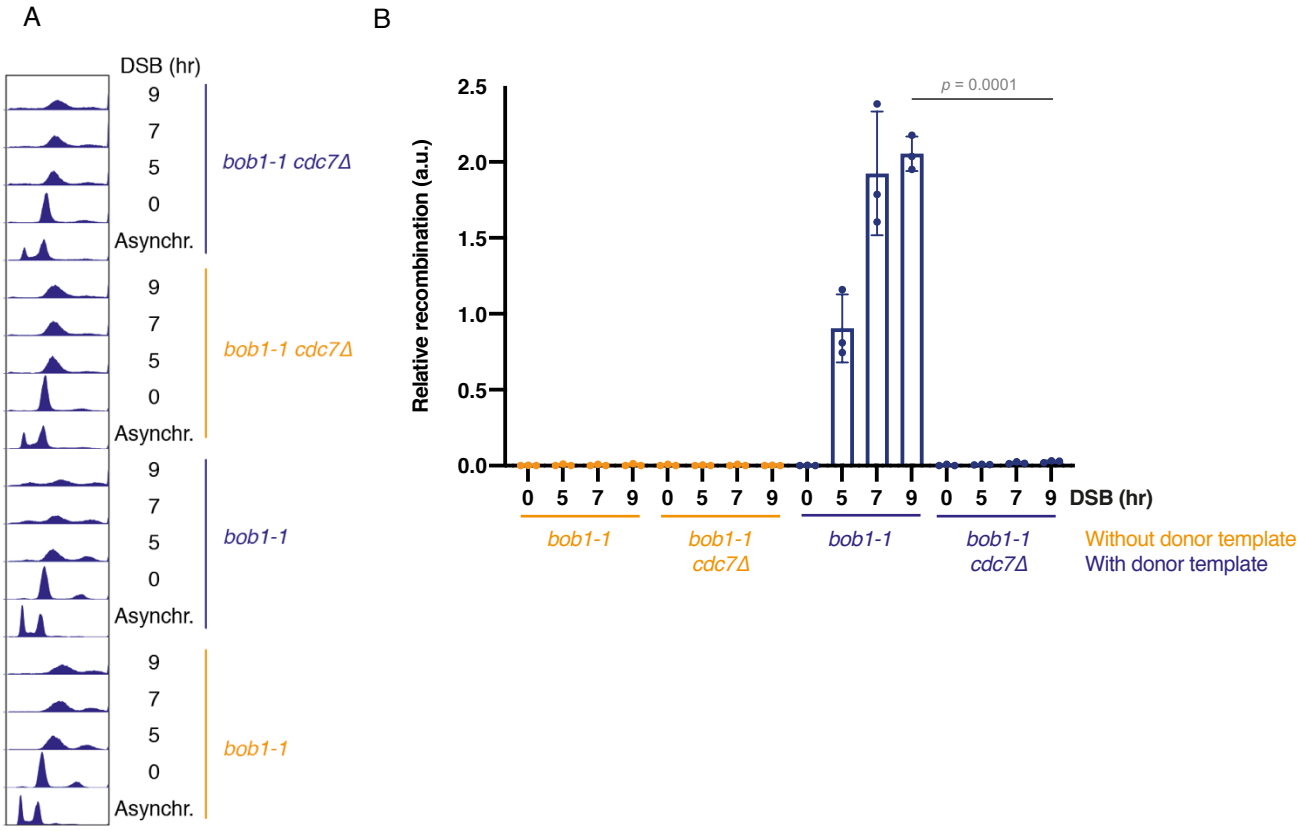

Figure 11-**DDK is required for HR**

bob1-1 or *bob1-1cdc7Δ* carrying the gene conversion system with or without a donor template were arrested in nocodazole and break induction was performed for 0-9 hours. A) Proper arrest of cells was monitored via FACS analysis of the DNA content (profiles from one biological replicate, representative of all replicates, are shown). B) Cells depleted of DDK are defective in HR. After genomic DNA extraction, each sample was subjected to two qPCRs. One using a primer pair giving a product only after homology-mediated repair, and one with a primer pair annealing on a control locus on chromosome XV (to correct for the amount of DNA). Results from three biological replicates (n=3) are shown, with 3 technical replicates each. Bars represent the mean of the three biological replicates (dots represent values of each biological replicate), and error bars denote the standard deviation (SD). The reported *p*-value (for the 9 hours-time points) was calculated performing an unpaired *t*-test using the GraphPad web-tool "*t*-test calculator" (https://www.graphpad.com/quickcalcs/ttest1.cfm).

2.3 DDK is required for DNA end resection

Our mass spectrometry analysis suggested an involvement of DDK in DNA end resection. Therefore, we tested if DDK was required already at the resection step. First, we used a genetic assay that measures single strand annealing (SSA). In the SSA assay system, a single DSB can be induced by galactose, having the HO endonuclease under control of the GAL promoter. The SSA assay system uses a *RAD51* deletion and therefore cells cannot repair the DSB by canonical HR. However, a region homologous to the DSB site has been engineered in this strain and if cells can resect an extended tract (25 Kb) as shown in figure 12, homologous sequences can anneal, and upon flap removal and ligation, cells are able to survive to chronic HO endonuclease expression [141].

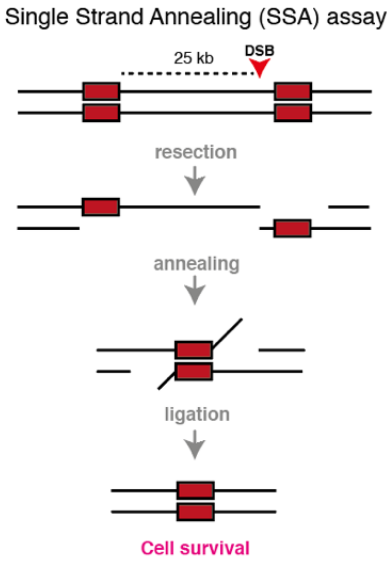

Figure 12- **Graphical representation of single strand annealing (SSA) and the genetic assay system**

Single strand annealing (SSA) allows the repair of a DSB by resection dependent annealing of a homologous sequence. A DSB is induced (via galactose-mediated induction of the HO-endonuclease) at a specific genomic location close to one of two homologous sequences. A homologous sequence can be found at defined distance (25 kb) and can be activated by extensive resection. Homology-directed annealing, flap removal and ligation allow for DSB repair and cell survival in the galactose-containing medium (due to the loss of the original DSB site) as shown in the figure.

As shown in figure 13, DDK mutants were not able to survive chronic induction of the HO endonuclease. Lack of cell survival in SSA assay is suggestive of a resection defect, providing first evidence that DDK might be required for DNA end resection.

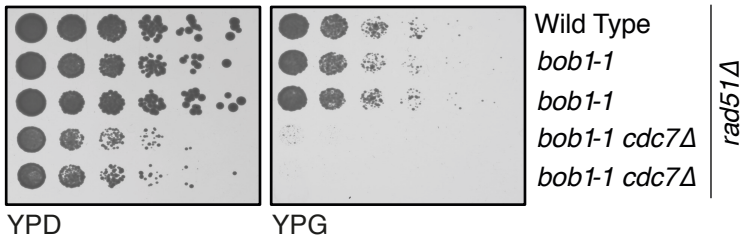

Figure 13-**DDK is required for single strand annealing (SSA)**

Serial dilutions of Wild Type, *bob1*-1 or *bob1-1cdc7Δ* cells harboring the SSA genetic assay system were spotted on either glucose (YPD) or galactose (YPG) containing plates. The experiment is performed in *rad51Δ* cells to force repair via SSA rather than canonical HR. With this system, a DSB is generated via galactose-mediated induction of the HO-endonuclease. DNA end resection is required for cells to repair the DSB via SSA (see figure 12) and survive to chronic induction of the HO-endonuclease (growth on YPG). *bob1-1cdc7*Δ cells are not able to grow on YPG, suggesting defective repair of the DSB due to lack of DNA end resection. The experiment was performed in two biological replicates (n=2).

We next monitored DNA end resection in a physical resection assay. Specifically, we measured the occurrence of single stranded DNA at a specifically localized DSB. As proxy for ssDNA formation, we measured the enrichment of RPA using RPA-ChIP followed by strand specific sequencing. An unrepairable DSB was induced with the GAL-HO system. Additionally, we used an inducible system for depletion of DDK. We fused an Auxin inducible degron (AID) to Dbf4. The AID system allows to obtain rapid degradation of the AID-tagged protein upon addition of indole-3-acetic acid (IAA) or naphthalene-1-acetic acid (NAA), in a strain expressing the plant protein Tir1 [142,143]. As shown in figure 14 we can induce depletion of Dbf4-AID via addition of IAA or NAA, and consistent with the essential function of DDK, cells are not able to survive chronic exposure to NAA.

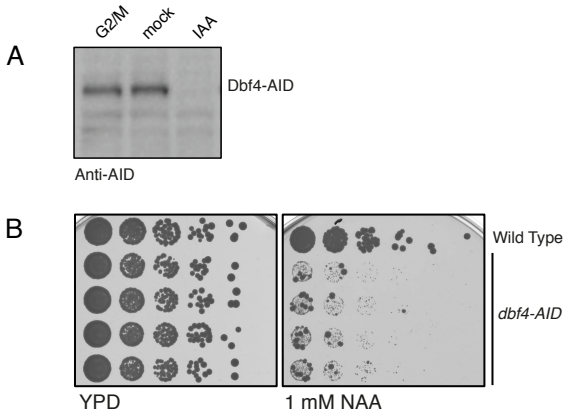

(Figure legend on the following page)

Figure 14- **Dbf4-AID allows for quick depletion of endogenous Dbf4 in the presence of IAA or NAA**

A) *dbf4-AID* cells were arrested in M-phase with nocodazole, and subsequently either mock treated (DMSO) or treated with 3 mM IAA. Western blot was performed to monitor Dbf4-AID degradation. B) Wild Type or *dbf4-AID* cells were serially diluted and spotted on YPD plates as control or on YPD plates containing 1 mM NAA.

For our RPA-ChIP sequencing experiment we arrested cells in M. We either mock treated our cells, or added 1 mM IAA to induce degradation of Dbf4 and therefore depletion of DDK. DSB induction was then performed and samples were collected after 2 and 4 hours post DSB-induction. Western blot analysis confirmed that treatment with IAA induced depletion of Dbf4 before break induction, and throughout the experiment (figure 15-B), while DNA content measurement confirmed the cell cycle arrest (figure 15-A).

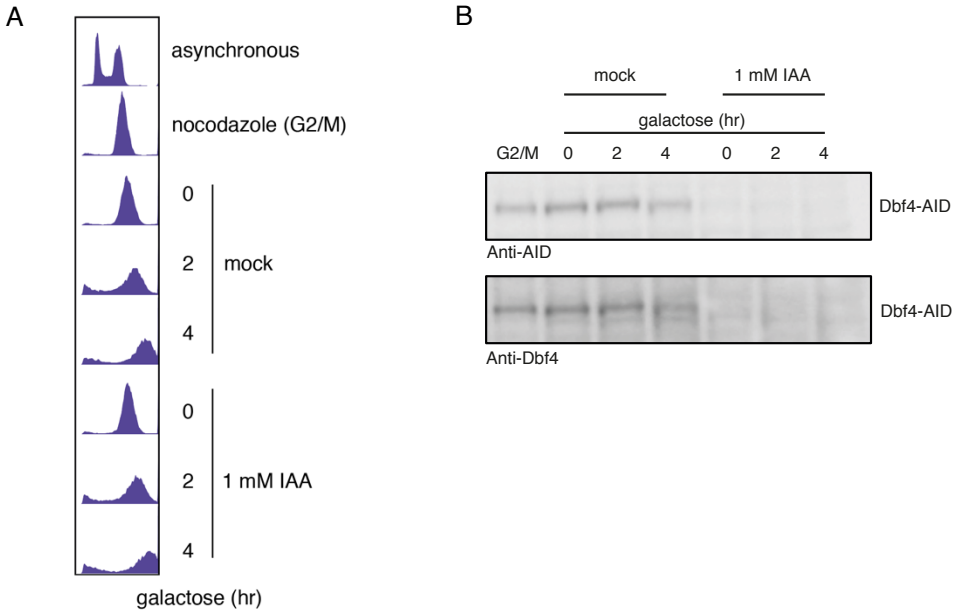

(Figure legend on the following page)

Figure 15- **Dbf4 degradation in Dbf4-AID test system for RPA-ChIP seq experiments**

To monitor DNA end resection via RPA-ChIP seq, *dbf4-AID* cells were arrested in the M-phase using nocodazole. Cells were then split and either mock treated (DMSO) or treated with 1 mM IAA (IAA is dissolved in DMSO) for 2 hours to induce depletion of Dbf4-AID. A single DSB was then induced via galactose-mediated induction of the HO-endonuclease. Samples were collected before galactose addition (0 hour) and 2- and 4-hours after HO induction. A) The DNA content was measured via FACS to confirm the arrest in the M-phase via nocodazole. B) The degradation of Dbf4-AID in the presence of IAA was confirmed with a western blot using antibodies against the AID tag (top) or Dbf4 (bottom). Experiments were performed in two biological replicates (n=2). Representative DNA content profiles and western blots are shown.

RPA-ChIP followed by strand specific sequencing allowed us to monitor the occurrence of ssDNA by resection. As shown in figure 16 we can monitor the enrichment of RPA at each side of the break in a strand specific manner. Importantly, cells that are depleted of DDK have a strong reduction in the enrichment of RPA, therefore confirming that DDK is required for DNA end resection.

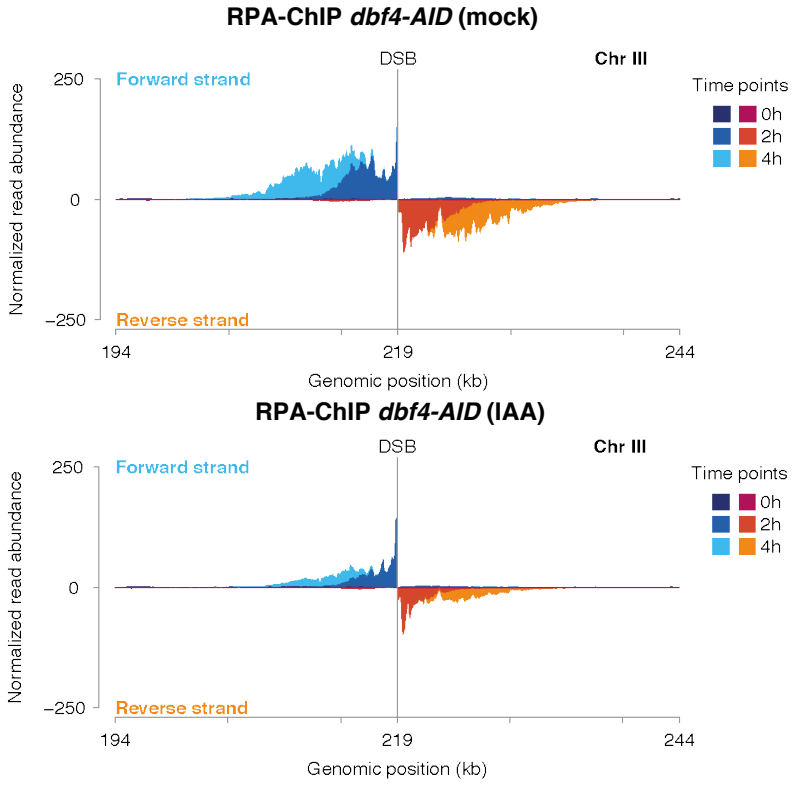

(Figure legend on the following page)

Figure 16-**DDK is required for DNA end resection**

Samples collected as shown in figure 15 were used for RPA-ChIP seq experiments to monitor RPA enrichment at a single induced DSB in the presence (mock) or absence (IAA) of DDK, which was depleted by using the auxin-inducible assay system. Mock treatment refers to addition of DMSO (as IAA is dissolved in DMSO). Crosslinked DNA was fragmented (200-500 bp fragments) and subjected to an RPA immunoprecipitation. Strand-specific libraries were prepared and DNA was paired-end sequenced. Normalized read abundance (normalization to the total number of reads) is displayed, showing the strand-specific enrichment of RPA of cells mock-treated (top) or IAA-treated (bottom). The reduction in the number of reads in cells depleted of DDK suggests an involvement of DDK in DNA end resection. The experiment was performed in two biological replicates (n=2). Shown are plots from one biological replicate, representative of the two biological replicates.

The resection defect in DDK mutants is already visible when looking at the total DNA samples (figure 17). DNA end resection represents nucleolytic degradation of the 5' broken DNA strand around the DSB. DNA end resection therefore leads to a strand specific loss of DNA at each site of the break, which can be observed in the input DNA of the mock treated cells. Consistent with a defect in resection, cells depleted of DDK have less pronounced strand specific loss of DNA around the DSB.

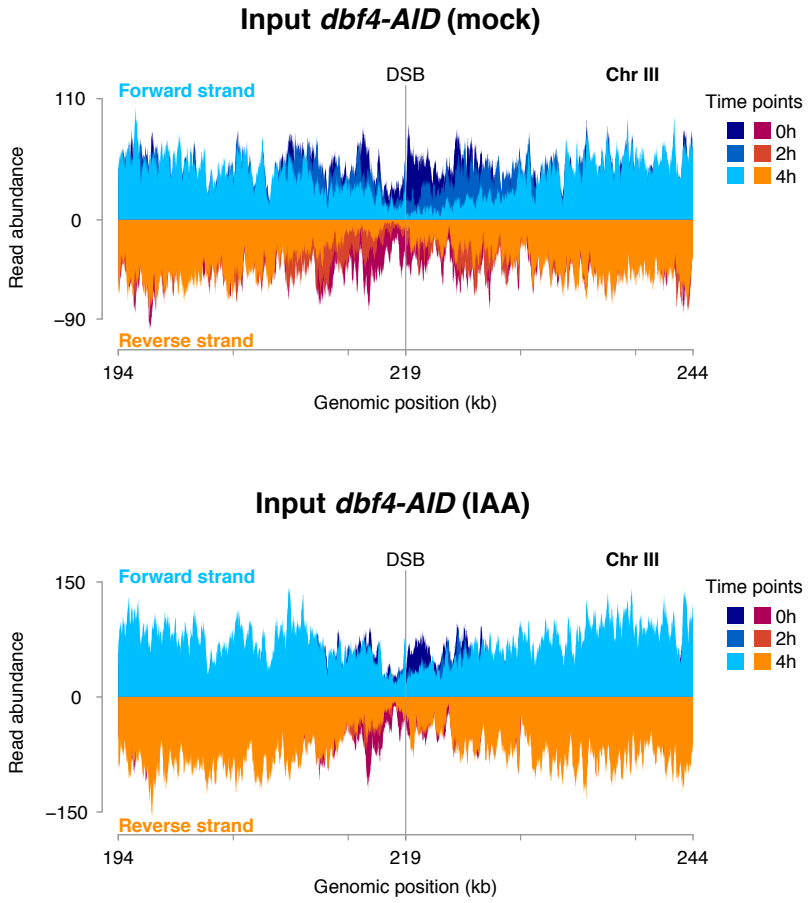

Figure 17-**DDK is required for DNA end resection**

Read abundance of the DNA input samples of the experiment presented in figure 16 is plotted showing input DNA in each sample at the indicated time points; mock-treated sample (top) and IAA-treated samples (bottom). Resection is visible by the respective loss of 3' DNA at the DSB. Cells depleted of DDK display reduced loss of 3'DNA, consistent with a defect in DNA end resection. The experiment was performed in two biological replicates (n=2). Shown are plots from one biological replicate (same experiment as in figure 16), representative of the two biological replicates.

We also performed similar experiments in both *dbf4-AID* and *bob1-1* systems, and measured RPA-ChIP followed by qPCR. For the *dbf4-AID* system the experiment was performed as the experiment shown in figure 16. For the comparison between *bob1-1* and *bob1-1cdc7Δ,* cells were arrested in M and break induction was achieved via addition of galactose in the medium and monitored for 4 hours. As observed in figure 18 we obtained similar results with both systems.

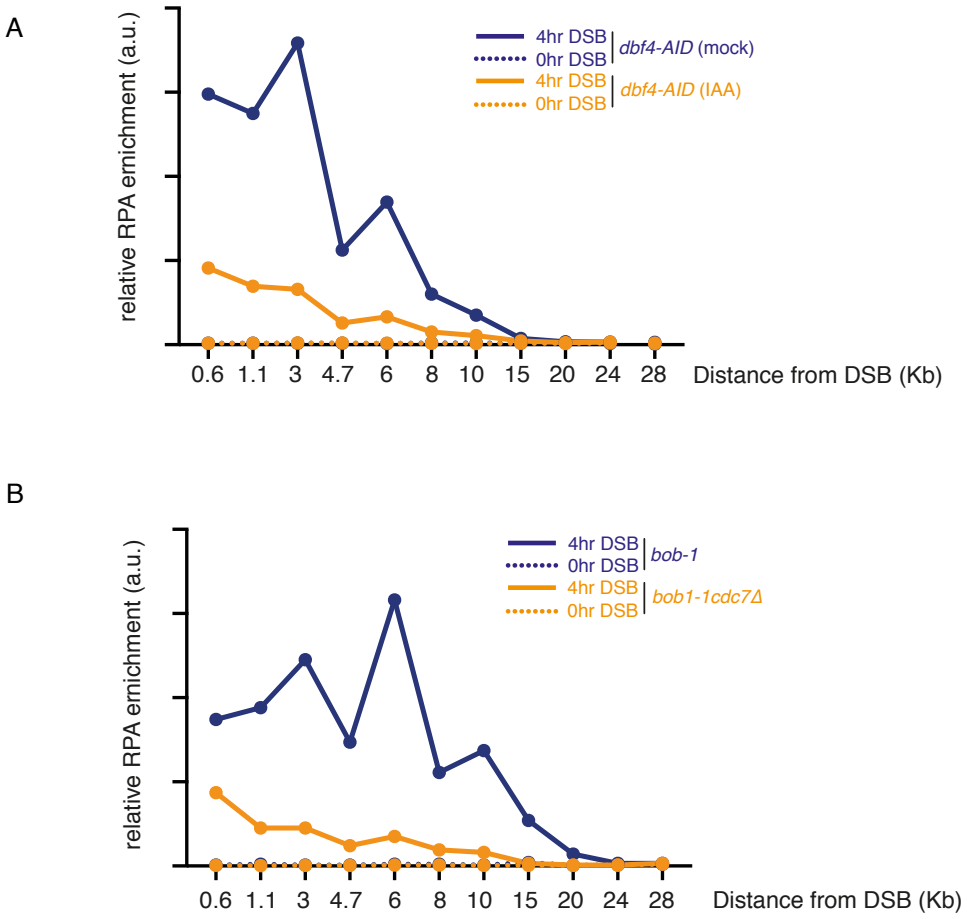

Figure 18- **Resection in different systems lacking DDK**

RPA-ChIP followed by qPCR to monitor the effect of DDK on resection with A) the *dbf4-AID* or B) the *bob1-1* system. Cells were arrested in M-phase with nocodazole and galactose-mediated induction of the HO endonuclease was used for DSB induction. Samples were collected before, and 4 hours after the induction of the DSB. For the *dbf4-aid* system, nocodazole-arrested cells were treated for 2 hours with 1 mM IAA (or mock treated) before induction of the DSB, to achieve depletion of Dbf4. For each time point, a sample before (input) and after the RPA-immunoprecipitation was measured via qPCR with three control primer pairs (to control for the amount of DNA) annealing on control loci on chromosome V, VI and XV, and with 11 primer pairs annealing from 0.6 kb up to 28 kb from the DSB. Depletion of DDK, either via auxin-inducible degradation of Dbf4-AID or via deletion of CDC7 in the *bob1-1* background, lead to defect in DNA end resection as shown by the reduction in RPA enrichment in the surrounding of the DSB, consistent with a role of DDK in DNA end resection. Each experiment was performed in two biological replicates (n=2). Shown are plots from one biological replicate, representative of the two biological replicates.

Altogether our experiments identify DDK as being required for the cellular response to repair DSBs via HR, already at the initial step of DNA end resection. Considering that end resection is the critical step that commits cells to repair via HR over NHEJ, this also suggests that DDK might be a critical player in the DSB repair pathway choice.

3. DDK phosphorylation of the Sae2-MRX complex promotes DNA end resection

3.1 DDK phosphorylates Sae2 *in vivo*

Despite not identifying Sae2 as DDK phosphorylation substrate in our phosphoproteomics screen, we identified a slower migrating band of Sae2 from samples of cells arrested in M-phase via nocodazole, when running samples on a 10% gel for 3hr or more. Knowing that Sae2 is phosphorylated in cell cycle dependent manner by CDK [9], we investigated if the observed shift on gels might be due to CDK phosphorylation. *cdc28-as1* is an engineered allele of *CDC28* (the single gene coding for CDK in *S. cerevisiae*) which can be inhibited by the nucleoside-analog 1-NM-PP1 [144]. We therefore arrested *cdc28-as1* cells in the G1 phase of the cell cycle, via the mating pheromone alpha factor, or in the M-phase of the cell cycle via Nocodazole. After the arrest, cells were split and either mock treated, or treated with the chemical 1-NM-PP1 for 1hr. We observed the shifted band in cells arrested in M, but not in G1 cells. Importantly, M-phase arrested cells even after 1 hour of treatment with 1-NM-PP1 showed a shift for Sae2, showing that the observed gel shift was not dependent on CDK (figure 19). Sld2 is a known CDK substrate [8], which served as a positive control for the effectiveness of the 1-NM-PP1 treatment and CDK inhibition (figure 19).

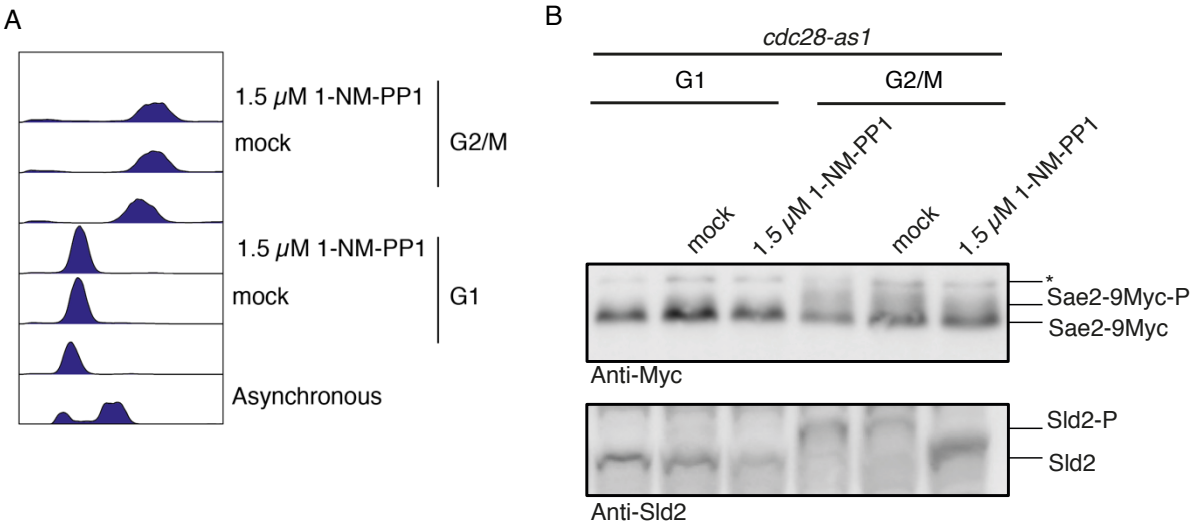

(Figure legend on the following page)

Figure 19-**Sae2 gel-shift is independent of CDK**

Yeast cells harboring Sae2-9Myc and carrying the *cdc28-as1* allele were arrested in M-phase with nocodazole or in G1 with alpha factor, and either mock treated (DMSO) or treated with 1.5 μM 1-NM-PP1 (dissolved in DMSO) to inhibit CDK (Cdc28-as1). A) DNA content measurement via FACS confirms cell cycle arrest. B) Samples were run on a 10% acrylamide gel to resolve the Sae2 shift. Sld2 phosphoshift (run on 12% Bis-Tris acrylamide gel) was used as a control of CDK inhibition. The asterisk indicates an unspecific band. The presence of the Sae2 gel-shift in M-phase cells also after CDK inhibition shows that the shift is cell-cycle dependent, but CDK independent. The experiment was performed in two biological replicates (n=2). Shown are DNA content profiles and western blots from one biological replicate, representative of the two biological replicates.

The gel shift was not dependent on CDK, but treatment of cells extracts from M arrested cells with λ phosphatase completely abolished the slower migrating band, showing that this band represented a phosphorylated form of Sae2 (figure 20)

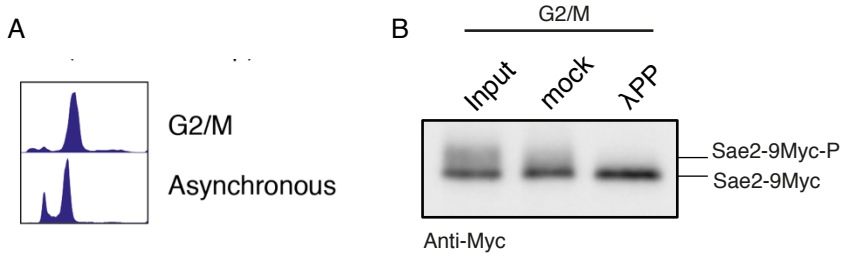

Figure 20-**Identification of phosphorylation-dependent gel shift for Sae2**

Cells harboring Sae2-9Myc were arrested in M-phase with nocodazole. A) DNA content measured via FACS confirms the cell cycle arrest. B) Cells were lysed and extracts were supplemented with 2 mM $MnCl_2$, split, and either mock treated (no addition of λ phosphatase) or treated with λ phosphatase (λPP) for 1 hour at 30°C. Samples were separated on 10% acrylamide gels and Sae2-9Myc detected using an anti-Myc antibody. The loss of Sae2-shift after treatment with λ phosphatase shows that the slower migrating band represent a phosphorylated form of Sae2. The experiment was performed in two technical replicates (two separate "mock versus λ phosphatase" reactions were performed on extracts coming from the same cells).

The cell cycle-dependent but CDK-independent phosphoshift of Sae2 prompted us to analyze if phosphorylation could be due to DDK. We performed a similar experiment as the one in figure 19, but with DDK mutants. Briefly, we arrested *bob1-1, bob1-1dbf4Δ* and *bob1-1cdc7Δ* cells in G1 or in M-phase, and analyzed the Sae2 phosphoshift as previously described. Again, we could observe the appearance of the phosphoshifted Sae2 band only

in M arrested cells. Interestingly, the phosphorylated Sae2 band was completely absent in cells depleted either of *DBF4* or *CDC7*, showing that Sae2 is phosphorylated *in vivo* by DDK in a cell cycle specific manner (figure 21).

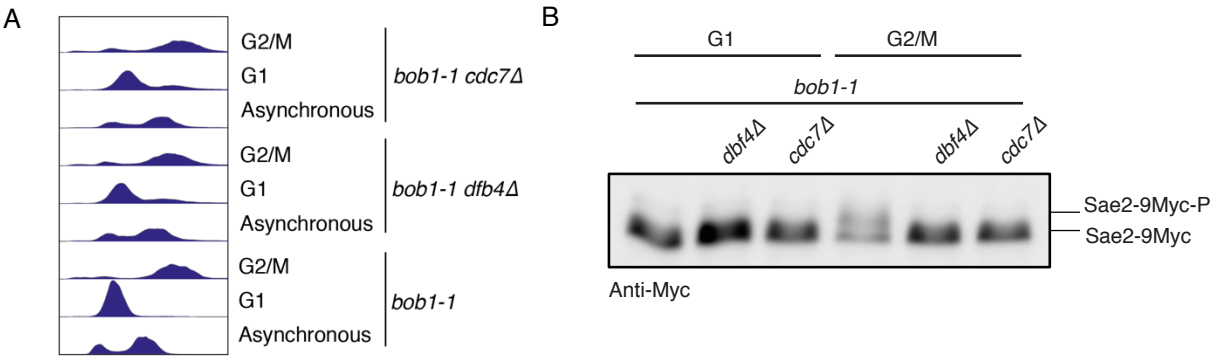

Figure 21-**The phosphorylation-dependent shift of Sae2 is dependent on DDK (*bob1-1* system)**

bob1-1, bob1-1 dbf4Δ and *bob1-1 cdc7Δ* cells harboring Sae2-9Myc were arrested in M-phase with nocodazole or in G1 with alpha factor. A) DNA content measured via FACS confirms cell cycle arrest. B) Samples were run on a 10% acrylamide gel to resolve the Sae2 phosphoshift. The phosphoshift is lost in DDK mutants, revealing DDK to be the kinase required for the observed phosphoshift. The experiment was performed in three biological replicates (n=3). Shown are DNA content profiles and western blots from one biological replicate, representative of the three biological replicates.

Having developed also the inducible system for Dbf4 depletion, we analyzed if we could observe loss of Sae2 phosphoshift also upon Dbf4 depletion. We again arrested cells in G1 or in M, and treated them with IAA to induce Dbf4-AID degradation. As shown in figure 22 we could observe the phospho-shift of Sae2 in cells arrested in M and in M cells mock treated. Cells in M in which Dbf4 was degraded via IAA lost the Sae2 phosphoshift consistent with our pervious result.

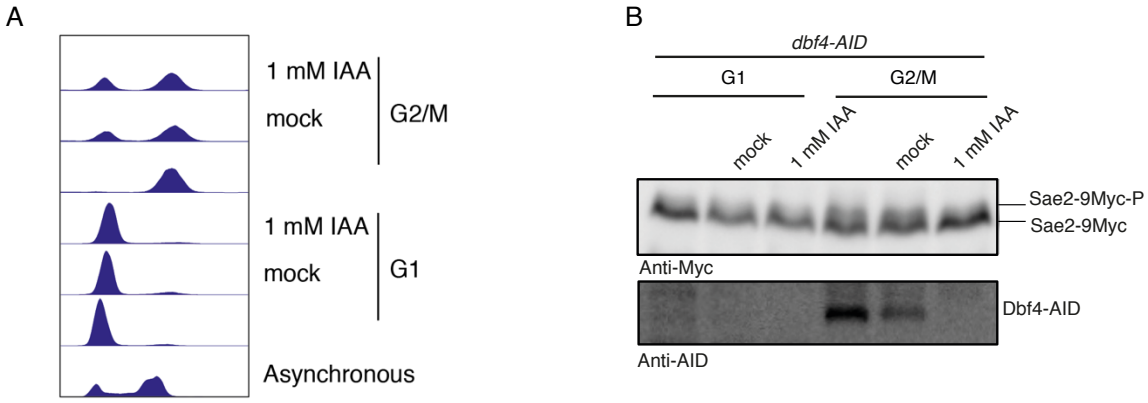

Figure 22-**The phosphorylation-dependent shift of Sae2 is dependent on DDK (*dbf4-AID* system)**

dbf4-AID cells harboring Sae2-9Myc were arrested in M-phase with nocodazole or in G1 with alpha factor and either mock treated (DMSO) or treated with 1 mM IAA (IAA is dissolved in DMSO) A) DNA content measured via FACS. B) Samples were run on a 10% acrylamide gel to resolve the Sae2 shift and to confirm Dbf4 degradation. The phosphoshift is lost after Dbf4-AID degradation, confirming DDK to be the kinase required for the observed phosphoshift. The experiment was performed once.

DDK was shown to form a kinase complex with Cdc5 in order to phosphorylate a series of substrates [13,24]. We therefore wondered if the DDK mediated phosphorylation of Sae2 would be dependent on the kinase complex with Cdc5. DDK interacts with Cdc5 through the N-terminal domain of Dbf4. A N-terminal truncation lacking amino acids 1 to 109 of Dbf4 is therefore not able to interact with Cdc5, despite being fully active [44]. As shown in figure 23 we observe a cell cycle dependent phosphoshift of Sae2 in cells harboring an interaction deficient mutant of Dbf4, showing that the phosphorylation of Sae2 requires DDK on its own, and not DDK as part of the kinase complex with Cdc5.

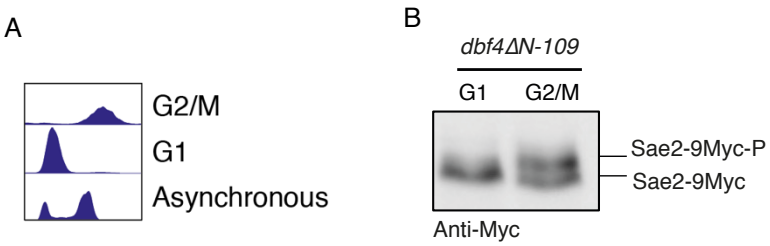

Figure 23-**The phosphoshift of Sae2 is dependent on DDK, but not on its interaction with Cdc5**

dbf4ΔN-109 cells harboring Sae2-9Myc were arrested in M-phase with nocodazole or in G1 with alpha factor. A) DNA content measured via FACS. B) Samples were run on a 10% acrylamide gel to resolve the Sae2 shift. In *dbf4ΔN-109* cells the cell cycle-dependent Sae2-phosphoshift is observed, showing that the phosphoshift requires DDK (see figure 21,22), but not its interaction with Cdc5. The experiment was performed in two biological replicates (n=2). Shown are DNA content profiles and western blots from one biological replicate, representative of the two biological replicates.

3.2 DDK phosphorylation of Sae2-MRX stimulates the nucleolytic activity of the Sae2-MRX complex

CDK-dependent phosphorylation of Sae2 on serine 267 is an essential step for the cell cycle specific activation of the Sae2-MRX complex, but it also does not seem sufficient. Having discovered that DDK is required for DNA end resection and that Sae2 is a substrate of DDK *in vivo,* we tested if DDK-dependent phosphorylation of Sae2 could be important to activate the nucleolytic activity of the Sae2-MRX complex and hence to initiate DNA end resection.

To directly analyze the effect of Sae2 phosphorylation on the nucleolytic activity of the Sae2-MRX complex we used an *in vitro* reconstituted system developed in the Cejka lab to monitor the endonucleolytic activity of the Sae2-MRX complex on a template DNA [71,145]. A radioactively labelled DNA with streptavidin at its extremities to block exonucleolytic digestion is used as a substrate. Endonucleolytic cleavage is monitored by the appearance of degradation products at lower molecular weights compared to the intact DNA (figure 24) providing a quantitative measurement of Sae2-MRX enodnucleolytic activity.

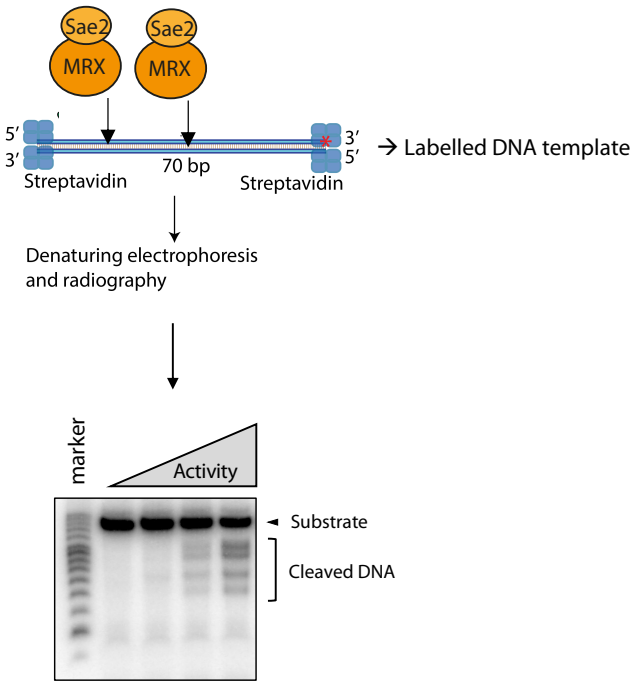

Figure 24- **Endonuclease/DNA end resection assay**

Schematic of the Sae2-MRX endonuclease assay. Radioactively labelled DNA (red asterisk) of 70 bp length with streptavidin blocked ends is used as a substrate and incubated with recombinant MRX and Sae2. Endonucleolytic cleavage by the Sae2-MRX complex can be monitored as appearance of cleaved DNA products with lower molecular weights after electrophoresis.

We purified Sae2 separately from the MRX complex, enabling us to phosphorylate it *in vitro* prior to adding it to the reaction mixture.

For CDK phosphorylation, CDK was purified as a complex of the human Cdk2 with a GST tag and the bovine CycA (ΔN170) with a 6xHis tag from *E.coli* cells [146]. Extracts of cells expressing GST-CDK2 and extracts of cells expressing CycA (ΔN170)-His were pooled together and subjected to a GST pulldown first (with Pre-Scission mediated elution), and a Ni-NTA pulldown afterwards to recover the self-assembled complex of Cdk2/CycA (ΔN170) (hereafter called CDK for simplicity) (figure 25).

DDK was purified from yeast cells using a plasmid harboring yeast Dbf4 with a N-terminal CBP tag and Cdc7 under control of a bidirectional GAL promoter, integrated in the genome. Both sequences were codon optimized. Briefly, yeast cells were grown to log phase and galactose was added to the medium for 6 hours. Cells extract were then

subjected to a CBP pulldown, followed by washes with ATP to remove a copurifying chaperone (figure 25). Both kinases were tested for their activity.

The yeast MRX complex was purified from Sf9 insect cells, as well as yeast Sae2. To this end, the MRX complex contained a His-tag and a FLAG-tag at the C-termini of Mre11 and Xrs2, respectively and was purified via affinity chromatography [147]. Sae2 had a MBP tag at its N-terminus and a HIS tag at its C-terminus and was purified via a double pulldown. First a MBP pulldown followed by a Ni-NTA pulldown (after MBP pulldown, the MBP tag was cleaved using PreScission protease) [120] .

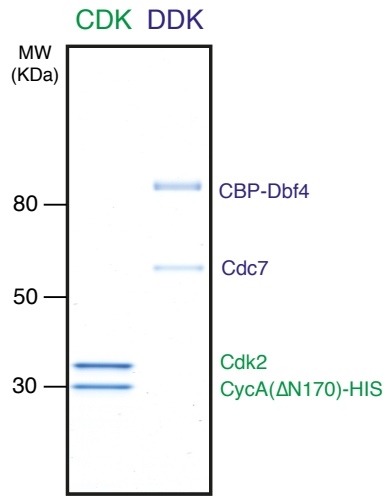

Figure 25-**DDK and CDK purification**

CDK and DDK were purified via affinity chromatography from bacteria and yeast cells, respectively. CDK was purified as a complex of the human Cdk2 and a construct of the bovine Cyclin A (CycA(ΔN170)). The two proteins were separately expressed in bacteria cells and extracts were pooled together to assemble an active Cdk2-CycA complex. Cdk2 carries a GST tag at its N-terminus while CycA(ΔN170) carries a HIS-tag at its C-terminus. Pooled extracts were subjected to a GST pulldown followed by a Ni-NTA pulldown (for His-tag affinity chromatography) to purify reconstituted Cdk2-CycA complexes (CDK). Yeast DDK was purified from yeast cells harboring a construct allowing galactose-mediated overexpression of CBP-Dbf4 (Dbf4 with a CBP-tag at its N-terminus) and Cdc7. Extracts were subjected to CBP pulldown to recover active DDK. A representative image of the purified proteins is shown.

We tried to recapitulate CDK and DDK mediated phosphorylation of Sae2 *in vitro*. By performing a kinase assay with Sae2 and CDK, DDK or both, we observed that both kinases can independently phosphorylate Sae2, as shown by incorporation of

radioactively labelled ATP. Note that DDK can also auto-phosphorylate itself as previously observed (figure 26).

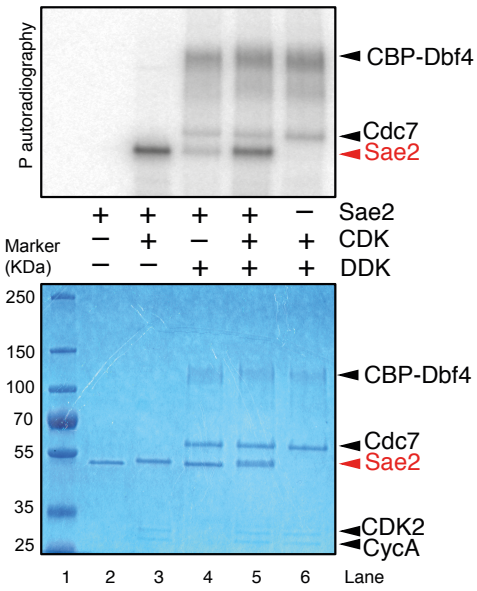

Figure 26- **CDK and DDK phosphorylate Sae2 *in vitro***

Purified, recombinant Sae2 was incubated with purified CDK, DDK or both for 30 minutes at 30°C in the presence of radioactive ATP. Autoradiography was performed to monitor the incorporation of radioactive ATP, showing that both CDK and DDK can phosphorylate Sae2 *in vitro*. The experiment was performed once.

Next, we tested endonucleolytic cleavage. First, we analyzed if DDK mediated phosphorylation of Sae2 is able to promote the nucleolytic activity of the MRX complex. 100nM of Sae2 was pre-phosphorylated with DDK, and subsequently added to the reaction mixture with the MRX complex and the template DNA. A reaction with mock treated Sae2 was used as a control. We observed an increase in the endonucleolytic activity of the MRX complex over time when it was provided with DDK-phosphorylated Sae2 compared to the mock treated Sae2 (figure 27). We conclude that DDK can phosphorylate Sae2 *in vitro* and that this phosphorylated form enhances the stimulation by Sae2 of the nucleolytic activity of the MRX complex.

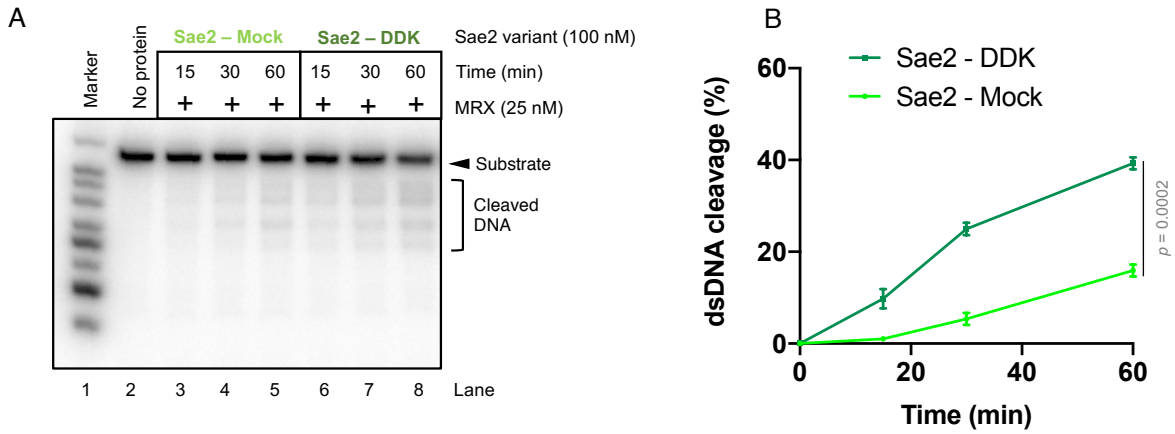

Figure 27- **DDK stimulates the endonucleolytic activity of Sae2-MRX**

Endonuclease assay performed using Sae2 (mock treated (no pre-incubation with DDK) or pre-incubated with DDK). After mock/kinase reactions, Sae2 was incubated with MRX and the DNA template at 30˚C and samples collected at the indicated times. Three separate in vitro assays were performed independently (n=3), but with the same protein preparations. A) Samples were resolved on a gel to measure the amount of cleaved DNA. Shown is a gel from one of the experiments, representative of the three replicates. B) Quantification of the experiments. The DNA cleavage was calculated as [products/(substrates + products)] for each lane. DDK-phosphorylated Sae2 was observed to stimulate the endonucleolytic activity of the Sae2-MRX complex. The mean of three replicates is plotted. Error bars denote standard error of the mean (SEM). The reported *p*-value (for the 60 minutes time points) was calculated performing an unpaired *t*-test using the web-tool "*t*-test calculator" (https://www.graphpad.com/quickcalcs/ttest1.cfm) from GraphPad.

Next, we analyzed the possible interplay with the CDK mediated phosphorylation. First, we performed an endonuclease end point assay by pre-incubating Sae2 either with DDK or with CDK before adding it to the reaction with MRX and the template DNA. Again, mock treated Sae2 was used as control. As shown in figure 28 we observed that both CDK or DDK pre-phosphorylation of Sae2 lead to a stimulation of the nucleolytic activity of MRX, to a similar degree.

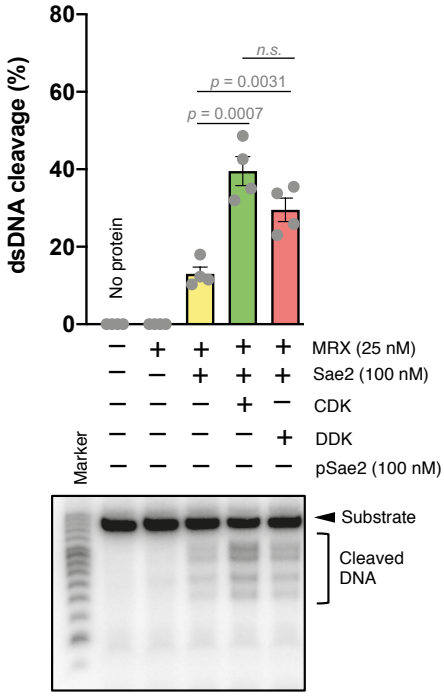

Figure 28- **DDK stimulates the endonucleolytic activity of Sae2-MRX to the same extent as CDK**

Endonuclease assay performed using mock treated Sae2 (no incubation with kinases) or Sae2 pre-incubated with DDK or CDK. After treatment, Sae2 was incubated with MRX and the DNA template for 30 minutes at 30°C. Four separate assays were performed independently, but with the same protein preparations. Quantification of the different experiments (top). Samples were resolved on a gel to measure the amount of cleaved DNA; shown is a gel from one of the experiments, representative of the four replicates (bottom). The DNA cleavage was calculated as [products/(substrates + products)] for each lane. DDK-phosphorylated Sae2 could stimulate the endonucleolytic activity of the Sae2-MRX complex to the same extent as CDK-phosphorylated Sae2. The mean of the four experiments is plotted. Dots represent values calculated for the single experiments. Error bars denote standard error of the mean (SEM). The reported *p*-values were calculated performing an unpaired *t*-test using the GraphPad web-tool "*t*-test calculator" (https://www.graphpad.com/quickcalcs/ttest1.cfm). *p*-values > 0.05 are reported as not significant (n.s.).

It was previously shown that CDK phosphorylation of Sae2 on serine 267 is required for the CDK mediated stimulation of the Sae2-MRX complex activity [9,120]. serine to alanine mutations of serine 267 on Sae2 are indeed defective for DNA end resection *in vivo* and for stimulation of the nucleolytic activity of the MRX complex *in vitro*, while phosphomimic serine to glutamate mutations of serine 267 (S267E) can only partially activate the nucleolytic activity of the Sae2-MRX *complex in vitro* [11,120]. Interestingly, serine 267 was shown to be the only CDK site that is important for this function, as mutating two other CDK consensus sites of Sae2 (serine 134 and 179) to alanine does not have an effect on phosphorylated Sae2 ability to stimulate the MRX complex [120]. We therefore wondered if activation by DDK depended on serine 267. As shown in figure 29 Sae2 S267E was able to stimulate Sae2-MRX endonuclease activity after DDK phosphorylation compared to mock treated Sae2 S267E. This experiment shows that DDK can stimulate the nucleolytic activity of the Sae2-MRX complex on top of phosphorylation of the key CDK site. It also provides an important control, showing that the DDK mediated stimulation observed is due to phosphorylation of specific sites on Sae2 and that DDK does not simply phosphorylates the known CDK sites.

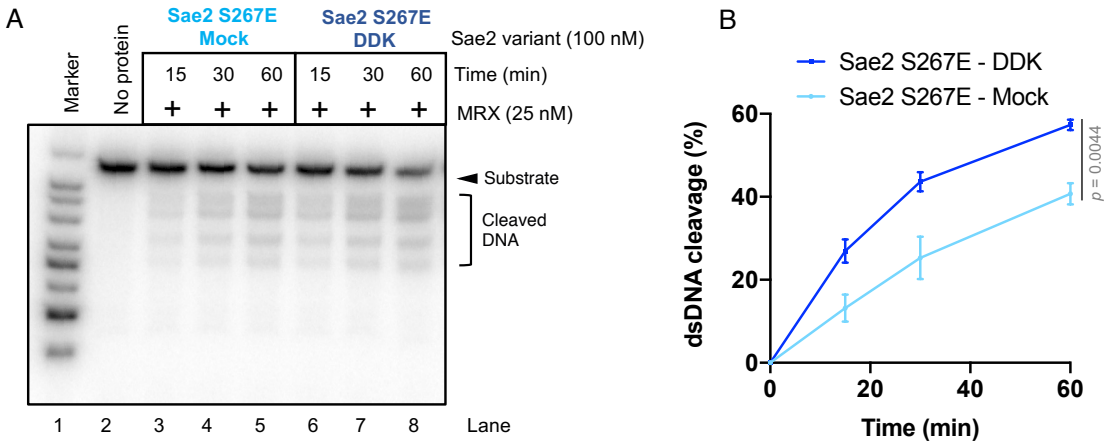

Figure 29- **DDK stimulates the endonucleolytic activity of Sae2-MRX independently of serine 267**

Endonuclease assay performed using Sae2 S267E (mock treated (no pre-incubation with DDK) or pre-incubated with DDK). After the mock/kinase reactions, Sae2 S267E was incubated with MRX and the DNA template at 30˚C and samples collected at the indicated times. Three separate in vitro assays were performed independently (n=3), but with the same protein preparations. A) Samples were resolved on a gel to measure the amount of cleaved DNA. Shown is a gel from one of the experiments, representative of the three replicates. B) Quantification of the experiments. The DNA cleavage was calculated as [products/(substrates + products)] for each lane. DDK was observed to stimulate the endonucleolytic activity of the Sae2-MRX complex independently of serine 267. The mean of three replicates is plotted. Error bars denote standard error of the mean (SEM). The reported *p*-value (for the 60 minutes time points) was calculated performing an unpaired *t*-test using the web-tool "*t*-test calculator" (https://www.graphpad.com/quickcalcs/ttest1.cfm) from GraphPad.

We also performed an experiment where we pre-phosphorylated Sae2 with CDK or with CDK and DDK together before starting the clipping reaction of MRX on the template DNA. Here, Sae2 phosphorylated with both DDK and CDK activated the MRX complex more strongly than Sae2 only phosphorylated by CDK (figure 30), even though the effect was weak (and not statistically significant).

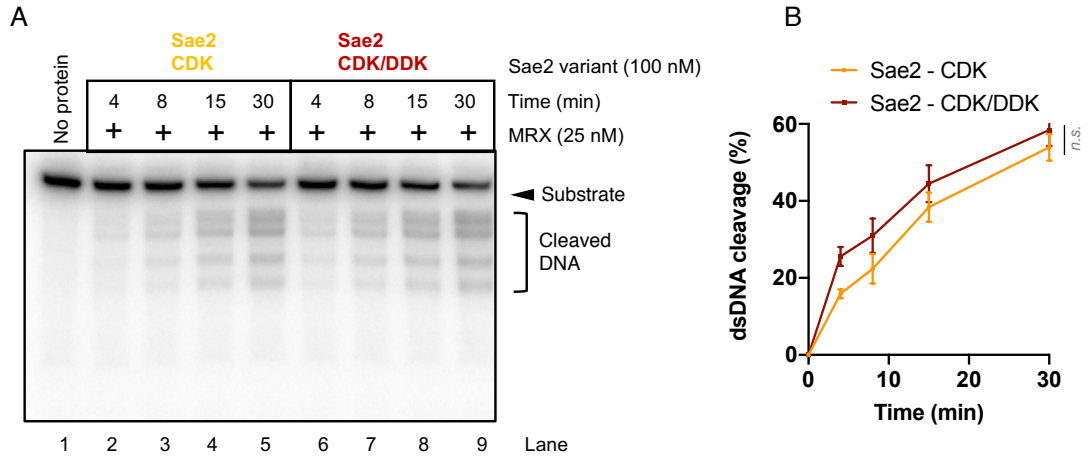

Figure 30- **Combined effect of DDK and CDK on Sae2-MRX endonucleolytic activity**

Endonuclease assay performed using Sae2 pre-incubated with DDK and CDK or with CDK only. After the kinase reactions, Sae2 was incubated with MRX and the DNA template at 30˚C and samples collected at the indicated times. Three separate in vitro assays were performed independently (n=3), but with the same protein preparations. A) Samples were resolved on a gel to measure the amount of cleaved DNA; shown is a gel from one of the experiments, representative of the three replicates. B) Quantification of DNA cleavage calculated as [products/(substrates + products)] for each lane. The mean of the three experiments is plotted. Error bars denote standard error of the mean (SEM). The *p*-value calculated (for the 60 minutes time points) was > 0.05 (reported as not significant; n.s.). Calculation was performed via an unpaired *t*-test using the GraphPad web-tool "*t*-test calculator" (https://www.graphpad.com/quickcalcs/ttest1.cfm).

Our *in vitro* analysis of Sae2-mediated stimulation of the nucleolytic activity of the MRX complex led us to conclude that DDK phosphorylated Sae2 stimulates the activity of the Sae2-MRX complex.

Currently it is known that phosphorylation of Sae2 can modulate the oligomeric state of Sae2, switching from an inactive high order aggregate to an active tetramer [120,125,126]. Additionally, it was shown that the interaction between Sae2 and the MRX complex might be influenced by phosphorylation [120]. To test if DDK phosphorylation of Sae2 might be important to regulate the oligomeric state of Sae2 we decided to pulldown Sae2 from M arrested *bob1-1* or *bob-1dbf4Δ* cells and monitor the oligomeric state of Sae2 via Size exclusion chromatography. However, as shown in figure 31 we did not observe any

difference in the running behavior of Sae2 pulled down from arrested *bob1-1* or *bob1-1dbf4Δ* cells, suggesting that DDK phosphorylation does not affect the oligomeric state of Sae2.

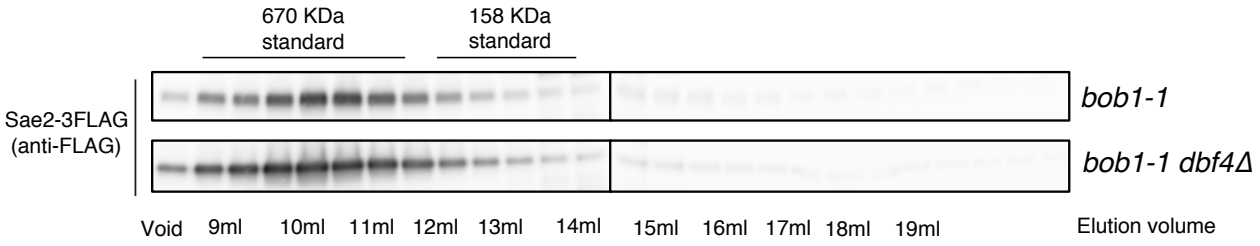

Figure 31-**Analysis of the Sae2 oligomeric state**

bob1-1 or *bob1-1dbf4Δ* cells harboring Sae2-3FLAG were arrested in M-phase with nocodazole, and after FLAG pulldown samples were subjected to a gel filtration on a Superdex200 10/300. Samples from each fraction were loaded on gel. Elution volume and the peaks of molecular weight standards are reported. The similarity in the elution profile of Sae2-3FLAG from *bob1-1* and *bob1-1dbf4Δ* cells suggests that DDK does not affect the oligomeric state of Sae2. The experiment was performed in one biological replicate. Two technical replicates for the size exclusion chromatography run were performed. The elution profile from one of the technical replicates is shown. The standard peaks were defined by running a proteins standard on the same column.

It was shown that phosphorylation can regulate the binding of Sae2 (CtIP/Ctp1) to the MRX/N complex in budding yeast, fission yeast and human [71,73,79,120,128-130,148]. Different interaction surfaces appear to exist which depends on the FHA domain of Nbs1/Xrs2 that mediates binding to phosphorylated Sae2/CtIP/Ctp1. We therefore decided to test if the FHA domain of Xrs2 could bind Sae2 in a phosphospecific manner. We first purified a fragment corresponding to the FHA domain of Xrs2 via sequential affinity purification followed by Size exclusion Chromatography (figure 32).

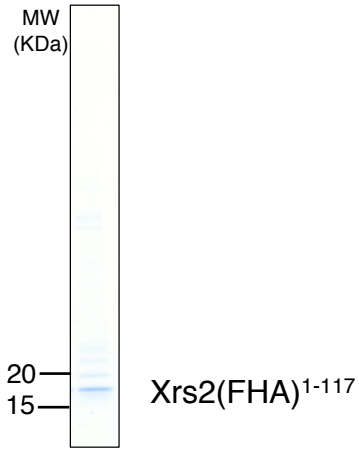

Figure 32-**Xrs2 (FHA)$^{1-117}$ purification**

A construct consisting of residues 1 to 117 spanning the FHA domain of Xrs2 was purified from *E. coli* via affinity chromatography followed by size exclusion chromatography. The Xrs2 construct carried at its N-terminus a Strep-tag. Cells were lysed after overnight induction of the Xrs2 construct, and extracts were subjected to a Strep-pulldown. Recovered Xrs2 (FHA)$^{1-117}$ was then additionally purified via size exclusion chromatography. A representative gel image of the purified construct is shown.

To analyze the binding between the FHA construct and Sae2, we performed *in vitro* pulldown experiments. Our FHA construct carries a Strep-tag at the N-terminus, while Sae2 carries a HIS-tag at its C-terminus. We therefore performed mock/kinase reactions of Sae2 followed by addition of the FHA construct, and subsequently utilized Strep-Tactin beads to pulldown the FHA domain together with binding partners. As shown in figure 33, we observed binding of FHA to Sae2 independently of pre-incubation with DDK or not. We can therefore not exclude that our in vitro kinase reaction might have not been fully proficient, and does not allow to distinguish from phosphorylation dependent and independent binding. Taken together, these experiments did not allow to elucidate specific mechanistic detail, but could serve as a basis for development of additional assays that could monitor specifically the relationship between Sae2-kinase specific phosphorylation and its function.

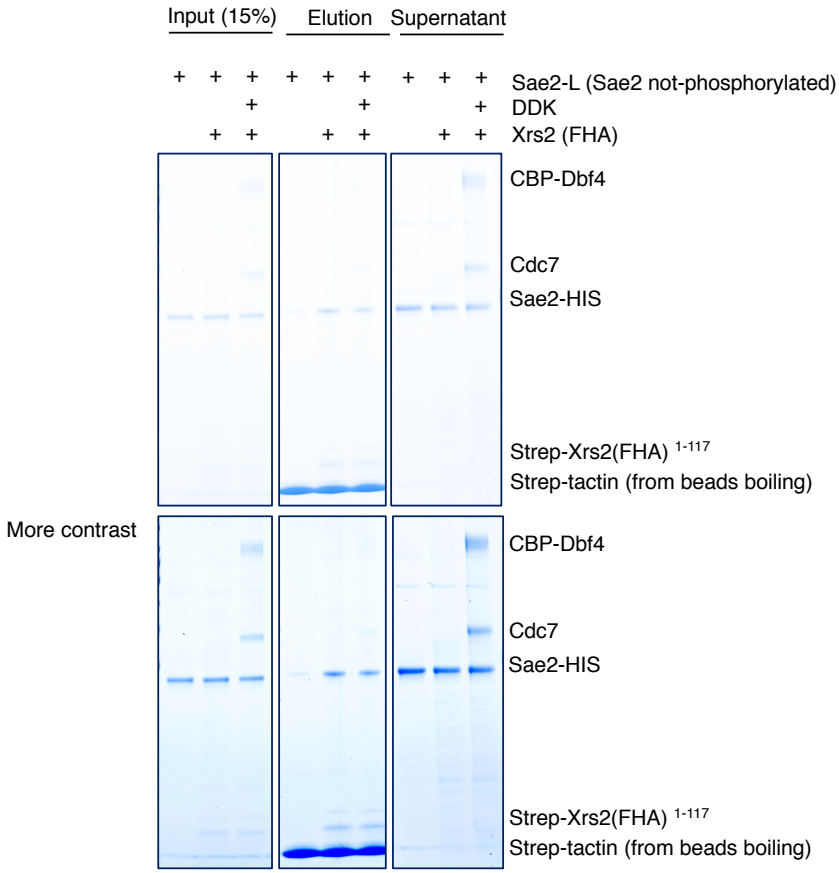

Figure 33- **Sae2-Xrs2(FHA)$^{1-117}$ interact independently of their phosphorylation status**

To investigate the interaction (and its possible phospho-mediated regulation) between Sae2 and the FHA-domain of Xrs2, Sae2 was either mock treated (no pre-incubation with DDK) or pre-incubated with DDK. Addition of Xrs2(FHA)$^{1-117}$ was used to test the Sae2-Xrs2 interaction. Strep-magnetic beads were then added to retrieve Xrs2(FHA)$^{1-117}$ and bound interactors. Samples were run on a gel and stained with Coomassie. A sample lacking Xrs2(FHA)$^{1-117}$ was used as control for unspecific binding of Sae2 to Strep-beads. The experiment was performed once. It nonetheless indicates that Sae2 might be bound by Xrs2 in a phosphorylation-independent manner.

4. DDK activation in G1 cells promotes cell cycle independent DNA end resection and homologous recombination

4.1 Premature activation of DDK leads to Sae2 phosphorylation already in G1 cells

DDK is a two subunit complex [15]. While Cdc7 levels are constant throughout the cell cycle, Dbf4 is degraded during late M and G1 phase, establishing cell cycle regulation of the kinase [16] [17,18]. Since we discovered that DDK phosphorylates Sae2 *in vivo* in a cell cycle specific manner, we reasoned that synthetic expression of DDK in G1 cells might lead to

premature Sae2 phosphorylation. In order to bypass the cell cycle regulation of DDK, we placed Dbf4 and Cdc7 under control of a bidirectional GAL promoter, the same system that we used for the purification of DDK in section 3 (referred to as GAL-DDK). Therefore, we were able to induce expression of both Dbf4 and Cdc7 by addition of galactose in the medium, allowing to induce DDK expression in any cell cycle phase of interest, being particularly interested in the G1 phase. Given that Dbf4 is degraded during the G1 phase of the cell cycle, we used a *DBF4* construct containing 4-point mutations in the D-box that are known to render Dbf4 resistant to cell cycle dependent degradation in G1 [17].

We arrested cells in the G1 phase of the cell cycle with the mating type pheromone alpha factor. After cell cycle arrest, we induced DDK expression via addition of galactose for up to 4 hours. DDK expression was confirmed by performing a western blot against the subunit Dbf4. Wild type cells were used as a negative control. Interestingly, we observed that induction of DDK in G1 cells can lead to phosphorylation of Sae2 already in G1 cells, as judged by the Sae2 phosphoshift observed on gels (figure 34).

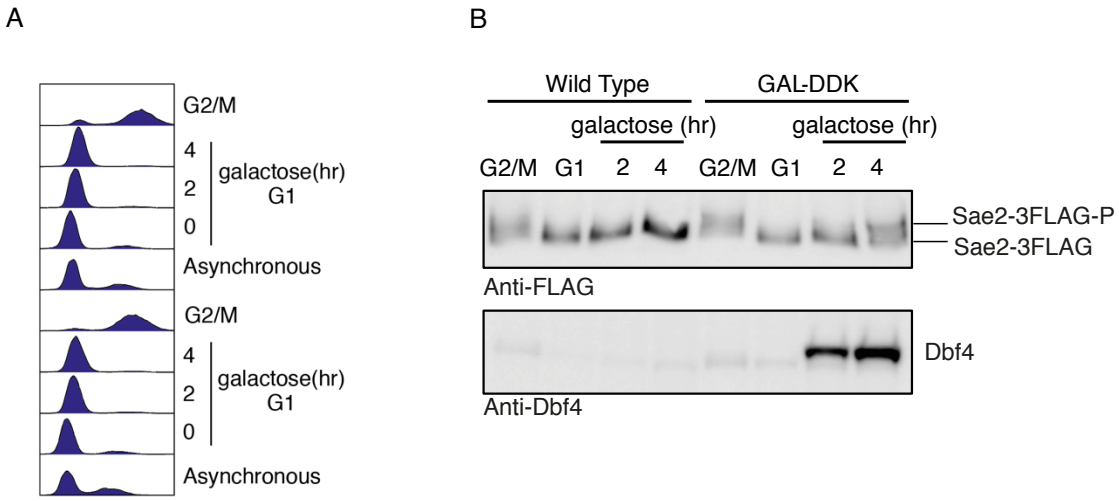

Figure 34-**DDK expression in G1 leads to premature Sae2 phosphorylation**

Sae2-3FLAG cells or Sae2-3FLAG cells harboring an inducible system for galactose-mediated over-expression of DDK were arrested in G1 with alpha factor. Galactose was then added for up to 4 hours to monitor Sae2 phosphorylation status. A) DNA content analysis via FACS (Wild Type; bottom and GAL-DDK; top). B) Western blot to resolve the Sae2 phosphoshift (anti-FLAG, top and to confirm DDK overexpression (anti-Dbf4, bottom)). DDK expression in G1 appears sufficient to induce the Sae2 phosphoshift prematurely during the cell cycle. The experiment was performed in two biological replicates (n=2). Shown are DNA content profiles and western blots from one biological replicate, representative of the two biological replicates.

4.2 Premature activation of DDK in G1 allows cell cycle independent activation of DNA end resection

Some degree of activation of DNA end resection in G1 cells was so far achieved mainly via depletion of the Yku70Yku80 heterodimer [149]. The Yku complex is central for DSB repair via NHEJ [48]. Not only it is involved in the re-ligation process, but it also inhibits HR being an obstacle towards DNA end resection. Given that activation of DDK led to Sae2 phosphorylation in G1 cells, we monitored if premature expression of DDK could also allow for activation of DNA end resection in G1 cells. We performed RPA ChIP-seq experiments at a single DSB induced by the HO endonuclease as quantitative measure of the occurrence of single-stranded DNA and resection. The system that we developed relies on galactose induction for the expression of the HO endonuclease, and as previously described, also for the induction of DDK. Next to it we also tested a CDK phosphomimic mutant of Sae2 (Sae2 S267E), present as endogenous copy of Sae2, either alone or in combination with premature induction of DDK. To perform the experiment, we first arrested cells in the G1 phase of the cell cycle via alpha factor. Upon cell cycle arrest, HO endonuclease (and DDK) expression was induced via addition of galactose, and time points were collected up to 4 hours. We could confirm cell cycle arrest and induction of DDK (in the respective strains) by western blot.

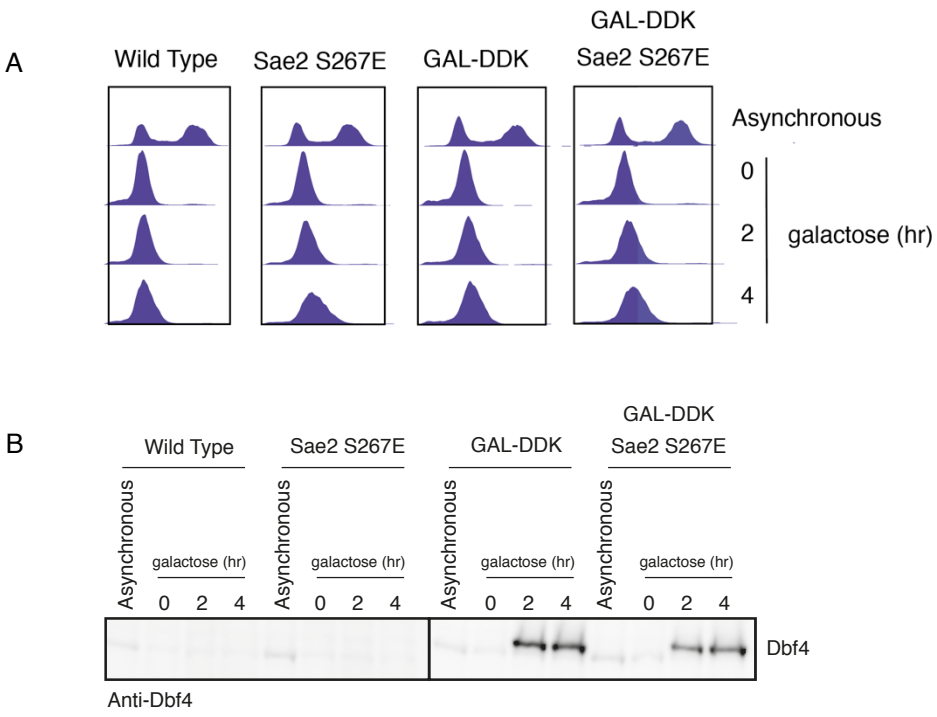

(Figure legend on the following page)

Figure 35-**DNA content measurement and western blot analysis (Figure 36)**

To monitor DNA end resection via RPA-ChIP seq, cells were arrested in the G1-phase using alpha factor, before inducing a DSB via galactose-mediated induction of the HO-endonuclease. Cells carrying the GAL-DDK system also carry an inducible system for galactose-mediated overexpression of DDK. Samples were collected before DSB induction, and 2-and 4- hours after DSB induction (galactose addition). A) the DNA content was measured via FACS to confirm the arrest in the G1 phase via alpha factor. B) The expression of DDK was monitored via western blot (anti-Dbf4 antibody). The experiment was performed in two biological replicates (n=2). Shown are DNA content profiles and western blots from one biological replicate, representative of the two biological replicates.

As shown in figure 36 the CDK phosphomimic mutant of Sae2 (Sae2 S267E) did not lead to a major activation of DNA end resection, as judged by the low enrichment of RPA observed at both sides of the break. Interestingly, G1 cells expressing DDK (GAL-DDK) showed a stronger enrichment of RPA at both sides of the break compared to Wild Type or *sae2 S267E* cells, showing that the premature expression of DDK can lead to activation of DNA end resection in G1 cells. The combination of GAL-DDK and *sae2 S267E* led to an even higher enrichment of RPA compared to GAL-DDK on its own (figure 36). Our resection analysis allowed us to conclude that DDK induction in G1 cells activates DNA end resection and therefore bypass, at least to a certain extent, the cell cycle dependency. As previously mentioned, we confirmed that the CDK phosphomimic mutant of Sae2 on its own have a minor effect in activating resection in G1 cells [11].

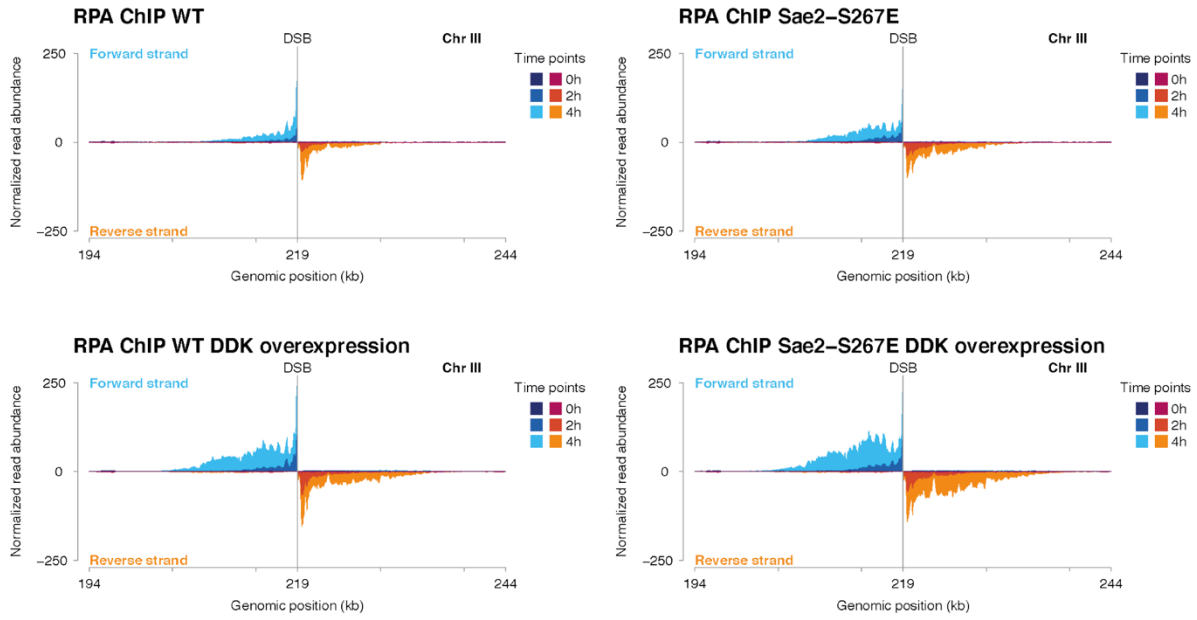

(Figure legend on the following page)

Figure 36-**DDK expression in G1 leads to cell cycle independent activation of DNA end resection**

RPA-ChIP seq experiment to monitor RPA enrichment at a single induced DSB in Wild Type, *sae2 S267E*, GAL-DDK and GAL-DDK *sae2 S67E* cells arrested in the G1-phase. Samples were collected as shown in figure 35. Crosslinked DNA was fragmented (200-500 bp fragments) and subjected to an RPA immunoprecipitation. Strand-specific libraries were prepared and DNA was paired-end sequenced. Normalized read abundance (normalization to the total number of reads) is displayed, showing the strand-specific enrichment of RPA. Cells expressing DDK display a higher number of reads suggestive of an increase in the enrichment of RPA (and hence of DNA end resection), overall showing that DDK expression in G1 allow for cell cycle-independent activation of DNA end resection in G1. The experiment was performed in two biological replicates (n=2). Shown are plots from one biological replicate, representative of the two biological replicates.

4.3 Premature activation of DDK in G1 allows cell cycle independent activation of homologous recombination

Our data showed that premature expression of DDK in G1 is enough to phosphorylate Sae2, and to initiate DNA end resection. It was therefore of interest if also HR could be activated in G1 cells. In order to measure repair via HR, we made use of the same system previously described in figure 9. We arrested cells in the G1 phase, and subsequently induced the DSB via addition of galactose in the medium. Note that addition of galactose will also induce the expression of DDK in the strains harboring the GAL-DDK system. We then collected time points up to 9 hours to monitor repair of the DSB vis qPCR. Interestingly, as presented in figure 37, in cells expressing DDK (GAL-DDK), we observed repair via HR, showing that there is activation and repair via HR in G1 cells, at least to a certain extent. In contrast, the CDK phosphomimic mutant of Sae2 does not show HR mediated repair of the DSB. Also, when DDK premature induction and CDK phosphomimic mutant Sae2 S267E were combined, we observed activation of HR similar to GAL-DDK alone.

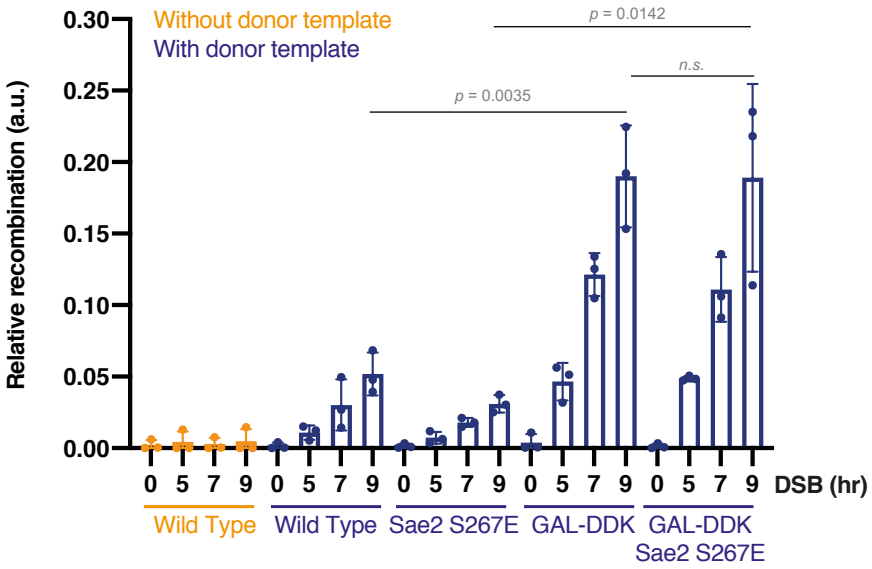

Figure 37-**DDK expression in G1 allow for cell cycle independent activation of HR**

Wild Type, *sae2 S267E*, GAL-DDK and GAL-DDK *sae2 S67E* cells carrying the gene conversion test system with (blue) or without (orange) a donor template were arrested in G1 and DSBs were induced via galactose-mediated induction of the HO endonuclease for 9 hours. After genomic DNA extraction, each sample was subjected to two qPCRs. One using a primer pair giving a product only after homology-mediated repair, and one with a primer pair annealing on a control locus on chromosome XV (to correct for the amount of DNA). Cells expressing DDK in G1 display a four-fold increase in recombination-mediated repair, showing that DDK expression in G1 can activate (to a certain extent) HR in a cell cycle independent manner. Results from three biological replicates (n=3) are shown, each having 3 technical replicates. Bars represent the mean of the three biological replicates (dots represent values for each biological replicate), and error bars denote the standard deviation (SD). The reported *p*-values (for the 9 hours-time points) were calculated performing an unpaired *t*-test using the web-tool "*t*-test calculator" (https://www.graphpad.com/quickcalcs/ttest1.cfm) from GraphPad; *p*-values > 0.05 are reported as not significant (n.s.).

We also carefully checked that the observed differences were not coming from a leaky G1 arrest. As shown in figure 38, the percentage of cells that are in G1 is similar for all strains in each experiment (figure 38 C). Western blots against Dbf4 confirmed DDK induction (figure 38 B).

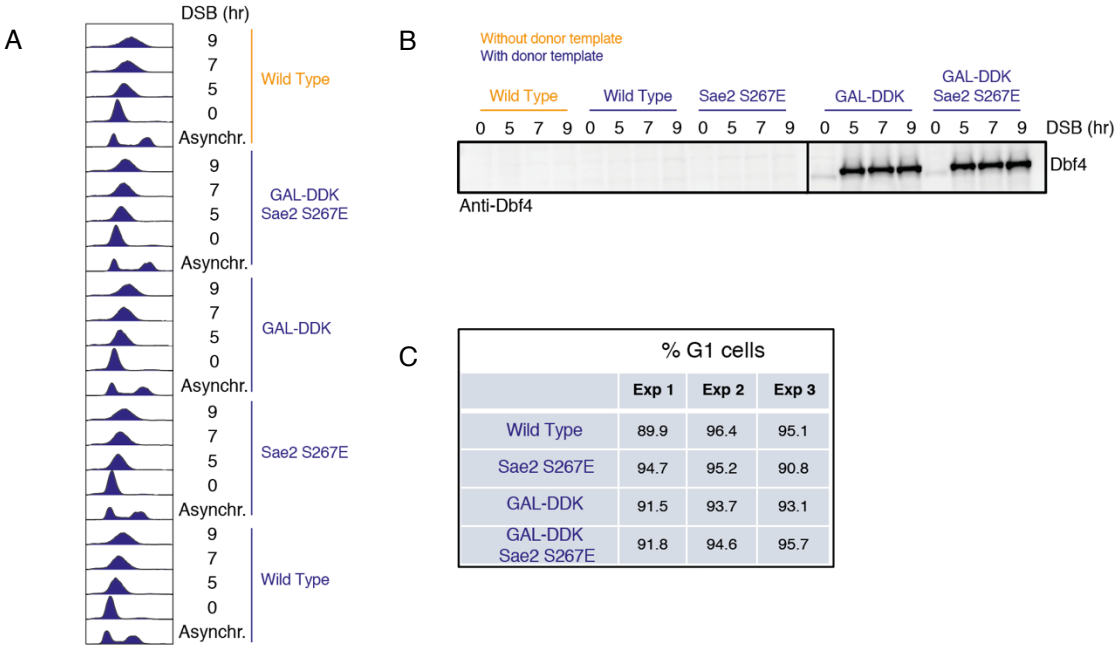

Figure 38-**Technical controls of HR assay (Figure 37)**

A) DNA content analysis via FACS confirms that cells were arrested in G1 (and kept the arrest throughout the experiment); shown are the profiles from one of the biological replicates, representative of the three replicates B) Western blot to confirm the overexpression of DDK (western blots from one of the biological replicates, representative of the three replicates) C) The 0-hour time point for each strain was used to measure the number of cells in G1 for each replicate. The percentage was calculated via the FlowJo software, calculating the percentage of cells in the G1 peak.

Our resection and HR assay showed that expression of DDK in G1 cells can activate DNA end resection, and consistently HR. Next, we tested if depletion of the Yku complex would further enhance HR in G1 [149]. We therefore combined induction of DDK with depletion of the Yku complex (via deletion of *YKU80*). Interestingly we observed that both GAL-DDK and *yku80Δ* cells showed similar rates of HR in G1 cells and also the double-mutant (figure 39).

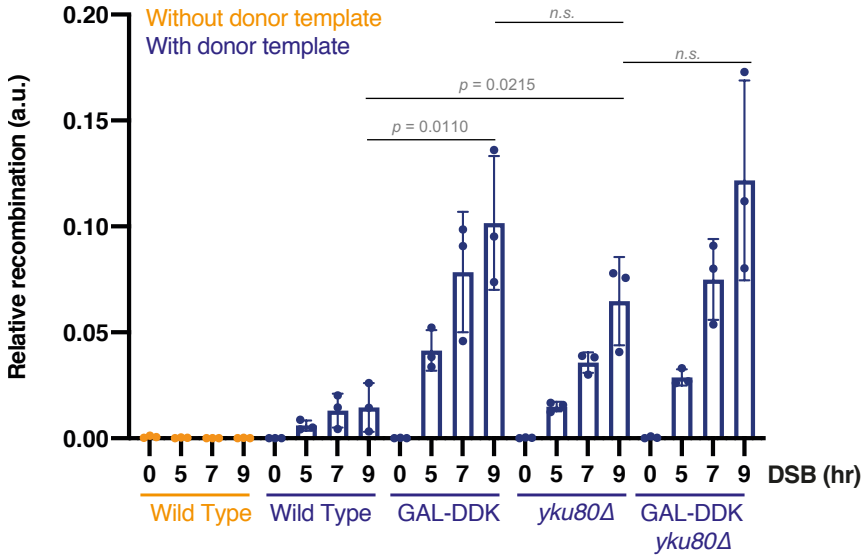

Figure 39-**DDK expression in G1 allows for cell cycle independent activation of HR similar to *yku80* mutants**

Wild Type, *yku80Δ*, GAL-DDK and GAL-DDK *yku80Δ* cells carrying the gene conversion test system with a donor template were arrested in G1 and break induction with HO was performed for 9 hours. After genomic DNA extraction, each sample was subjected to two qPCRs. One using a primer pair giving a product only after homology-mediated repair, and one with a primer pair annealing on a control locus on chromosome XV (to correct for the amount of DNA). Cells expressing DDK can activate HR in G1 cells (also shown in figure 37), similar to cells depleted of Yku80. Results from three biological replicates (n=3) are shown, with 3 technical replicates each. Bars represent the mean of the three biological replicates (dots represent values of each biological replicate), and error bars denote the standard deviation (SD). The reported *p*-values (for the 9 hours-time points) were calculated performing an unpaired *t*-test using the web-tool "*t*-test calculator" (https://www.graphpad.com/quickcalcs/ttest1.cfm) from GraphPad; *p*-values > 0.05 are reported as not significant (n.s.).

We again confirmed that the number of cells arrested in G1 from each population was similar (figure 40 C). Western blots against Dbf4 confirmed DDK induction (figure 40 B).

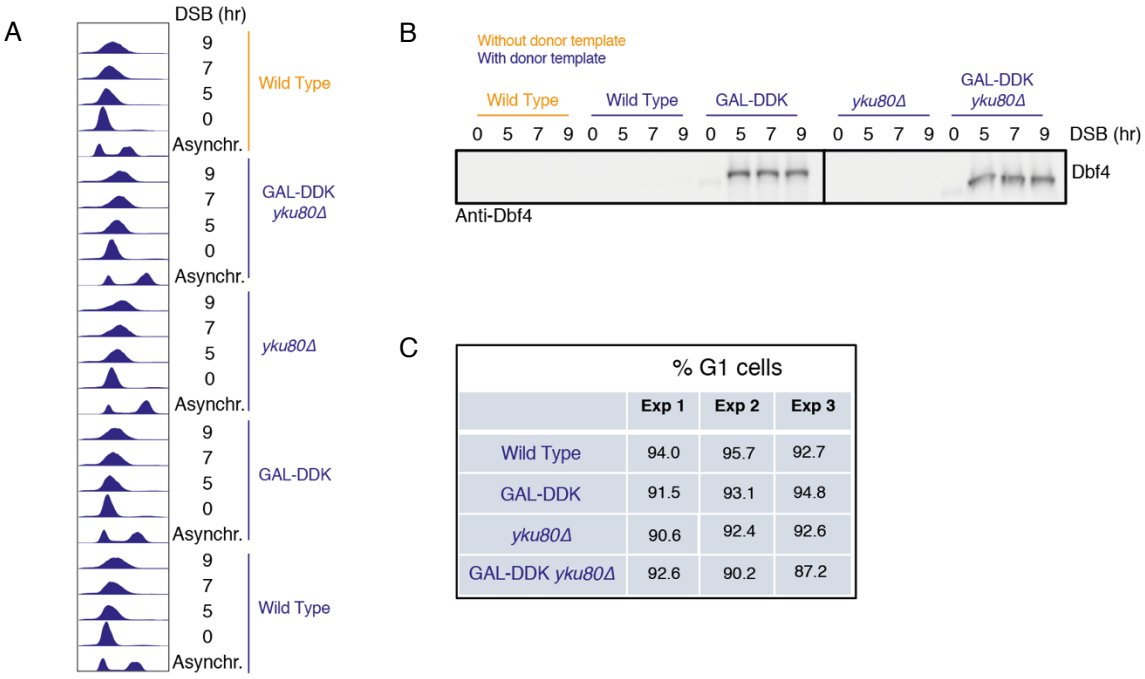

C

	% G1 cells		
	Exp 1	**Exp 2**	**Exp 3**
Wild Type	94.0	95.7	92.7
GAL-DDK	91.5	93.1	94.8
yku80Δ	90.6	92.4	92.6
GAL-DDK *yku80Δ*	92.6	90.2	87.2

Figure 40-**Technical controls of HR assay (Figure 39)**

A) DNA content analysis via FACS confirms that cells were arrested in G1 (and kept the arrest throughout the experiment); shown are the profiles from one of the biological replicates, representative of the three replicates B) Western blot to confirm the overexpression of DDK (western blots from one of the biological replicates, representative of the three replicates) C) The 0-hour time point for each strain was used to measure for each replicate the number of cells in G1. The percentage was calculated via the FlowJo software, calculating the percentage of cells in the G1 peak.

We therefore conclude that DDK expression in G1 cells activates initiation of DNA end resection similar to the absence of the resection inhibitor Yku80, but that additional regulatory pathways exist which restrict HR in G1 cells.

5. The DDK-Cdc5 kinase complex

Physical interaction between DDK and Cdc5 was observed in both meiosis and mitosis, and it was shown that the Polo Box Domain (PBD) of Cdc5 is important for the interaction with DDK via a short stretch of amino acids (83-88) within the N terminus of Dbf4 [44,45].

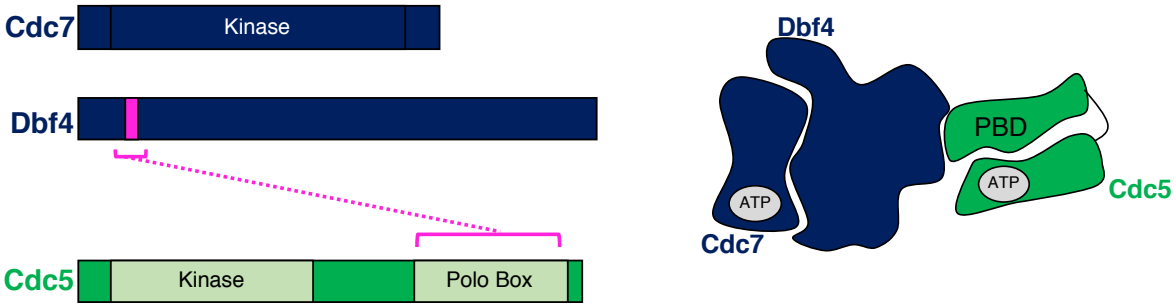

Figure 41-**The DDK-Cdc5 kinase complex**

Schematics of the interaction between DDK and Cdc5. On the left, in pink are highlighted the regions known to be required for the interaction. In particular, the polo-box domain (PBD) of Cdc5 and a short peptide of Dbf4 (amino acids 83-88). On the right a fictional representation of the two kinases, highlighting the requirement for the interaction (Dbf4 (within the DDK complex) and the polo-box domain (PBD) of Cdc5).

In meiosis the interaction was shown to be important for the regulation of chromosome segregation, while in mitosis it was suggested that DDK could overall inhibit Cdc5 by titrating the polo kinase away from its substrates [24,25,44,45]. However, a more recent paper discovered that also in mitosis the DDK-Cdc5 complex was an active kinase and phosphorylated the endonuclease Mus81-Mms4 [13]. We therefore decided to investigate if the DDK-Cdc5 kinase complex might be a more general mechanism used by cells to regulate also other DDK and Cdc5 mediated phosphorylation events.

5.1 The DDK-Cdc5 kinase complex is a general mitotic regulator

Replication factor Sld2 degradation in mitosis, is dependent on prior phosphorylation of a phosphodegron motif. Among the kinases phosphorylating Sld2 within the phosphodegron are both DDK and Cdc5 (figure 42) [8].

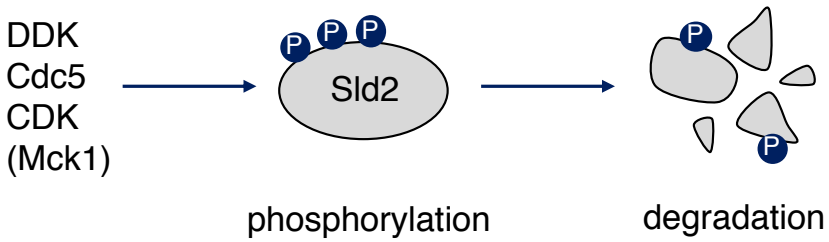

Figure 42-**Scheme of the Sld2 phosphorylation dependent degradation**

Sld2 is phosphorylated by different kinases (DDK, Cdc5, CDK and Mck1). Phosphorylation of Sld2 is required for degradation by the ubiquitin-proteasome system in M-phase.

Sld2 was therefore an interesting candidate for being a possible substrate of the kinase complex. We reasoned that if this was the case, a mutant of Dbf4 which cannot interact with Cdc5 should abolish Sld2 degradation. We performed cycloheximide (CHX) experiments to monitor Sld2 stability in M arrested Wild Type cells and compared it to a strain harbouring the *dbf4ΔN109* allele, which induces a defect in the interaction between DDK and Cdc5 [44,45]. Wild Type cells showed fast degradation of Sld2, but cells harbouring an active but Cdc5-interaction deficient DDK displayed stable Sld2 (figure 43). A strain harbouring an N-terminal truncation of Dbf4 (*dbf4ΔN66),* but still containing the Cdc5 interaction region was used as a control.

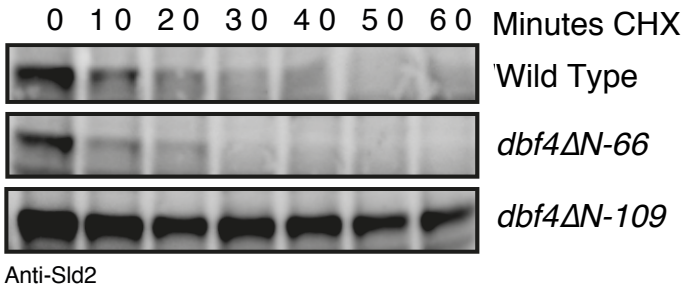

Figure 43-**Sld2 is a substrate of the DDK-Cdc5 kinase complex**

Wild Type, *dbf4ΔN-66* and *dbf4ΔN-109* cells were arrested in the M-phase with nocodazole, and then treated for 1 hour with cycloheximide (CHX). Samples were then run on a 4-12% Bis-Tris acrylamide gel to monitor the levels of Sld2 by western blot using an anti-Sld2 antibody. The experiment was performed in three biological replicates (n=3). Shown are western blots from one experiment, representative of the three replicates. The *dbf4ΔN-109* mutation, which abolishes the interaction of DDK and Cdc5 (but not *dbf4ΔN-66,* which does not abolish the interaction) leads to a marked stabilization of Sld2, indicating the DDK-Cdc5 complex targets Sld2 for degradation.

Given that phosphorylation is essential to induce degradation, we can conclude that also Sld2 is phosphorylated via DDK and Cdc5 in an interdependent manner, that involves the DDK-Cdc5 kinase complex, suggesting that the two-kinase complex has a more widespread role than previously anticipated.

5.2 Analysis of the DDK-Cdc5 kinase complex

In order to get mechanistic and structural insights into the kinase complex, we developed systems to purify the complex, as well as the single kinases. DDK was purified as previously described, via overexpression of both Dbf4 with and N-terminal CBP-tag and Cdc7 in yeast cells, followed by a CBP pulldown (and ATP wash for removal of an otherwise copurifying chaperone). Cdc5 with a 3FLAG tag at its C terminus was also purified via overexpression in yeast cells followed by FLAG pulldown. The constructs for the overexpression of both DDK and Cdc5 are integrated in the genome. To copurify the kinase complex we therefore integrated both the "DDK plasmid" and "Cdc5 plasmid" into the genome of the same yeast strain. After overexpression, a CBP pulldown followed by a FLAG pulldown was performed. In figure 44 A representative gel images of the purified proteins are shown. To confirm that the double pulldown for co-purification of the complex allowed us to copurify a stable complex, we performed a size exclusion chromatography and observed co-elution of all the subunits of the complex (figure 44 B).

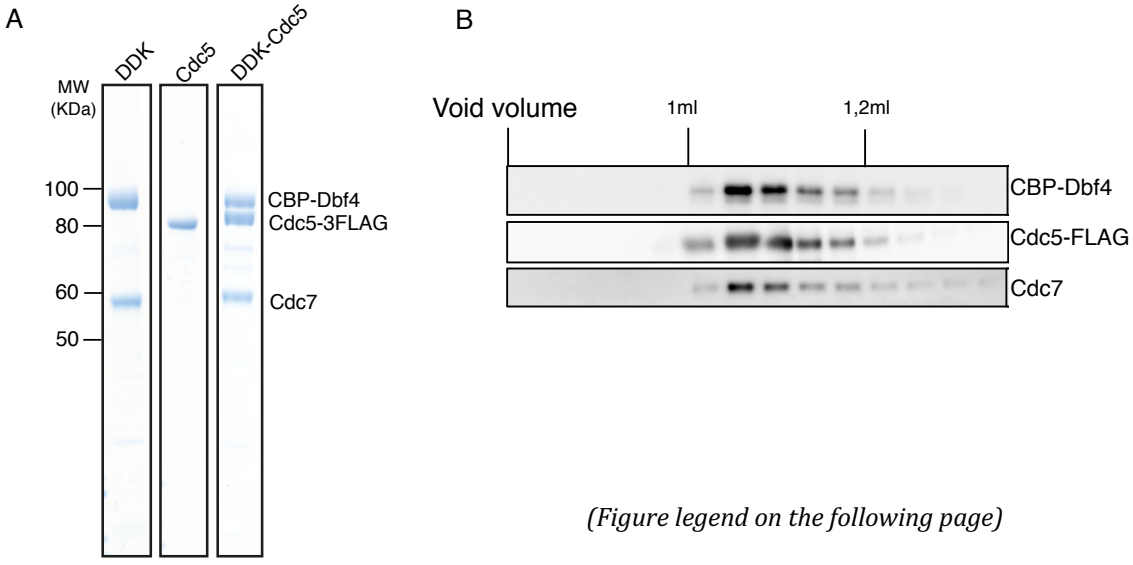

(Figure legend on the following page)

Figure 44-**Single kinases and kinase complex purification**

A) DDK, Cdc5 and the DDK-Cdc5 kinase complex were purified via affinity chromatography from yeast cells. Cells carrying constructs for galactose-mediated overexpression of DDK, Cdc5 or both were used to induce overexpression of the protein of interest. DDK carries a CBP tag at the N-terminus of Dbf4, while Cdc5 carries a 3FLAG tag at its C-terminus. DDK was purified performing a CBP pulldown, while Cdc5 was purified performing a FLAG pulldown. For the complex, extracts of cells overexpressing both DDK and Cdc5 were used; the complex was purified via a CBP pulldown followed by a FLAG pulldown. Representative images of the purified proteins are shown. B) The DDK-Cdc5 kinase complex was subjected to size exclusion chromatography on a Superdex200 10/300 column. Western blots to monitor the presence of each component of the complex in the different fractions were performed using Anti-Dbf4 (top), Anti-Cdc5 (middle) or Anti-Cdc7 (bottom) antibodies. The co-elution of the subunits of the complex shows that the co-purified complex is stable over a size-exclusion chromatography run.

With our co-purified kinase complex we also decided to test if we could fit the currently limited structural information available to our purified complex. We applied crosslinking mass spectrometry (XL-MS) to obtain information on the 3D conformation of the complex. For XL-MS, the protein of interest is treated with a suitable crosslinker, inducing crosslinking of lysines in close proximity (generally within 10 to 30 Angstrom (Å), depending on the length of the crosslinker spacer, and considering the approximately 6 Å of the lysine side-chain [150,151]). After digestion, LC-MS allow for identification of the crosslinked peptides. For our experiments we used the PhoX crosslinker. PhoX is a recently developed crosslinker which contains phosphonic acid, allowing for an enrichment step of crosslinked peptides that is highly similar to phosphopeptide enrichment used in phosphoproteomics [152]. For our purpose 100 µg of DDK-Cdc5 kinase were crosslinked with 100x molar excess of PhoX for 45 minutes, and subsequently quenched with 100 mM Tris-HCl, pH 7.5 to avoid over-crosslinking of the sample. Additionally, to render the phospho-based enrichment step more specific for the PhoX crosslinked peptides, samples were supplemented with 2 mM MnCl2 and treated with λ phosphatase. We identified a total of 232 crosslinks (inter + intra crosslinks). A highlight of the inter-links is shown in figure 45.

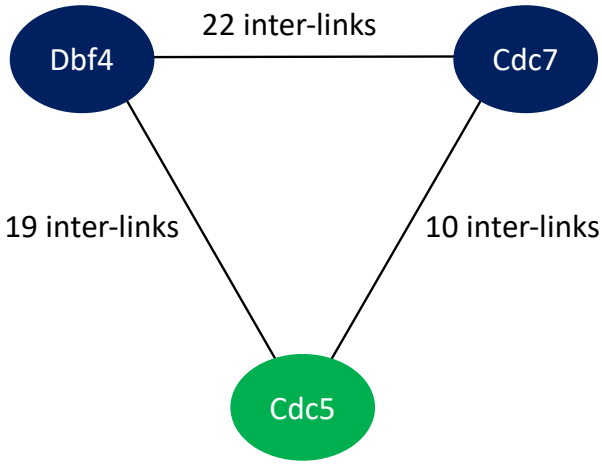

Figure 45- **XL-MS of the DDK-Cdc5 kinase complex shows interlinks between all three proteins**

Scheme showing the number of inter-links detected between each subunit of the kinase complex in the crosslinking-MS experiment of the DDK-Cdc5 kinase complex.

A crystal structure showed binding of the PBD of Cdc5 to a short peptide of Dbf4 spanning the Cdc5-interacting region [153]. In order to control if the inter-crosslinks detected could fit with the few structural information that we have about the kinase complex, we analyzed our crosslinked peptides using the recently published structure as a reference. We observed that 3 lysines within the PBD (K502, K507 and K509) are facing the Dbf4 binding region and were crosslinked with lysines at the N terminus of Dbf4 (where the Cdc5 interaction region resides), allowing us to fit to our analysis of the full length complex the information that we have available about the interaction between the PBD of Cdc5 and the Dbf4 peptide (figure 46). Moreover, our data suggest that also the N-terminal region of Cdc5 and not only the PBD is making contacts with the N terminus of Dbf4. We also found inter-links measured between Cdc7 and Cdc5. This indicates that the two active sites could be close to each other in the complex. This raises the question on a possible interplay between both active sites.

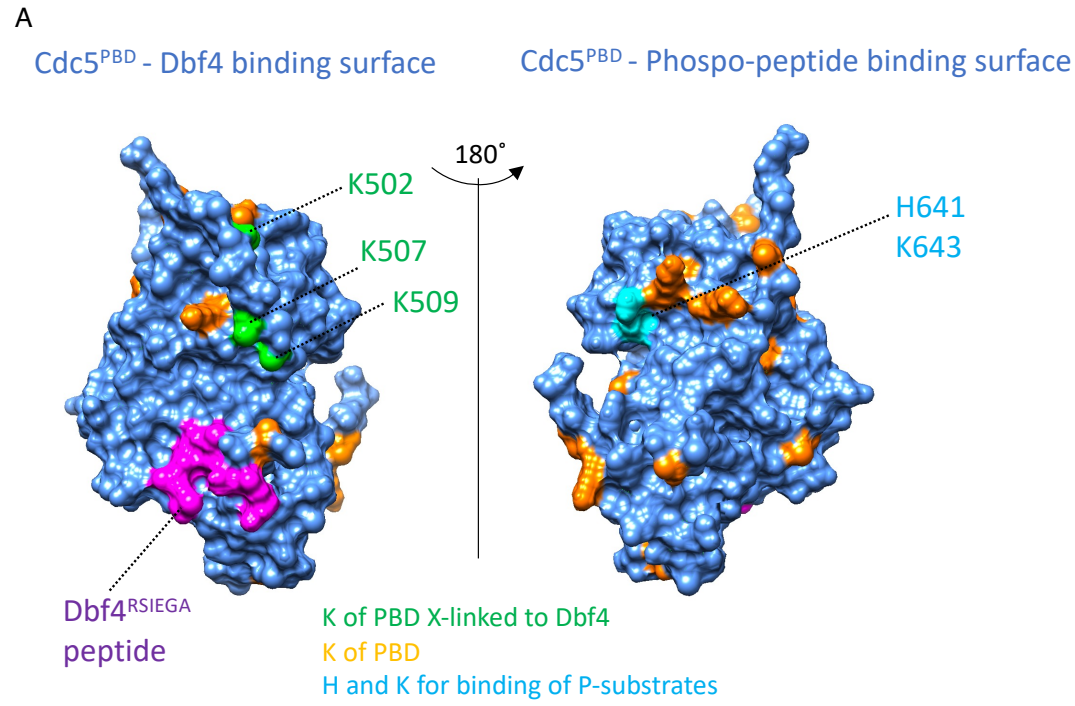

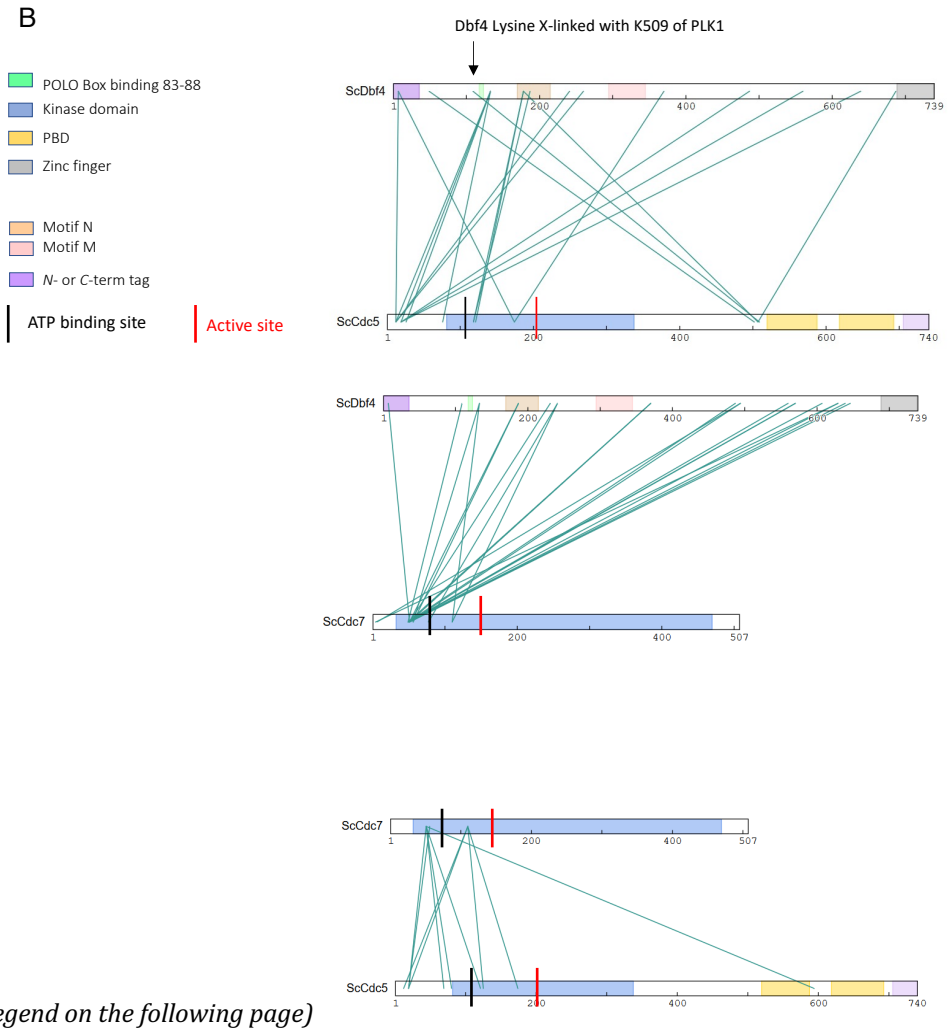

(Figure legend on the following page)

Figure 46-**XL-MS of the DDK-Cdc5 kinase complex**

A) Using the software Chimera, based on the structure from Alwami et al., 2020 (PDB: 6MF6) [153], in green the lysines of the polo-box domain (PBD) of Cdc5 that were found to be crosslinked with Dbf4, in Purple the Dbf4 peptide. The Dbf4 binding surface and the phosphobinding surface of the PBD are shown. B) Graph showing the positions of the inter-links (depicted as green lines) between lysines in the different subunits of the kinase complex. The ATP binding site is shown in black; the active site is depicted in red. The crosslinking-MS experiment was performed once.

Having the single kinases and the DDK-Cdc5 kinase complex available as purified proteins, we also purified a known substrate, the Mus81-Mms4 complex. The latter was purified via overexpression in yeast cells of the two subunits, followed by a FLAG pulldown and Size Exclusion Chromatography (figure 47). We performed *in vitro* kinase assays to test the kinase activity of the single subunits compared to the complex. It would indeed be reasonable to think that one model how the complex might work is by modulating the kinase activity of the kinases once they get together. As shown in figure 47 B, we observed similar activity in the phosphorylation of Mus81-Mms4 by Cdc5 or the DDK-Cdc5 kinase complex as we observed similar incorporation of radioactive ATP in Mus81-Mms4. We therefore reason that DDK may act as scaffold for the phosphorylation,

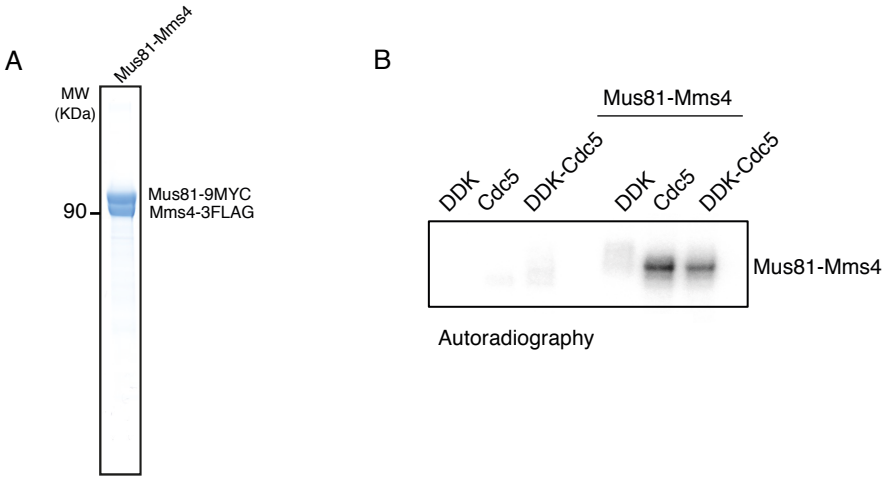

(Figure legend on the following page)

Figure 47-**Mus81-Mms4 purification and use as substrate in a kinase assay**

Yeast Mus81-Mms4 was purified via affinity chromatography from yeast cells carrying a system for galactose-mediated overexpression of Mus81 (Myc-tagged) and Mms4 (FLAG-tagged). After overexpression, cells were lysed and extracts subjected to a FLAG-pulldown. After elution Mus81-Mms4 was additionally purified via size exclusion chromatography. A) A representative image of the purified complex is shown. B) Radioactive kinase assays using Mus81-Mms4 as a substrate of either DDK, Cdc5 or the DDK-Cdc5 kinase complex were performed. For kinases (single kinases and the kinase-complex) as well as the Mus81-Mms4 substrate, proteins from two different preparations were tested (n=2). The DDK-Cdc5 kinase complex appears to be active similarly to Cdc5 on its own. Shown is an image from one of the replicates, representative of the different replicates.

Additionally, we performed experiments using the novel substrate of the complex that we identified, Sld2. In particular we used a N-terminal construct (GST-Sld2$^{(1-150)}$) that was previously successfully used for *in vitro* phosphorylation reactions [8]. Note that the DDK mediated phosphorylation of Sld2 was also shown to require a priming step mediated by CDK, and we therefore included an additional "CDK-priming" step in our reactions. Again, with the Cdc5-DDK complex we did not observe enhanced phosphorylation compared to the single kinases (figure 48).

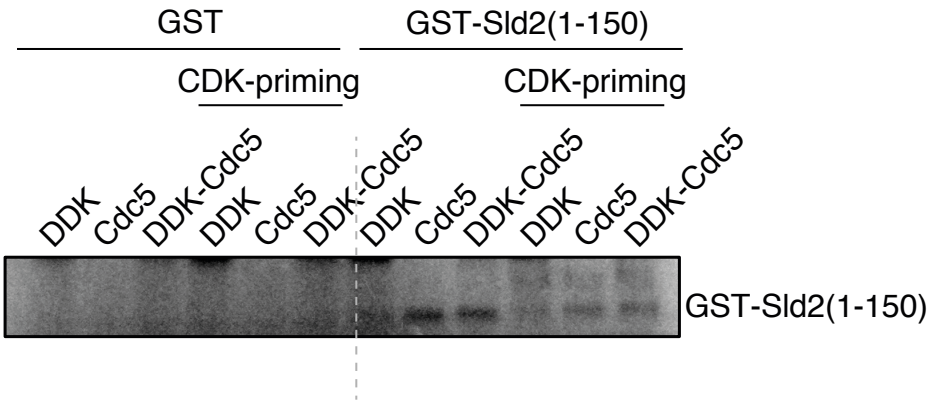

Figure 48-**Kinase assay with GST-Sld2$^{(1-150)}$ as substrate**

Radioactive kinase assay using GST-Sld2$^{(1-150)}$ as a substrate and either DDK, Cdc5 or the DDK-Cdc5 kinase complex as kinase. Reactions also included a negative control with GST, and reactions with a CDK priming step. Overall, the incorporation of radioactive ATP in reactions containing the DDK-Cdc5 complex did not appear different from the other reactions. This experiment was performed once.

Our kinase assays overall suggests that the kinase complex per se does not change the kinase activity of the single kinases.

Another possible model for how the kinase complex might work is via one of the two kinases being important to target the second kinase to certain substrates. If this was the case, the activity of the docking kinase per se might not be important. Also, such a mechanism might be difficult to observe in the simplified kinase reactions performed *in vitro.* We therefore performed *in vivo* experiments and reasoned that if a "docking mechanism" would be the function of the kinase complex, we should observe a positive effect towards the substrate phosphorylation independently of the kinase activity of the docking kinase. We again made use of Sld2 degradation as a readout of proper phosphorylation and performed experiments where we arrested cells in M, but before addition of CHX we overexpressed the single kinases either in their Wild Type version or as kinase-dead mutants; the overexpressed protein would then be over-represented and be the main source of DDK or Cdc5 in cells. Interestingly, we noticed that cells overexpressing DDK as Wild Type or kinase-dead mutant displayed a quicker degradation of Sld2. Conversely, only Cdc5 in its Wild Type version behaved similarly, while the kinase dead-mutant showed an overall increase in the amount of Sld2, suggesting a defect in the phosphorylation of Sld2 (and therefore a defect in its degradation) (figure 49 A). This was also mimicked when looking at the kinetics of degradation, with overexpression of DDK in either form and overexpression of Cdc5 as Wild Type which led to quicker degradation kinetics compared to the Wild Type or to cells overexpressing Cdc5 in its kinase dead version (figure 49 B).

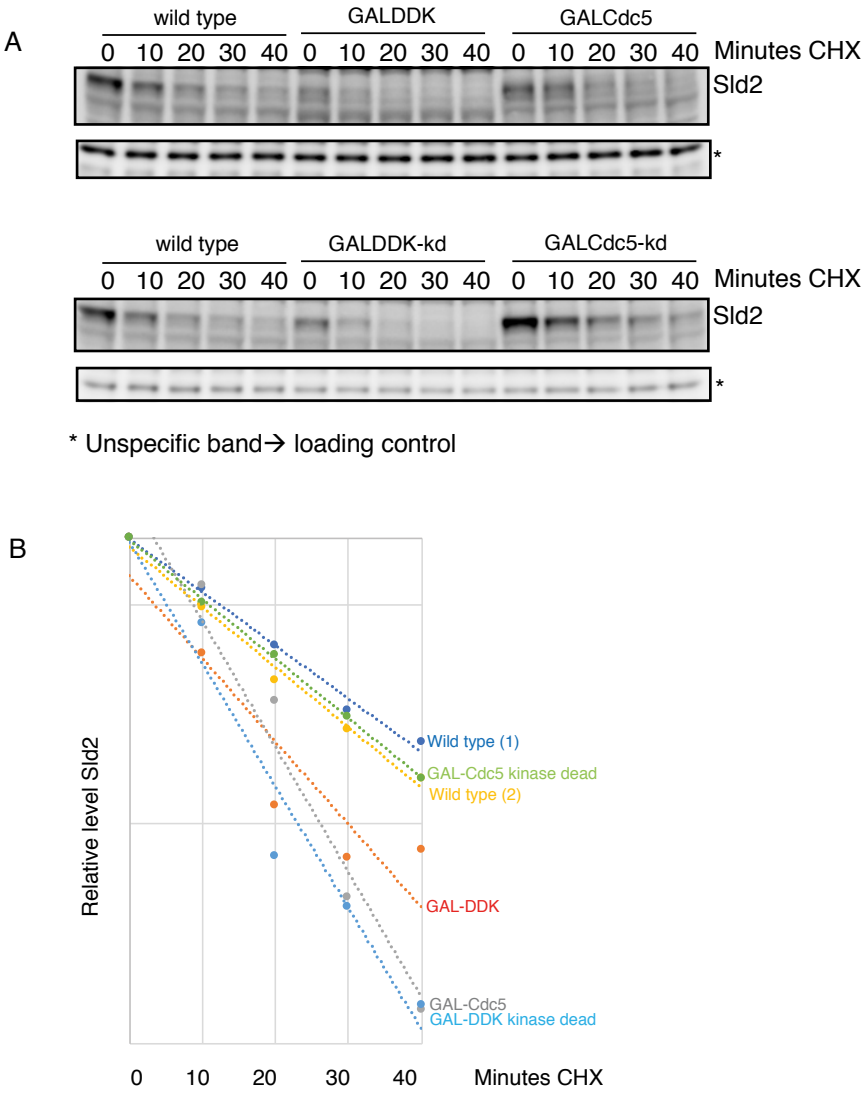

Figure 49-**DDK can function in the kinase complex independently of its kinase activity**

Phosphorylation dependent degradation of Sld2 was tested by arresting cells in M-phase with nocodazole prior to overexpression of the kinase of interest (in the Wild Type or kinase dead form). Cycloheximide (CHX) shut-off experiments were conducted by addition of CHX and measurement of protein degradation for 40 minutes. A) Samples were loaded on a gel to monitor the levels of Sld2 via western blot using an anti-Sld2 antibody. Overexpression of DDK as Wild Type or kinase dead or of Cdc5 as Wild Type (but not kinase dead) have a similar effect on Sld2 degradation, suggesting that DDK can function in the complex independently of its kinase activity. The experiment was performed in two biological replicates (n=2). Shown are western blots from one replicate, representative of the two replicates. B) Quantification of the Sld2 levels from the gel shown in A to monitor degradation kinetics. The levels of Sld2 were quantified from the western blot using ImageJ (the unspecific band shown in the figure was quantified and used to normalize in order to account for possible differences coming from sample loading). Normalized values are plotted on semi-log scale. The quantification to monitor degradation kinetics was performed only for one of the biological replicates.

Our *in vivo* experiments therefore suggests that DDK overexpression has a positive effect towards the phosphorylation of Sld2 and hence its degradation independently of its kinase activity, and could therefore suggest a model where DDK is rather important as a scaffold rather than for its catalytic activity, while Cdc5 is actually required with its kinase activity. Cdc5 was indeed shown to be the key kinase in setting the timing of degradation of Sld2 [8] Interestingly, a similar mechanism was recently suggested with Exo1 acting as scaffold for recruitment of Cdc5 in the regulation of meiotic crossover formation [154]. What is of particular interest is that the sequence in Exo1 found to interact with Cdc5 share high similarity with the Dbf4 sequence known to interact with Cdc5 [44,154].

Cdc5/PLK1 is believed to undergoes conformational changes from an autoinhibited closed conformation with the PBD blocking the Kinase Domain to an active conformation upon phospho-dependent binding of its substrates via the PBD, which would lead to an opening of the structure [155]. In the recently published crystal structure of the PBD of Cdc5 bound to a short peptide of Dbf4 spanning the Cdc5-interaction region of Dbf4 [153], the authors suggested that the interaction of DDK and Cdc5 could be important to modulated Cdc5 kinase activity due to a conformational change that would make the kinase domain of Cdc5 more exposed. Our *in vitro* analysis however revealed that the kinase complex overall does not lead to changes in the kinase activity of the single kinases, suggesting that Cdc5 might not go through structural changes after binding to DDK. To test for a conformational change in Cdc5 we used crosslinking Mass Spectrometry and compared the intra-protein crosslinks of Cdc5 when part of the kinase complex (measured when performing crosslinking Mass Spec of the complex) and Cdc5 when alone. For Cdc5 alone we crosslinked the sample as previously explained for the kinase complex, with only difference that we used 60 µg of Cdc5 and a 75x molar excess of PhoX. It is important to notice that unstructured and flexible regions will give generally rise to a higher number of intra cross-links. We overall observe a series of intra-links also between the PBD and Kinase domain of Cdc5, known to be structured, therefore overall suggesting that the N and C terminus make contacts with each other, as previously shown, but also showing that Cdc5 when part of the complex seems to have a similar conformation to that of Cdc5 on its own (figure 50). This overall fits to our data suggesting that the complex does not have a different activity compared to the single subunits, given that the previously

proposed idea of a conformational change was based on the idea that this would lead to a change in the activity.

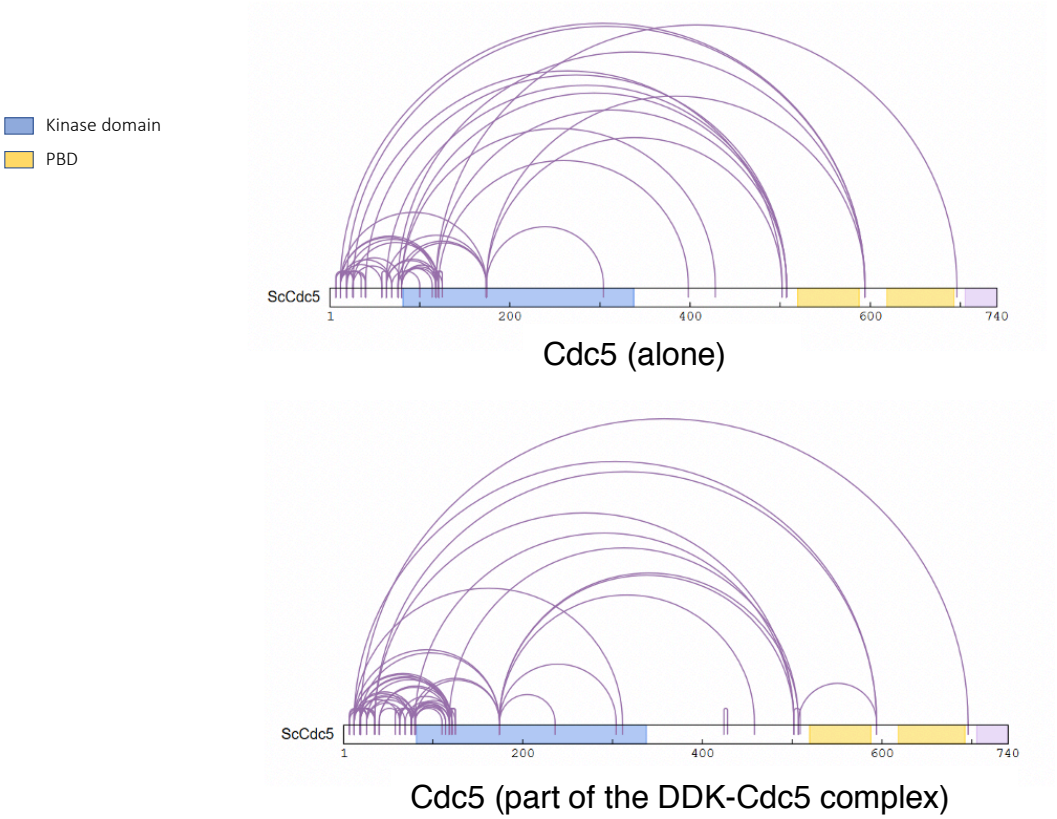

Figure 50-**XL-MS analysis of Cdc5**

Intra-links within Cdc5 measured on PhoX crosslinked Cdc5 (alone) or on Cdc5 when part of the DDK-Cdc5 kinase complex. The similar pattern of the intra-links between Cdc5 on its own and Cdc5 as part of the complex, suggests that Cdc5 might keep a similar 3D conformation when part of the kinase complex. This experiment was performed once.

5.3 Conservation of the DDK-Cdc5/PLK1 kinase complex

DDK and Cdc5 are key cell cycle kinases, highly conserved from yeast to humans. We therefore evaluated if the psychical interaction between DDK and Cdc5 is conserved as well. In humans there are different PLKs, but the ortholog of Cdc5, the only polo-like kinase in yeast, is PLK1.

We tested for a physical interaction via co-immunoprecipitations (co-IP) of endogenous proteins. We therefore collected extracts from U2OS cells arrested in M with Nocodazole, lysed cells and split the lysate to perform co-IP using IgG (as a negative control) or a DBF4 antibody. Interestingly we could detect a specific immunoprecipitation of PLK1 with DBF4, therefore showing that DDK and PLK1 can physically interact also in human cells (figure 51).

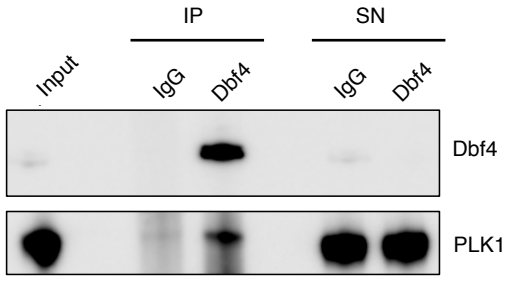

Figure 51-**DDK and PLK1 interact in U2OS cells**

U2OS cells were arrested in nocodazole, and after lysis cells extracts were split to perform an immunoprecipitation with either anti IgG (as negative control) or anti DBF4 antibodies. Samples of the immunoprecipitated proteins were the loaded on 4-12% Bis-Tris acrylamide gels to monitor the presence of DBF4 and PLK1 via western blot. PLK1 immunoprecipitates with DBF4 (but not with the IgG negative control) providing evidence for the physical interaction of DDK and PLK1. The experiment was performed once.

Having observed the interaction between DDK and PLK1, we decided to develop a system that would allow us to map the interaction using overexpression of construct of interest in HEK293T cells. In particular, we based our analysis on the use of plasmids that allow to constitutively overexpress the constructs of interest via CMV promoter upon transient transfection. In a first experiment we tested our system to confirm the previously observed interaction. We used HEK293T cells co-transfected with plasmids for overexpression of PLK1 with a N-terminal GFP tag, DBF4 and CDC7 (a GFP only construct was also used as a control of unspecific binding to the GFP itself). 48 hours after transfection, cells were harvested and an IP using GFP beads was performed. As shown in figure 52 we observed binding of DDK (both DBF4 and CDC7) to GFP-PLK1, while the GFP negative control showed no interaction.

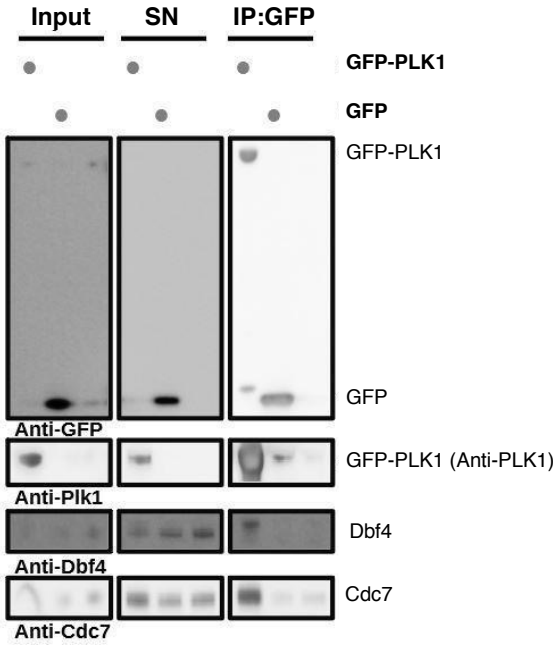

Figure 52- **DDK and PLK1 interact after overexpression in HEK293T cells**

HEK293T cells were transfected with constructs carrying under control of a CMV promoter DBF4, CDC7 and GFP-PLK1, for overexpression of the respective proteins. As control, cells were also transfected with constructs for overexpression of DBF4, CDC7 and the GFP-tag only or with constructs for overexpression only of DBF4 and CDC7. After transfection cells were lysed and a GFP pulldown was performed. Samples eluted from the GFP pulldown were loaded on gel, showing that both DBF4 and CDC7 (DDK) are immunoprecipitated by GFP-PLK1 (but not by GFP on its own). The experiment was performed in two biological replicates (n=2); shown are western blot images from one of the replicates, representative of the two replicates.

In yeast the PBD of Cdc5 is required for the interaction with Dbf4 [44,45]. We tested if this was the case also for PLK1. We used a construct of PLK1 lacking the PBD, and also a construct consisting just of the PLK1-PBD, both with a GFP-tag. GFP IP showed us that PLK1 lacking the PBD is not able to interact with DDK, and interestingly, that the PBD of PLK1 on its own is able to bind DDK (figure 53 A). We can therefore conclude that similar to yest, also in humans the interaction requires the PBD of PLK1. We also identified which part of DDK is important for the interaction. By performing GFP immunoprecipitations experiments similarly to the previously presented experiments, we observed that lack of the C-terminus of DBF4 led to loss of interaction with PLK1 (figure 53 B)

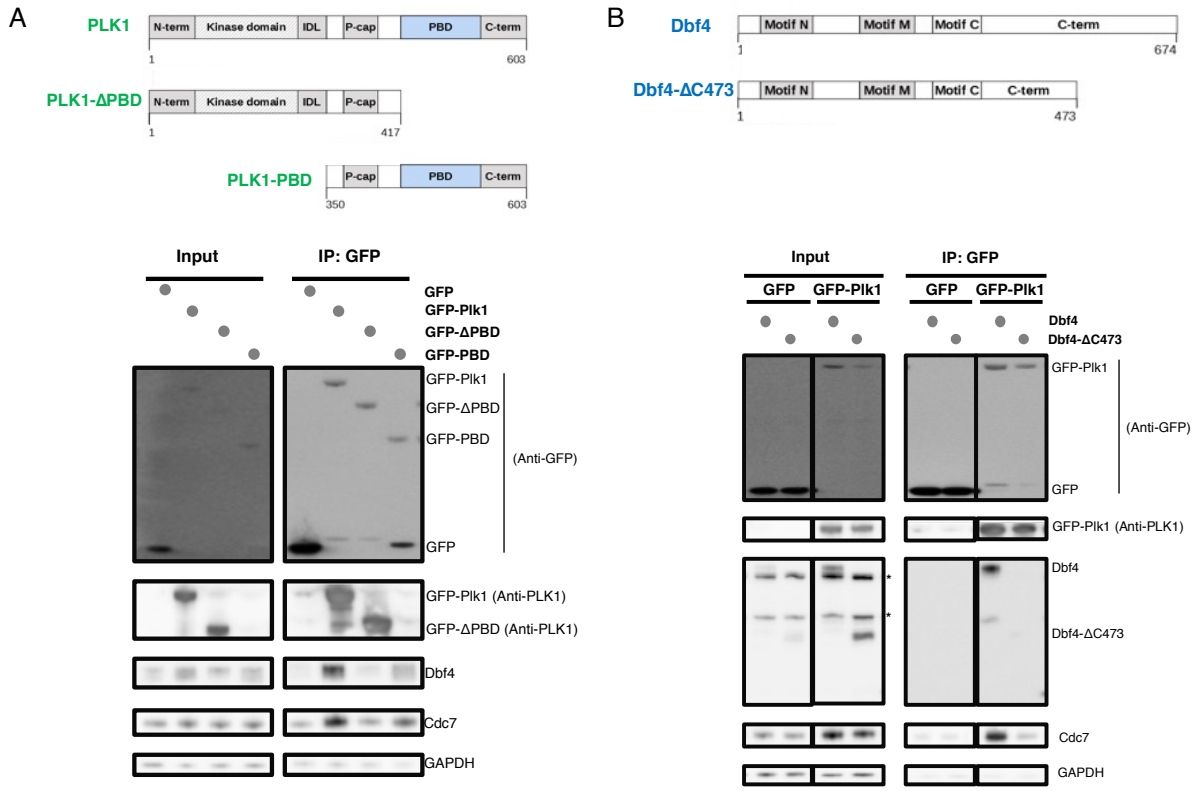

Figure 53- **DDK-PLK1 interaction requires the PBD of PLK1 and the C-terminus of Dbf4.**

HEK293T cells were transfected with different combinations of constructs to map the interaction region in PLK1 and DBF4. A) Cells were transfected with constructs for CMV based overexpression of DBF4, CDC7 and either GFP (as control), GFP-PLK1, GFP-PLK1-ΔPBD (a PLK1 construct lacking the polo-box domain) or GFP-PBD (a construct consisting only of the polo-box domain). A schematic representation of the construct is shown on the top. After transfection cells were lysed and a GFP pulldown was performed. Samples eluted from the GFP pulldown were loaded on gel. The interaction with DDK is lost if the polo-box domain is deleted, and the polo-box domain on its own can interact with DDK, overall showing that the polo-box domain of PLK1 is required for the interaction with DDK. The experiments were performed in two biological replicates (n=2). Shown are western blot images from one of the replicates, representative of the two replicates. B) Cells were transfected with constructs for CMV based overexpression of GFP-PLK1, CDC7 and either DBF4 or a construct of DBF4 lacking 200 amino acids at its C-terminus (DBF4-ΔC473). A schematic representation of the construct is shown on the top. The interaction between DDK and PLK1 is lost in the construct lacking the C-terminus of DBF4, showing its requirement for the interaction with PLK1. The experiments were performed in two biological replicates (n=2). Shown are western blot images from one of the replicates, representative of the two replicates.

Our analysis of the human proteins therefore allowed us not only to show conservation, but also provided first insights into the interaction which requires the PBD of PLK1 and the C-terminus of DBF4.

Results obtained in collaboration

Mass spectrometry experiments (phosphoproteomic experiment shown in figure 5 and crosslinking mass spectrometry experiment shown in figure 46 B and figure 50) were conducted in collaboration with the Mass Spectrometry core facility at *the Max Planck Institue of Biochemistry, Martinsried*. The phosphoproteomic samples were measured by Dr. Nagarjuna Nagaraj, while the crosslinking mass spectrometry samples were measured by Dr. Barbara Steigenberger. Data were analyzed in collaboration with Dr. Barbara Steigenberger.

Strand-specific RPA-ChIP seq experiments presented in figure 16 and figure36, and RPA-ChIP qPCR experiments presented in figure18 were performed and analyzed by Martina Peritore (*Boris Pfander laboratory, Max Planck Institue of Biochemistry, Martinsried*) and measured at the NGS core facility at *Max Planck Institue of Biochemistry, Martinsried* by Rin Ho Kim.

The *in vitro* kinase experiment presented in figure 26 and the clipping assays presented in figure 27,28,29,30 were performed and analyzed by Elda Cannavo (*Petr Cejka laboratory, Institute for Research in Biomedicine, Faculty of Biomedical Sciences, Università della Svizzera italiana (USI), Bellinzona, Switzerland*) and Petr Cejka (*Institute for Research in Biomedicine, Faculty of Biomedical Sciences, Università della Svizzera italiana (USI), Bellinzona, Switzerland and Department of Biology, Institute of Biochemistry, Eidgenössische Technische Hochschule (ETH), Zürich, Switzerland*).

The plasmids used for CMV based overexpression of GFP-tagged or untagged proteins used for immunoprecipitations experiments are unpublished plasmids that were kindly provided by Dr. Christian Biertuempfel (*Laboratory of Structural Cell Biology, National Heart, Lung, and Blood Institute, National Institutes of Health, 50 South Dr., Bethesda, MD 20892, USA and Max Planck Institue of Biochemistry, Martinsried*). The experiments in figure 52 and figure 53 were performed by Simone Mosna (*Boris Pfander laboratory, Max Planck Institue of Biochemistry, Martinsried*) as part of his master thesis entitled "Molecular characterization of the interaction between Polo-like Kinase 1(Plk1) and Dbf4/Drf1-dependent Kinase (DDK)" at the *University of Bologna, Italy*, which I supervised.

Discussion

Many cellular processes and pathways must be strictly coordinated with the cell cycle, as they must be active in certain phases, but inactive in others. A common way to achieve such strict regulation within different phases of the cell cycle, is by post-translational modifications (PTMs) such as phosphorylation [156]. Eukaryotic cells indeed rely on several cell cycle kinases. One of the key cell cycle kinases, conserved from yeast to humans, is the Dbf4-dependent kinase (DDK). DDK is well studied for its essential function during the initiation of DNA replication [19,20]. Together with CDK, DDK phosphorylation is essential to activate the replicative helicase and initiate DNA replication [4-6,21]. DDK is however important also for functions in mitosis. It was shown to be important to control DNA replication regulating Sld2 degradation and the Rif1-mediated replication repression [22,157]. Moreover, upon formation of a kinase complex with Cdc5, DDK is important to regulate the resolution of Holliday junction in the final step of homologous recombination [13]. DDK functions are not restricted to mitosis, as it was found to be important also in meiosis for the regulation of meiotic recombination and chromosome segregation [12,14,25-27]. DDK is therefore a key cell cycle kinase with several functions, and it is also of high clinical interest given that overexpression of DDK is known to be associated with several cancers [158-162].

By performing phosphoproteomics experiments we discovered that DDK phosphorylates proteins involved in homologous recombination (HR) and DNA end resection. We therefore went on to analyze the role of DDK in HR, and not only discovered that DDK is crucial to activate repair via HR, by promoting the initiation of DNA end resection via stimulation of the Sae2-MRX complex, but also that premature expression of DDK can bypass the cell cycle regulation of DNA end resection and HR.

1. DDK phosphorylates Homologous Recombination and DNA end resection proteins

In order to identify possible novel substrates of DDK in an unbiased high-throughput manner, we decided to make use of phosphoproteomics. We measured the phosphoproteome of cells with DDK and compared it to the one of cells depleted of DDK. A general aspect important to consider is that independently of the system used to deplete cells of DDK (chemical inhibition or depletion of DDK or the use of bypass

mutants that allow the deletion of *DBF4* or *CDC7*), cells lacking an active DDK do not cycle as Wild Type cells and will eventually die in the long run. Working with cycling cells therefore requires to check that differences observed in the outcome of the experiment of interest, are specifically coming from the depletion of DDK, and not indirectly due to a cell cycle difference induced by the depletion of DDK. In order to overcome this issue, we generally decided to perform our experiments from budding yeast cells arrested at specific phases of the cell cycle.

Our phosphoproteome analysis identified DDK as being required for the phosphorylation of several proteins involved in the response to DSBs. DDK was already known to be required for the activation of the endonuclease complex Mus81-Mms4, important for the late steps of HR [13]. We indeed identified the Mus81-Mms4 complex as DDK substrate in our analysis, but we also identified proteins known to be important for the initial steps of HR, such as nucleases or chromatin remodelers which are known to be important to initiate HR via the processing of the broken ends during DNA end resection, therefore showing that DDK might have an unprecedented key role in the regulation of DSB repair and in the DSB repair pathway choice.

2. The cell cycle regulation of DNA end resection and Homologous Recombination

DSBs can be repaired via two main pathways - non-homologous end joining (NHEJ) and homologous recombination (HR). Cellular pathway choice is determined by the cell cycle state and installed at the stage of DNA end resection. In this work we identified DDK as being required for DNA end resection via stimulation of the nucleolytic activity of the Sae2-MRX complex. This finding, not only elucidate a novel key function of DDK but also offers a potential tool to attempt cell cycle independent activation of HR, which is of increasing interest given the CRISPR-Cas revolution and the current limitations and obstacles towards precise genome editing [163,164].

2.1 DDK and Homologous recombination

Based on our phosphoprotemics experiment we investigated a possible more general role of DDK in the response to DSBs, and discovered that DDK is essential for the response to DSBs as it is required for repair via HR (figure 11). Interestingly, it was also more

recently shown that inhibition of DDK in human cells leads to a HR defect [165]. To monitor repair via HR, the authors used a gene conversion assay based on the DR-GFP system developed in the Jasin lab, in which repair leads to conversion of a mutated GFP to a functional GFP and can therefore be monitored by the amount of GFP+ cells. [166,167]. Cells with DDK inhibited showed a reduction of GFP+ cells and hence of HR [165]. While these data could be consistent with evolutionary conservation of our findings, indirect effects cannot be completely ruled out, for example cell cycle specific changes after DDK inhibition. Interestingly, the experiments performed by Iwai and colleagues were aimed to identify potential combination drugs of the DDK inhibitor TAK-931. Consistent with a role of DDK in the response to DSBs, a synergistic effect was observed between TAK-931 and DNA damaging agents, providing promising insights into the potential clinical applications of the DDK inhibitor TAK-931. Our data thus not only confirms a direct role of DDK in repair of DSBs via homologous recombination, but also offers an explanation of what the requirement of DDK for HR could be.

2.2 DDK and DNA end resection

Our data suggest that Sae2 phosphorylated by DDK (and CDK) can stimulate the nucleolytic activity of MRX and therefore initiate DNA end resection, committing cells to repair via HR during the S, G2 and M phases of the cell cycle. Recently, two studies proposed a role for DDK in the resection of reversed replication forks in human cells [168,169]. Replication forks can slow down or stall during replication stress. A newly synthetized strand can anneal back to the template in such a condition, leading to a cruciform structure called reversed fork [170]. Moderate processing and resection of a reversed fork was suggested to be important for fork restart, particularly in BRCA-deficient cells. It was indeed observed that in BRCA-deficient cells there is active resection of reversed forks to promote their restart, and that this replication fork specific resection is impaired upon inhibition of DDK [169]. This finding would be consistent with a defect in resection of these structures in the absence of DDK, even though a direct connection between these two events is still missing [169]. In contrast, the Jallepalli lab recently uncovered novel functions of DDK during DNA replication, but did not observe a role in the resection of reversed forks [171]. It should be noted that these experiments were performed in BRCA+ cells, a condition in which it is indeed thought that BRCA1 and

BRCA2 overall protect reversed forks from nucleolytic degradation. It is therefore possible that the resection of reversed forks relies on DDK but this can only be observed in BRCA-deficient cells. It is however clear that insights into novel functions of DDK in regulating DSB repair and DNA resection have implications for genome stability in the context of cancer, as well as for potential therapy.

3. homologous recombination and chromatin remodelers

An important aspect of all processes that act on DNA, is that their template within cells is not simply naked DNA, but is chromatin. Different chromatin remodelers were shown to be important for DNA end resection and indeed some remodelers are also cell cycle regulated by the cell cycle kinases, e.g. Fun30 (human SMARCAD1). It was shown that CDK phosphorylation of Fun30 is important to recruit it to DSBs where via a still unknown mechanism, it can promote extension of the resected tracts during long-range resection [11]. Other chromatin remodelers were shown to be important for resection, such as the RSC, SWI/SNF and INO80 complexes (the latter being important also during presynaptic filament formation) [134-138]. Our phosphoproteomic analysis identified subunits of both the INO80 and RSC complex to be phosphorylated by DDK, therefore raising the idea that DDK could not only be important to initiate resection via stimulation of the nucleolytic activity of the Sae2-MRX, but potentially also modulating the activity of chromatin remodelers. Interestingly, also Fun30 was identified as DDK substrate in our phosphoproteomic experiment. It was excluded in the most stringent filtering due to a change in the protein levels in the total proteome measurement of one of the control conditions (*bob1-1*). However, the fact that there were no significant differences when comparing the total proteomes of the Wild Type and the DDK mutant strongly suggest, that the difference observed in the phosphosites is real. Two interesting putative DDK phosphosites that were identified are serine 19 and serine 27. It is known that CDK mediated recruitment of Fun30 to DSBs is achieved by phosphorylation of serine 20 and 28. The fact that we identified serine 19 and 27, might suggest that not only CDK, but also DDK phosphorylation might be important for its cell cycle regulation (note that the phosphorylated peptides were identified in multi phosphorylated peptides with a localization probability of >0.8 for S19 and 1 for S27). CDK phosphorylation of Fun30 on serine 20 and 28 mediates Fun30 binding to Dpb11, as serine to alanine mutations of serine 20 and 28 leads to a loss of interaction between Fun30 and Dpb11. By yeast two

hybrid we observed that serine to alanine mutations of the serine 19 and 27, the DDK consensus sites that we identified, also abolished the interaction between Fun30 and Dpb11 (data not shown). These data are still preliminary, but nonetheless the overall identification of phosphosites in several chromatin remodelers involved in DNA resection, strongly suggest that this could be an additional layer of the DDK mediated regulation of DSB repair.

4. DDK mediated stimulation of DNA end resection

After identifying Sae2 as a DDK substrate *in vivo*, we decided to analyze the role of DDK mediated phosphorylation of Sae2 using an *in vitro* reconstituted system developed in the Cejka lab [71,120,145]. These experiments allowed us to directly look into the effect of DDK phosphorylation of Sae2, leading to the finding that DDK-phosphorylated Sae2 can stimulate the nucleolytic activity of the MRX complex. Our experiments show that both DDK and CDK phosphorylation of Sae2 stimulates the nucleolytic activity of the MRX complex.

In vivo we observe a major effect for the bypass of cell cycle regulation of both DNA end resection and HR when expressing DDK in G1 cells, but not when expressing the CDK phosphomimic mutant of Sae2. Expression of DDK in G1 cells lead to premature phosphorylation of Sae2, but most likely of other DDK substrates working in HR. Our phosphoproteomic experiment will be a valuable tool to direct research towards specific substrates and their possible DDK mediated regulation during resection and HR. It will also be of high interest to identify the DDK targeted sites in Sae2, to try and develop a mutant that bypasses cell cycle regulation (for example phospho-mimikry).

Discovering the cell cycle regulation and PTMs that regulate resection and HR is also really important when considering the *in vitro* reconstitution of these processes. Full reconstitution will indeed not only require knowledge of the minimal set of proteins, but also their regulation. Our finding that DDK is critical for activation of DNA end resection and HR via stimulation of Sae2-MRX will be important for the *in vitro* reconstitution of end resection. Again, our phosphoproteomic experiment will be a valuable base to orient the research towards some of the novel identified DDK substrates.

5. Phospho-regulation of the Sae2-MRX complex assembly and activity

On a mechanistic level, it is still not entirely clear how the phosphorylation of Sae2 regulate the overall activity of the Sae2-MRX complex. This is unsurprising given the complexity of phosphor-regulation of this complex, where cell cycle dependent phosphorylation by CDK and DDK interplays with DNA damage induced phosphorylation by the Mec1/Tel1 checkpoint kinases [9,124,127].

It was observed that Sae2 exist in different oligomeric states, and that its oligomeric state can change after phosphorylation, both *in vivo* and *in vitro* [120,126]. It was indeed shown that phosphorylated Sae2 shifts from a higher order-inactive oligomer to an active tetramer [120]. We tested if lack of DDK would alter the oligomeric state of Sae2 pulled-down from M arrested cells via size exclusion chromatography, but we did not observe any difference when Sae2 was pulled down from Wild Type cells or DDK mutants. More extensive analysis might be required to find conditions, testing not only DDK but also CDK mutants, and eventually with DNA damage induction, to eventually take into account also the checkpoint kinases Mec1/Tel1. Induction of DDK-dependent phosphorylation of Sae2 in G1 may be a useful tool to investigate the function of DDK in the absence of CDK phosphorylation and these conditions may be used to test an influence on the oligomeric state.

It is currently unclear how the different phosphorylation events mediated by the aforementioned kinases could specifically influence the activity, oligomeric state or integrity of the complex. It is known from previous and our own data that CDK and DDK phosphorylation of Sae2 can stimulate the nucleolytic activity of the MRX complex. This could fit with the idea that cells could have Sae2 cell cycle phosphorylated in a state that is able to initiate resection and therefore activate HR. This would also fit recent *in vivo* data which overall suggest that cell cycle phosphorylation of Sae2 (by CDK) and DNA damage checkpoint mediated phosphorylation via Mec1/Tel1 kinases have different functions [127]. CDK phosphorylation of Sae2 was indeed suggested to be important for activation of DNA end resection via the MRX complex, while Mec1/Tel1 phosphorylation was proposed to attenuate the DNA damage checkpoint and indirectly affect resection. [127]. Our data fits well with this model, adding DDK phosphorylation of Sae2 as cell cycle regulator of resection.

There are also several phospho-dependent interactions identified between different components of the MRX/MRN complex and Sae2/Ctp1/CtIP involving different interaction surfaces. A recent study discovered Casein Kinase II (CKII)-mediated phosphorylation of the N terminus of Ctp1 as being required for interaction with the MRN complex, and hence for the stimulation of its activity, but also discovered that a short peptide within the C terminus of Ctp1 is important for the stimulation of the nuclease activity of the MRN complex [130]. Of interest, Casein Kinase II is related to DDK and phosphorylates similar sites, suggesting that CKII and DDK may activate MRX-Sae2 via the same sites. It will be of interest to get more insights into the phospho-dependent interactions within the Sae2/CtIP/Ctp1 and MRN/X reconstituting specifically the single kinases events, and comparing between cell cycle (CDK or DDK) and DNA damage induced phosphorylation.

6. DDK, the cell cycle regulation of DNA end resection and implications for genome editing

Endogenous DSB repair pathway choice is extremely relevant for genome editing, considering that a DSB induced during CRISPR-Cas9 based editing will be repaired by the DSB repair machinery of the cell [172,173]. Template-dependent genome editing involves HR based repair from template DNA with the desired modification that is extrinsically provided [173]. The template can be either provided as a dsDNA or, more recently, ssDNA donor templates (also known as single-stranded donor oligonucleotides; ssODNs) have been applied, leading to more efficient editing [174,175]. In contrast, repair via end-joining pathways will re-ligate the DSB, leading to possible insertions or deletions. If the broken ends are not compatible, or lack a 3'-hydroxyl or a 5' phosphate group, processing is required, and this can lead to mutagenic insertions or deletions (indels) [67,176,177]. Currently, this represents one of the biggest obstacles for precise genome editing, as repair by end-joining pathways will typically be preferred [163,164], given that typical human cells spend long time in the G1 phase of the cell cycle. Identifying cells or cell clones that have used precise editing will require intense and complicated screening and genotyping in order to obtain the desired modified clones. Currently, one strategy to favor HR is to inhibit NHEJ to promote homology mediated repair [178,179]. Also, cell-cycle specific expression of Cas9 in HR permissive cell cycle phases was shown to enhance homology-mediated repair [180,181]

6.1 DDK, the cell cycle regulation of DNA end resection and implications for genome editing-homologous recombination

In order to manipulate DSB repair pathway choice good knowledge of the pathway is required. Therefore, we used our knowledge of the pathway and induced expression of DDK in G1 cells. Notably, the expression of DDK in G1 cells is not only activating DNA end resection, but is also inducing actual repair of DSBs via HR providing a new tool for cell cycle independent activation of HR. The fact that we observe a similar activation of HR in cells depleted of *YKU80* (known to activate DNA end resection already in G1) strongly suggest that premature expression of DDK is able to induce repair via HR due to its ability of activating DNA end resection, likely via activation of the Sae2-MRX complex as our *in vitro* data suggests. Stimulation of the Sae2-MRX complex would be consistent with activation of resection already in close proximity to the break (short range resection). DNA end resection as previously described can also be extended via additional nuclease during the so-called long-range resection [66]. For example, the chromatin remodeler Fun30 is known to be required for long range resection [11], but cell cycle-independent activation did not allow to induce repair of DSBs in G1 cells and *fun30Δ* cells were suggested to not have defects in HR [182,183].

In our setup, activation of DDK in G1 enhanced repair via HR, but the amount of repair that we observe is not as much as the repair observed in M arrested cells, suggesting that additional events would be required to achieve full activation or efficacy of HR, similarly to what was observed with a bypass system developed in human cells [184]. It is of course highly plausible that other cell cycle events might be required. We indeed tested the CDK phosphomimic mutant of Sae2 in our experiments, but additional mechanisms remain to be tested and involve the nuclease Dna2, which is also cell cycle regulated by CDK phosphorylation [10] (our phosphoproteomic data identified Dna2 as a novel substrate of DDK as well).

It would be interesting to test if similar to what we observe in yeast, DDK expression in G1 cells could enhance the efficiency of CRISPR-Cas based genome editing in human cells. In this regard, it is important to discuss a recently published paper. In an impressive study, the Corn lab [185] developed a protocol to enhance the efficiency of CRISPR-based genome editing via XL-413 mediated inhibition of DDK. The fact that inhibiting DDK led to an increase in edited cells would rather suggest that in human cells DDK could be

inhibitory towards HR. There are however some points that have to be taken into account. In particular, DDK is essential for DNA replication also in humans. Therefore, complete lack of DDK activity will be lethal for cells. The DDK inhibition therefore reduced, but not abolished DDK activity. Reduced DDK activity will interfere also with the essential function of DDK in initiating DNA replication, leading to DDK inhibited cells that progress slower during the S-phase due to reduced DNA replication initiation. Therefore, an increased usage of HR based editing is indeed likely to come from a slower S phase, and cells spending more time in a HR-permissive cell cycle stages. Additionally, the authors observe that to induce increased HR upon DDK inhibition it is crucial to inhibit DDK post-editing treatment. Pre-exposure of cells with the DDK inhibitor and subsequent release during editing led to an actual reduction of the efficiency of HR. We therefore believe that this highly specific and detailed study does not contradict our idea that DDK could be a positive regulator of HR also in human cells, also considering that two studies reported that human cells are defective in HR after DDK inhibition [165,186]

6.2 DDK, the cell cycle regulation of DNA end resection and implications for genome editing-non homologous end joining

Another way to promote HR could come from inhibition of NHEJ. This strategy was employed experimentally for developing a system to increase the efficiency of HR based editing via inhibition of the DSB recruitment of 53BP1, which is a factor promoting NHEJ, therefore overall leading to an inhibition of NHEJ mediated repair [178]. In a similar direction, it was also observed that suppression of NHEJ via silencing of KU70 or KU80 can enhance HR mediated repair and hence increase the efficiency of genome editing [179]. This raises the possibility that DDK could also inhibit NHEJ. In such a situation, DDK would on the one hand activate HR during the S, G2 and M phases, and at the same time inhibit NHEJ. In this direction it was shown that in fission yeast, cell cycle regulated phosphorylation via CDK of a key component of the NHEJ machinery leads to inhibition of NHEJ in those cell cycle phases that are permissive for HR [187]. Interestingly, our DDK phosphoproteomic analysis also revealed Nej1, a key component of the ligase complex acting during NHEJ. Nej1 was proposed to have an inhibitory effect towards DNA end resection [188,189] Additionally, also the resection inhibitor Rad9 was found to be a substrate of DDK. Further analysis will be required to investigate whether DDK activates resection also by inhibiting resection inhibitors from the NHEJ pathway.

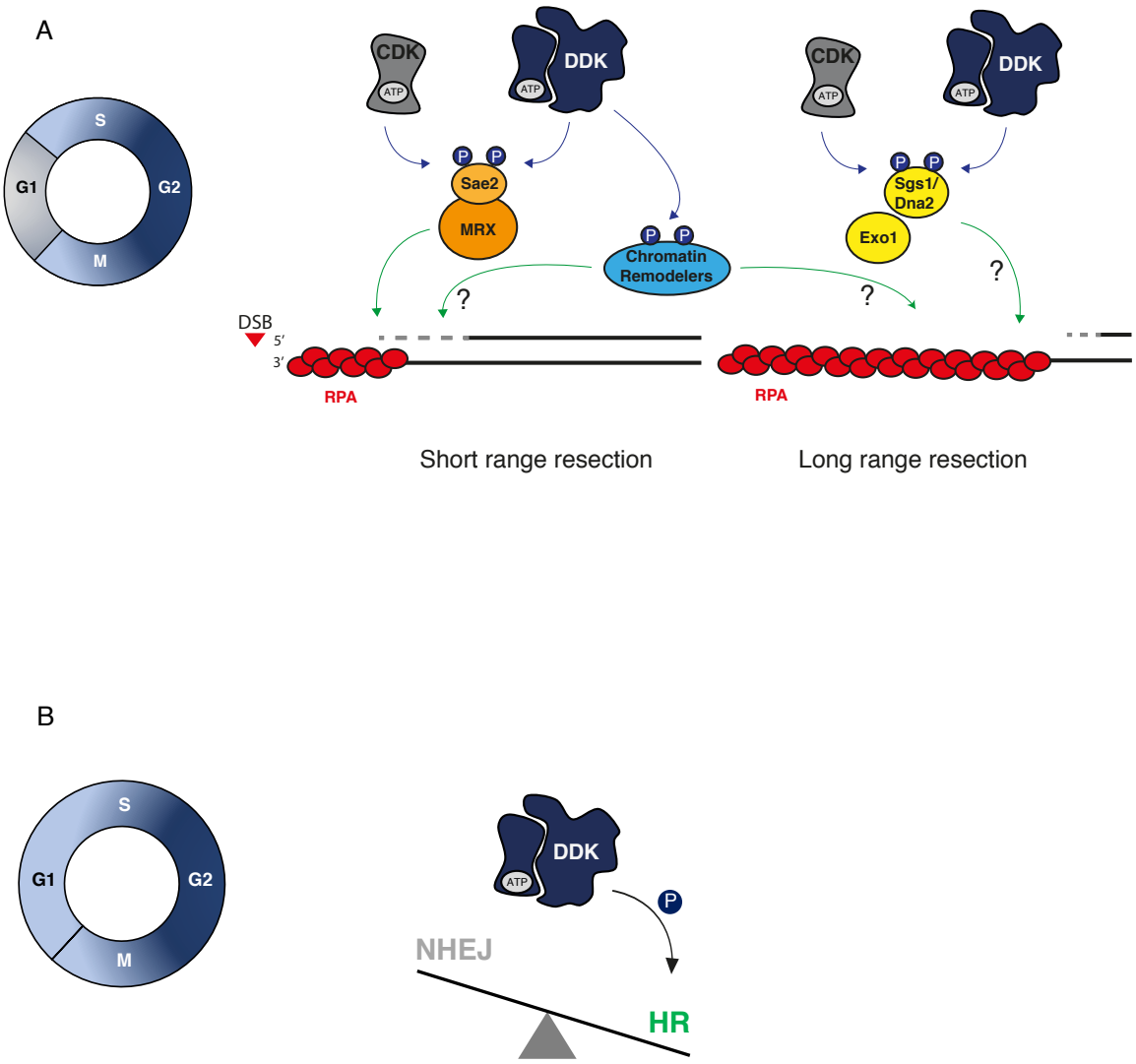

Figure 54-**Model for the DDK mediated regulation of DNA end resection**

A) During S, G2 and M phases of the cell cycle, DDK is active and phosphorylates Sae2. Via stimulation of the nucleolytic activity of the Sae2-MRX complex, DDK (and CDK) phosphorylated Sae2 is able to initiate DNA end resection if DSBs occur, initiating recombination-mediated repair. DDK also phosphorylates other important resection factors (some known to be phosphorylated also by CDK) suggesting that the DDK-dependent regulation of end resection might not be restricted only to Sae2-MRX. B) DDK act as a key regulator of DSB repair pathway choice, as synthetic activation of DDK in G1 cells allows to switch the balance from NHEJ to HR based repair of DSBs.

7. The DDK-Cdc5 kinase complex

Cdc5 is a third essential cell cycle kinase (next to CDK and DDK) which regulates several mitotic events. Interestingly, it was shown that DDK and Cdc5 can physically interact with each other in mitosis and meiosis [24,44,45]. Initially it was proposed that the interaction in mitosis would serve as an inhibitory mechanism towards Cdc5, with DDK blocking Cdc5 from targeting its substrates rather than inhibiting its kinase activity [45]. However, recent work from our lab discovered that DDK and Cdc5 need to interact with each other to phosphorylate a mitotic substrate (Mus81-Mms4) [13]. We therefore were interested in getting biochemical insights into the DDK-Cdc5 kinase complex. A two-kinase complex could form a novel enzymatic activity, consisting of two kinases which are completely functional and active on their own, but need to be together for the phosphorylation of specific substrates.

First, we tried to identify novel substrates. We know that Sld2 is a substrate of both DDK and Cdc5 [8], and interestingly we discovered that similar to Mus81-Mms4, also Sld2 requires specifically the kinase complex for its phosphorylation, overall suggesting that the regulation via the DDK-Cdc5 kinase complex is a more general mechanism. It will be of interest to find novel substrates of the kinase complex, for example by using phosphoproteomics experiments. We already performed phosphoproteomics experiments using Cdc5 mutants (data not shown), showing that there is an extensive overlap of proteins targeted by Cdc5 and proteins targeted by DDK. Among those targeted by both DDK and Cdc5, we expect further substrates of the kinase complex. For this analysis, we could use known interaction-deficient mutants that are not able to form the DDK-Cdc5 kinase complex [44,45].

What is the principal advantage of using such a two-kinase complex? One can speculate that the two kinases could somehow regulate/modulate their kinase activities when they get together. Another possibility could be that one kinase could serve as a scaffold for the recruitment of the other kinase to a set of substrates. In order to get insights into the activity of the kinase complex we purified the single kinases as well as the complex from yeast cells, and tested their activity by using *in vitro* kinase assays. Our analysis overall suggests that the kinase activity is not changing through complex formation. It is of course possible that our *in vitro* assay is an over-simplified system that does not allow the detection of all mechanistic details that might be particularly important *in vivo*. Our

preliminary *in vivo* experiments based on overexpression of catalytic-dead kinases suggest a model, where DDK functions as a scaffold. It will be important to verify these results in a better *in vivo* system which does not rely on protein overexpression, to analyse the requirement of the activity of each kinase, in order to definitively address whether a certain kinase activity is required or not. One possibility could be to have the endogenous kinase (Cdc5 or Cdc7) fused to an inducible degron (like the Aid tag [142]), and provide cells with a second copy of the kinase, either Wild Type or as a kinase-dead mutant. It would therefore be possible to test within the experimental conditions of interest the phenotype of kinase-dead mutants by inducing degradation of the endogenous copy of the kinase. Additional experiments aimed to reveal the role of DDK as an adapter could be of interest, such as co-localization-based experiments aimed to observe the DDK dependent recruitment of Cdc5 to the targets. The use of DDK mutants unable to interact with Cdc5 could allow to specifically observe a DDK-dependent co-localization of Cdc5. The coupling of these mutants with kinase dead mutants would allow to observe the DDK-dependent but kinase activity independent recruitment of Cdc5, if our preliminary model is correct.

The model appears similar to the one of a recent publication, which identified a mechanism for the recruitment of Cdc5 at sites of crossover in meiosis that depends on Exo1 [154]. The authors discovered that Cdc5 is recruited via binding to Exo1 and identified a short sequence within Exo1 which is highly similar to the sequence used by Dbf4 for the binding to Cdc5, suggesting that such a Cdc5-recrutiment mechanism could eventually work also via DDK.

A kinase complex with DDK and Cdc5 generates a really interesting enzyme. The complex has two active sites, one on Cdc5 and one on Cdc7. Our analysis suggest that the complex might be important despite the kinase activity of DDK, however, further experiments will be required to validate the hypothesis. Also, despite not observing differences in the kinase activity from the single subunits when compared to the complex, we cannot completely rule out the possibility of some interplay between the two kinases. It was previously suggested that Cdc5/PLK1 is generally in an autoinhibited state and that the binding to DDK could lead to a conformational change that could activate Cdc5 [153,155]. However, our XL-MS experiments do not provide support for a conformational change, suggesting that either Cdc5 is in an active state in both the complex and on its own, or that the structural resolution of the observed crosslinks is too low to detect such a

conformational change. Additionally, the observed inter-links of Dbf4 and Cdc5 nicely fit with the (still limited) structural information that we have available. Indeed, three lysines in the PBD of Cdc5 which were found to be crosslinked with the N terminus of Dbf4, are facing the Dbf4 binding surface of the PBD of Cdc5 in the available structure. Of interest, we could find a series of crosslinks between the kinase domains of Cdc5 and Cdc7 around both the ATP binding site and the active site, which could suggest proximity of the two active/ATP binding sites within the 3D structure of the kinase complex. Whether there could be some interplay between the two active sites is unclear. The results presented here, are still preliminary structural data, which would need to be complemented with more direct structural information. It could be also of interest to get structural data not only of the complex on its own, but also of the complex bound to a substrate. This could help better understanding the biochemical mechanism.

DDK and Cdc5 are highly conserved from yeast to human and in this work, we showed that also human DDK and PLK1 can interact with each other. Additionally, we could also map the interaction to the PBD of PLK1 and the C-terminal region of DBF4. The conservation of the interaction and hence of the kinase complex is of high interest. Both DDK and PLK1 are well known for being overexpressed in several cancers, and they are both considered as targets in cancer therapy [158,190]. Several inhibitors have been and are being developed for both DDK and PLK1. The fact that DDK and PLK1 can interact with each other, is worthy of interest given that the kinase complex might gain additional functions compared to the single kinases. For example, our preliminary data suggests a role of DDK, as part of the complex, that is not dependent on its kinase activity. Such a scenario would be really important to take into account for the human kinase complex, as it could for example be changed when DDK is overexpressed in the cancer setting. It should therefore be tested whether the kinase complex is equally affected by inhibitor treatment. Additionally, in humans different PLKs exist [28]. We focused our analysis on PLK1 given that it is the human ortholog of the yeast Cdc5, but exploiting the system we developed it would be interesting to test if other PLKs could interact with DDK, or if this interaction is specific for PLK1. On the same line, in humans there is the ortholog of yeast Dbf4, DBF4A (previously defined as DBF4), but is also present a second paralog called Drf1. It was suggested that the Drf1-CDC7 complex is the major form of DDK during development [191]. Again, it would be of interest to analyse if the human DDK-PLK1

complex is formed also with Drf1-CDC7. In all, our study provides the first step to an understanding of a new cell cycle regulator in human cells.

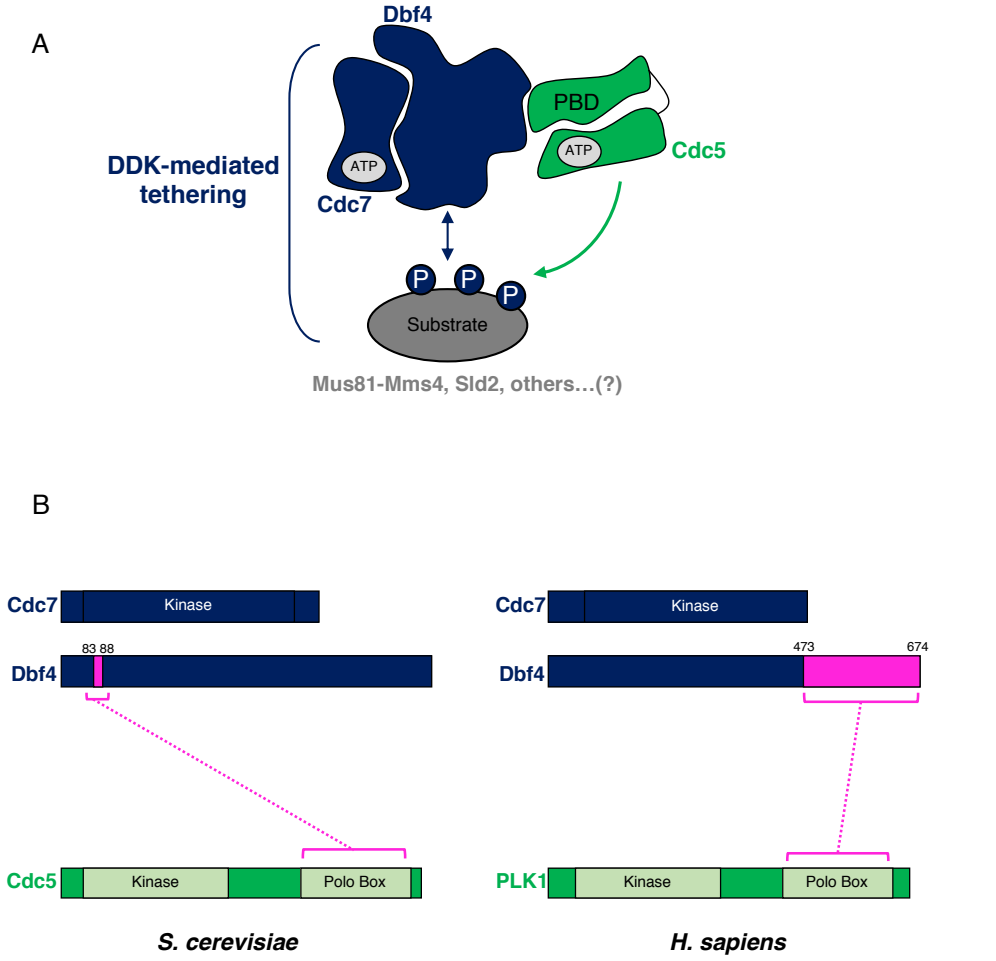

Figure 55-**Model for the proposed working mechanism of the DDK-Cdc5 complex and its conservation**

A) DDK and Cdc5 physically interact to form a two-kinase complex. As part of the kinase complex, DDK act as a tether for Cdc5, promoting phosphorylation of a series of substrates. B) In yeast DDK and Cdc5 interact via the Polo Box domain of Cdc5 and a short stretch of amino acids (83-88) in the N terminus of Dbf4. The interaction is conserved in humans, and require the Polo Box domain of PLK1 and the C terminus of DBF4.

Material and Methods

Yeast strains used in this study

Strain	Genotype	Reference
W303a	MAT**a** ade2-1 ura3-1 his3-11,15 trp1-1 leu2-3,112 can1-100	192
YBP388	MAT**a** ade2-1 ura3-1 his3-11,15 trp1-1 leu2-3,112 can1-100 pep4::LEU2	11
YLP100	MAT**a** ade2-1 ura3-1 his3-11,15 trp1-1 leu2-3,112 can1-100 bob1-1::HIS3 pep4::hph	13
YLP101	MAT**a** ade2-1 ura3-1 his3-11,15 trp1-1 leu2-3,112 can1-100 bob1-1::HIS3 dbf4Δ::nat-NT2 pep4::hph	13
JD2042	MAT**a** ade2-1 ura3-1 his3-11,15 trp1-1 leu2-3,112 can1-100 bob1-1::HIS3	This study
YKR101	MAT**a** ade2-1 ura3-1 his3-11,15 trp1-1 leu2-3,112 can1-100 bob1-1::HIS3 dbf4Δ::nat-NT2	This study
YKR102	MAT**a** ade2-1 ura3-1 his3-11,15 trp1-1 leu2-3,112 can1-100 bob1-1::HIS3 cdc7Δ::nat-NT2	8
YCL88	MATa, ade3::pGAL-HO, hmlΔ::pRS-1 hmrΔ::pRS-2 matHOcsΔ::pBR-1 ChrIV491kb::GFPHOcs-hphNT1	Dr. Claudio Lademann
YCL94	MATa, ade3::pGAL-HO, hmlΔ::pRS-1 hmrΔ::pRS-2 matHOcsΔ::pBR-1 ChrIV491kb::GFPHOcs-hphNT1 ChrIV795kb::GFPHOinc-kanMX4	Dr. Claudio Lademann
YLG243	MATa, ade3::pGAL-HO, hmlΔ::pRS-1 hmrΔ::pRS-2 matHOcsΔ::pBR-1 ChrIV491kb::GFPHOcs-hphNT1 bar1Δ::TRP	This study
YLG245	MATa, ade3::pGAL-HO, hmlΔ::pRS-1 hmrΔ::pRS-2 matHOcsΔ::pBR-1 ChrIV491kb::GFPHOcs-hphNT1 ChrIV795kb::GFPHOinc-kanMX4 bar1Δ::TRP	This study
YLG269	MATa, ade3::pGAL-HO, hmlΔ::pRS-1 hmrΔ::pRS-2 matHOcsΔ::pBR-1 ChrIV491kb::GFPHOcs-hphNT1 bob1-1::URA	This study
YLG271	MATa, ade3::pGAL-HO, hmlΔ::pRS-1 hmrΔ::pRS-2 matHOcsΔ::pBR-1 ChrIV491kb::GFPHOcs-hphNT1 ChrIV795kb::GFPHOinc-kanMX4 bob1-1::URA	This study
YLG337	MATa, ade3:pPGAL-HO, hmlΔ::pRS-1 hmrΔ::pRS-2 matHOcsΔ::pBR-1 ChrIV491kb::GFPHOcs-hphNT1 bob1-1::URA cdc7Δ::NAT	This study
YLG342	MATa, ade3::pGAL-HO, hmlΔ::pRS-1 hmrΔ::pRS-2 matHOcsΔ::pBR-1 ChrIV491kb::GFPHOcs-hphNT1 ChrIV795kb::GFPHOinc-kanMX4 bob1-1::URA cdc7Δ::NAT	This study
YMV80	hmlΔ::ADE1 mataΔ::hisG hmrΔ::ADE1 his4::NAT-leu2-(XhoI-to Asp718) leu2::HOcs ade3::GAL::HO ade1 lys5 ura3-52 trp1 (trp1::hisG)	141
YSB260	YMV80 rad51::hphNT1	11
YLG102	YMV80 bob1-1::URA rad51::hphNT1	This study
YLG104	YMV80 bob1-1::URA cdc7Δ::KAN rad51::hphNT1	This study
YLG136	MatA ade3::pGAL::HO bar1Δ::TRP1 hmlΔ::pRS-1 hmrΔpRS-2 pTDH3-OsTir1::leu2 DBF4-3AID::NAT	This study
YLG275	MatA ade3::pGAL::HO bar1Δ::TRP1 hmlΔ::pRS-1 hmrΔpRS-2 bob1-1::URA	This study
YLG348	MatA ade3::pGAL::HO bar1Δ::TRP1	This study

	hmlΔ::pRS-1 hmrΔpRS-2 bob1-1::URA cdc7Δ::NAT	
YLG65	MATa ade2-1 ura3-1 his3-11,15 trp1-1 leu2-3,112 can1-100 bob1-1::HIS3 SAE2-9MYC-KAN	This study
YLG467	MAT**a** ade2-1 ura3-1 his3-11,15 trp1-1 leu2-3,112 can1-100 cdc28::cdc28-F88G SAE2-9MYC::NAT	This study
YLG66	MATa ade2-1 ura3-1 his3-11,15 trp1-1 leu2-3,112 can1-100 bob1-1::HIS3 dbf4Δ::nat-NT2 SAE2-9MYC::KAN	This study
YLG123	MAT**a** ade2-1 ura3-1 his3-11,15 trp1-1 leu2-3,112 can1-100 bob1-1::HIS3 cdc7Δ::nat-NT2 SAE2-9MYC::KAN	This study
YLG436	MAT**a** ade2-1 ura3-1 his3-11,15 trp1-1 leu2-3,112 can1-100 pTDH3-OsTir1::leu2 DBF4-3AID::KAN SAE2-9MYC::NAT	This study
YLG71	MAT**a** ade2-1 ura3-1 his3-11,15 trp1-1 leu2-3,112 can1-100 MMS4-3Flag::hph-NT1 pep4::HIS3Mx4 Dbf4-NΔ109::KanMx SAE2-9MYC-NAT	This study
YLG194	MAT**a** ade2-1 ura3-1 his3-11,15 trp1-1 leu2-3,112 can1-100 pep4::LEU2 SAE2-3FLAG::KAN	This study
YLG223	MAT**a** ade2-1 ura3-1 his3-11,15 trp1-1 leu2-3,112 can1-100 pep4::LEU2 SAE2-3FLAG::KAN trp1::TRP1pRS304-Cdc7, CBP-Dbf4	This study
YSDK8	MATa ade2-1 ura3-1 his3-11,15 trp1-1 leu2-3,112 can1-100 pep4::KanMx trp1::TRP1pRS304-Cdc7, CBP-Dbf4	This study
YLG46	MAT**a** ade2-1 ura3-1 his3-11,15 trp1-1 leu2-3,112 can1-100 pep4Δ::LEU2 his3-11,15::Cdc5-3FLAG-pGAL1-10-GAL4(HIS3)	This study
YLG53	MATa ade2-1 ura3-1 his3-11,15 trp1-1 leu2-3,112 can1-100 pep4::KanMx trp1::TRP1pRS304-Cdc7, CBP-Dbf4his3-11,15::Cdc5-3FLAG-pGAL1-10-GAL4(HIS3) cdh1::NAT	This study
YLG211	MAT**a** ade2-1 ura3-1 his3-11,15 trp1-1 leu2-3,112 can1-100 bob1-1::HIS3 pep4::hph SAE2-3FLAG::KAN	This study
YLG214	MAT**a** ade2-1 ura3-1 his3-11,15 trp1-1 leu2-3,112 can1-100 bob1-1::HIS3 dbf4Δ::nat-NT2 pep4::hph SAE2-3FLAG::KAN	This study
YSB517	MatA ade3::pGAL::HO bar1Δ::TRP1 hmlΔ::pRS-1 hmrΔpRS-2	[11]
YSB802	MatA ade3::pGAL::HO bar1Δ::TRP1 hmlΔ::pRS-1 hmrΔpRS-2 SAE2 S267E::NAT	This study
YLG137	MatA ade3::pGAL::HO bar1Δ::TRP1 hmlΔ::pRS-1 hmrΔpRS-2 ura::URA3pRS306-Cdc7, CBP-Dbf4	This study
YLG142	MatA ade3::pGAL::HO bar1Δ::TRP1 hmlΔ::pRS-1 hmrΔpRS-2 ura::URA3pRS306-Cdc7, CBP-Dbf4 SAE2 S267E::NAT	This study
YLG256	MATa, ade3::pGAL-HO, hmlΔ::pRS-1 hmrΔ::pRS-2 matHOcsΔ::pBR-1 ChrIV491kb::GFPHOcs-hphNT1 ChrIV795kb::GFPHOinc-kanMX4 bar1Δ::TRP SAE2 S267E::NAT	This study
YLG308	MATa, ade3::pGAL-HO, hmlΔ::pRS-1 hmrΔ::pRS-2 matHOcsΔ::pBR-1 ChrIV491kb::GFPHOcs-hphNT1 ChrIV795kb::GFPHOinc-kanMX4 bar1Δ::TRP ura::URA3pRS306-Cdc7, CBP-Dbf4 SAE2 S267E::NAT	This study
YLG283	MATa, ade3::pGAL-HO, hmlΔ::pRS-1 hmrΔ::pRS-2 matHOcsΔ::pBR-1 ChrIV491kb::GFPHOcs-hphNT1 ChrIV795kb::GFPHOinc-kanMX4 bar1Δ::TRP ura::URA3pRS306-Cdc7, CBP-Dbf4 SAE2 S267E::NAT SAE2 S267E::NAT	This study
YLG457	MATa, ade3::pGAL-HO, hmlΔ::pRS-1 hmrΔ::pRS-2 matHOcsΔ::pBR-1 ChrIV491kb::GFPHOcs-hphNT1 ChrIV795kb::GFPHOinc-kanMX4 bar1Δ::TRP yku80Δ::NAT	This study
YLG459	MATa, ade3::pGAL-HO, hmlΔ::pRS-1 hmrΔ::pRS-2 matHOcsΔ::pBR-1 ChrIV491kb::GFPHOcs-hphNT1	This study

	ChrIV$_{795kb}$::GFPHOinc-kanMX4 bar1Δ::TRP ura::URA3pRS306-Cdc7, CBP-Dbf4 yku80Δ::NAT	
YLP344	MAT**a** ade2-1 ura3-1 his3-11,15 trp1-1 leu2-3,112 can1-100 MMS4-3Flag::hph-NT1 pep4::HIS3Mx4 Dbf4-NΔ66::KanMx	[13]
YLP345	MAT**a** ade2-1 ura3-1 his3-11,15 trp1-1 leu2-3,112 can1-100 MMS4-3Flag::hph-NT1 pep4::HIS3Mx4 Dbf4-NΔ109::KanMx	[13]
YLG48	*MAT**a** ade2-1 ura3-1 his3-11,15 trp1-1 leu2-3,112 can1-100 pep4Δ::LEU2 his3-11,15::Mus81-Myc Mms4-3FLAG-pGAL1-10(HIS3)*	This study
YLG82	MAT**a** ade2-1 ura3-1 his3-11,15 trp1-1 leu2-3,112 can1-100 pep4::LEU2 MMS4-9MYC::NAT	This study
YLG83	MAT**a** ade2-1 ura3-1 his3-11,15 trp1-1 leu2-3,112 can1-100 pep4Δ::LEU2 his3-11,15::Cdc5-3FLAG-pGAL1-10-GAL4(HIS3) MMS4-9MYC::NAT	This study
YLG85	MATa ade2-1 ura3-1 his3-11,15 trp1-1 leu2-3,112 can1-1*his3-11,15::Cdc5N209A 3FLAG-pGAL1-10-GAL4(HIS3)* MMS4-9MYC::NAT	This study
YLG87	MATa ade2-1 ura3-1 his3-11,15 trp1-1 leu2-3,112 can1-100 pep4::KanMx trp1::TRP1pRS304-Cdc7, CBP-Dbf4 MMS4-9MYC::NAT	This study
YLG89	MATa ade2-1 ura3-1 his3-11,15 trp1-1 leu2-3,112 can1-100 pep4::KanMx trp1::TRP1pRS304-Cdc7K76A, CBP-Dbf4 MMS4-9MYC::NAT	This study
YSDK8	MATa ade2-1 ura3-1 his3-11,15 trp1-1 leu2-3,112 can1-100 pep4::KanMx trp1::TRP1pRS304-Cdc7, CBP-Dbf4	John Diffley lab

Plasmids used in this study

Plasmid	Description	Reference
pLG10	pRS303 pGAL1-10 GAL4 Cdc5-3FLAG(codon optimized)	This study
pLG23	pRS306 pGAL1-10 Cdc7 CBP-Dbf4(codon optimized)	This study
1652	pRS304 pGAL1-10 Cdc7 CBP-Dbf4(codon optimized)	John Diffley lab
pJB164	pRS304 pGAL1-10 Mus81-9MYC Mms4-3FLAG	This study
pLG13	pRS303 pGAL1-10 GAL4 Cdc5 N209A-3FLAG(codon optimized)	This study
pLG14	pRS304 pGAL1-10 Cdc7 K76A CBP-Dbf4(codon optimized)	This study
pGST-CDK2	pGEX-GPI-CDK2/cak1 (for bacterial expression of ^{GST}CDK2)	[146]
pHIS-cycA$^{\Delta N170}$	Pet21-CycA$^{\Delta N170}$ (for bacterial expression of ^{His6}cycA$^{\Delta N170}$)	[146]
pLG35	pET-TwinStrep-3C-Xrs2-FHA$^{1-117}$ (for bacterial expression of TwinStrep-Xrs2-FHA $^{1-117}$)	This study
pSM48	CMV-GFP (control)	This study
pSM8	CMV-GFP-PLK1	This study
pSM15	CMV-DBF4A	This study
pSM23	CMV-CDC7	This study
pSM9	CMV-PLK1ΔPBD	This study
pSM11	CMV-PBD	This study
pSM21	CMV-DBF4AΔC	This study

Microbiology methods

Preparation of Chemically Competent *E. coli* cells

Chemically competent *E. coli* cells were prepared using the Inoue protocol. Briefly, cells were grown to an OD_{600} around 0.7 at 18°C and subsequently cooled down at 4°C. Cells were then washed and resuspended in Inoue Transformation buffer (10 mM PIPES pH 6.7; 250 mM KCl; 55 mM $MnCl_2$; 15 mM $CaCl_2$) supplemented with 7.5% DMSO. Aliquots were then stored at -80°C

Transformation of *E. coli* cells

Chemically competent cells were thawed on ice, then incubated with the plasmid of interest (in case of re-prepping of plasmids) or with the cloning reaction mixture (during cloning protocols) for 15 minutes on ice. Then cells were heat shocked at 42°C for 45 seconds, incubated another 5 minutes on ice and recovered in 1 ml LB at 37°C for 1 hour. Cells were afterwards plates on LB plates supplemented with the antibiotic of interest. Transformations for bacterial expression of proteins were conducted in the same way, but using chemically competent BL21 harboring the pRIL construct.

Genetic modifications of *S. cerevisiae* cells

PCR-based deletions and tagging in yeast strains were performed following standard protocols. Plasmid integration was performed using linearized integrative vectors. All strain constructions were confirmed by colony PCR.

Preparation of competent *S. cerevisiae* cells

Cells were inoculated overnight in 5 ml YPD (YP supplemented with 2% glucose) and grown to stationary phase, and diluted the morning after in 50 ml YPD to an OD_{600} around 0.15. When cells reached an OD_{600} of 0.5 they were washed with water, and then with SORB buffer (100 mM LiOAc; 10 mM Tris-HCl, pH 8.0; 1 mM EDTA; 1 M sorbitol). Subsequently, cells were resuspended in SORB buffer supplemented with previously boiled herring sperm DNA. 100 µl aliquots were then stored -80°C.

Transformation of competent *S. cerevisiae* cells

An aliquot of competent cells was thawed on ice, and supplemented with 10 µl of precipitated PCR product (or 1 µg of linearized plasmid) and 6 volumes of PEG buffer (100 mM LiOAc; 10 mM Tris-HCl, pH 8.0; 1 mM EDTA; 40% w/v PEG-3350). Cells were then incubated at room temperature for 30 minutes shaking at 900 rpm and subjected to a heat shock at 42°C for 15 minutes. For transformations based on auxotrophic markers, cells were then plated on selective plates, while for transformations based on antibiotic markers, cells were first grown in YPD without antibiotics for 3 hours at 30°C and then plated on the selective plates. After the transformation, single colonies were isolated, streaked on selective plates and genotyped via colony PCR, prior long-term storage at -80°C.

Cells treatment for cell cycle experiments

Cells were generally treated with the respective drugs when growing in log phase and being at an OD_{600} of 0.5. For arrest in the G1 phase cells were treated with 5 µg/ml mating pheromone alpha-factor, while for arrest in the M phase with 5 µg/ml nocodazole for at least 2 hours or more. The *cdc28-as1* allele was inhibited by treating cells with 1,5 µM 1NM-PP1. To induce degradation of Dbf4-AID, cells were treated with 3 mM indole-3-acetic acid (IAA). For protein translation inhibition, cycloheximide (CHX) was used at a final concentration of 500 µg/ml.

Spotting assay

Cells were grown overnight to stationary phase. A starting culture was then diluted to an OD_{600} of 0.5 and 5-fold serial dilutions were spotted on plates of interest.

Molecular biology methods

Plasmid DNA preparation

5 ml of LB with the appropriate antibiotic were inoculated with a single colony of *E. coli* harboring the plasmid of interest and grown for 12 to 16 hours at 37°C. Plasmid DNA extraction was then performed using the AccuPrep Plasmid Mini Extraction Kit (Bioneer) following manufacturer's instruction.

Ethanol precipitation of DNA

The DNA containing solution was supplemented with 0.1 volumes of 3 M NaOAc and with 2.5 volumes of 95% ethanol and incubated for 30 minutes at -20°C. The solution was then spun at 14000 rpm at room temperature and the supernatant was discarded. The pellet containing the DNA was left to dry for at least 30 minutes and then resuspended in water.

Agarose gel electrophoresis

DNA samples were generally run on 1% agarose gels with 2 µl Ethidium Bromide/50ml in TAE buffer and visualized using a UV-light detection system

Agarose gel extraction

Bands of interest were cut from the agarose gel and purified using the gel extraction kit (Clonthech) following manufacturer's instructions

Polymerase Chain Reaction (PCR)

Standard PCR reactions were performed and run using PCR programs here presented for amplification of deletion/tagging cassettes or for colony PCR to genotype yeast strains.

Standard PCR reaction
2 µl template
3.2 µl primer 1 (10 µM)
3.2 µl primer 2 (10 µM)
1.75 µl dNTPs (10 mM)
10 µl HF-buffer
1 µl DMSO
0.5 µl Phusion polymerase
28.35 µl water

PCR program Phusion
1) 98 °C for 30 sec
2) 98 °C for 30 sec
3) 58 °C for 30 sec
4) 72 °C for 2 min
repeat steps 2 to 4 for 35 cycles
5) 72 °C for 5 min
6) hold at 4 °C

PCR program CASTORP
1) 95 °C for 4 min
2) 95 °C for 1 min
3) 45 °C for 30 sec
4) 72 °C for 2 min
repeat steps 2 to 4 for 10 cycles
5) 95 °C for 1 min
6) 54 °C for 30 sec
7) 72 °C for 2 min
repeat steps 5 to 7 for 20 cycles
8) hold at 4 °C

Cloning

The insert of interest was amplified using either another vector or yeast genomic DNA as a template, using primers with 15 nucleotides overhangs complementary to the sequences upstream and downstream the cut site in the target vector. 5 µg of the target vector were incubated with the restriction enzyme(s) of choice and incubated at 37°C for at least 3 hours up to overnight. Both the PCR product and the linearized vector were then run on an agarose gel and purified. Subsequently, 50 ng of PCR product and 50 ng of vector were mixed together and cloned using SLIC cloning via the InFusion HD Cloning Kit (Clontech) following manufacturer's instructions. 2 µl of the cloning reaction were then used to transform competent *E. coli* cells and cells were then plated on selective plates. Single colonies were then inoculated to extract plasmid DNA which was sequenced to confirm correct integration of the insert of interest. For construction of plasmids for CMV-based overexpression of human proteins, Gibson assembly was performed. Inserts of interest for DFB4a, CDC7 and PLK1 were PCR amplified from cDNA retrieved from the MPIB core facility, and 80 fmol of purified PCR product were mixed with 20 fmol of BspQI (NEB) linearized plasmid of interest. Mixture was incubated at 50°C for 60 minutes in the presence of Gibson Assembly Mix (MPIB core facility). 2 µl of the cloning reaction were then used to transform competent E. coli cells and cells were plated on selective plates. Single colonies were then inoculated to extract plasmid DNA which was sequenced to confirm correct integration of the insert of interest

Sequencing of plasmid DNA and PCR

Samples were sequenced using the Mix2seq kit (Eurofins) and results were analyzed using the SeqMan Pro software

***S. cerevisiae* genomic DNA extraction-general**

Cells were inoculated overnight in 10 ml till they reached stationary phase and centrifuged. The pellet was then suspended in breaking buffer (2% Triton X-100; 1% SDS; 100 mM NaCl; 10 mM Tris HCl, pH 8.0; 1 mM EDTA) and supplemented with glass beads and an equal volume of phenol/chloroform/isoamyl alcohol solution (Roth). Cells were lysed by vortexing for 3 minutes. Upon addition of an equal volume of TE buffer (10 mM Tris HCl, pH 8.0; 1 mM EDTA), the aqueous layer was transferred to another tube and

precipitated with ethanol. The pellet containing the DNA was the resuspended in TE buffer, and treated with 30 µg RNase A for 5 minutes at 37°C. DNA was then precipitated with addition of 0.1 volumes ammonium acetate and 2.5 volumes 95% ethanol. After centrifugation, the pellet containing the DNA was dried for 30 minutes and resuspended in TE buffer.

Recombination assays

A stationary culture of cells grown in YPR (YP supplemented with 2% raffinose) + 40 µg/ml adenine was used to inoculate cells in YPR for the experiment. At OD_{600} of 0.5, cells were arrested at the desired phase of the cell cycle, and 2 ODs (1 OD corresponds to around $2x10^7$ cells) of cells were collected before addition of 2% galactose for break induction. 2 ODs of cells were then collected for each time point. Cells were spun down and the pellet frozen in liquid nitrogen and stored at -80°C till further use. Frozen pellets were then used for genomic DNA extraction using the Masterpure Yeast DNA Purification Kit (Epicentre) following manufacturer's instruction.

20 ng of genomic DNA were then used to perform qPCR using either control primers on a locus on Chromosome XV (for normalization of the amount of DNA) or primers to monitor repair. The ratio between the signal of the "repair" primer pair and the control locus on Chromosome XV was used as the relative recombination rate signal. Each recombination assay was performed in triplicates.

Cell cycle analysis via DNA content measurement with FACS

1 OD (1 OD corresponds to around $2x10^7$ cells) of cells at the time point of interest was collected, centrifuged and the pellet resuspended in FACS buffer (70% ethanol; 50 mM Tris-HCl, pH 8.0) and stored at 4°C till further use. Cells were then treated with 0.38 mg/ml RNaseA for at least 4 hours at 37°C and subsequently treated with 1 mg/ml proteinase K for 30 minutes at 50°C. Lastly, cells were resuspended in 50 mM Tris-HCl, pH 8.0. Before measurement, cells were sonicated and subsequently diluted 1:20 in SYTOX solution (SYTOX Green (Thermo Fisher)) diluted 1 to 1000 in 50 mM Tris-HCl, pH 8.0) and measured using a MACSquant Analyzer Flow Cytometer (Milteny Biotec) and data were analyzed using FlowJo (version 10.5.3) (FlowJo LLC).

Cell culture and transfections (human)

For immunoprecipitation of endogenous proteins, $1x10^6$ U2OS cells were seeded in medium without antibiotics and subsequently treated with 50 ng/ml nocodazole for 12 hours to arrest them in the M-phase. Cells were then harvested and pellets frozen until further use. For immunoprecipitation experiments with overexpressed constructs, HeK293T cells were grown in DMEM Glutamax medium (Gibco) supplemented with 10% FCS (Fetal Calf Serum) and 1 mM sodium pyruvate. 24 hours before transfection $2.5x10^6$ cells were seeded. For transfection, 10 µg of each plasmid to be transfected was diluted in 225 µl, and then75 µL $CaCl_2$ 2.5 M and 300 µL of 2x BBS (BES Buffered Solution: 50 mM N,N-bis(2-hydroxyethyl)- 2aminoethanesulfonic acid (BES; Calbiochem), 280 mM NaCl, 1.5 mM Na_2HPO_4, pH 6.95 with 1 M NaOH) were added and left for 20 minutes at RT priori transfection. 24 hours after transfection cells were harvested and used for the immunoprecipitation experiments (see session cell lysis and immunoprecipitation)

Lambda phosphatase treatment

100 ODs (1 OD corresponds to around $2x10^7$ cells) of nocodazole arrested cells were collected and washed twice with sorbitol buffer (25 mM HEPES-KOH, pH 7.6; 1 M sorbitol). The pellet was then resuspended in 1 volume of lysis buffer (50 mM HEPES-KOH, pH 7.6; 100 mM NaCl; 0.1% NP-40; 10% glycerol; 2 mM β-mercaptoethanol; protease inhibitors (400 µM PMSF, 4 µM aprotinin, 4 mM benzamidin, 400 µM leupeptin, 300 µM pepstatin A)), and frozen drop by drop in liquid nitrogen. Frozen pellet-drops were then lysed using Cryo Mill (Spex SamplePrep 6870) with 6 cycles at a rate of 15 cps (cycles per second) for 2 minutes each. Extracts were then supplemented with 2 mM $MnCl_2$ and split. One half was mock treated and the other half was treated for 90 minutes with 4000 U of λ phosphatase (NEB) at 30°C while shaking at 1200 rpm. Samples were then prepared by adding an equal volume of Laemmli 2X and run on 10% acrylamide gels.

Cell lysis and immunoprecipitation (human)

U2OS and HEK293T cells were lysed in lysis buffer (50 mM HEPES-KOH, pH 7.6; 200 mM potassium acetate; 5% glycerol; 1 mM EDTA; 1% Triton X-100; 10 mM sodium pyruvate; 2 mM β-mercaptoethanol, 1 mM PMSF, phoSTOP (Roche) and cOmplete protease inhibitor (Roche)). Extracts were then centrifuged at 13000 rpm for 10 minutes at 4°C

and supernatant was recovered. For U2OS cells-based experiments, the supernatant was split in two, and one half of the supernatant was supplemented with 2 µg of anti IgG antibody and the other half with 2 µg of anti DBF4 antibody and subsequently incubated for 3 hours at 4°C with rotation. 200 µl of protein A beads slurry (Thermo Fischer) were then added to each reaction and incubated for another 3 hours at 4°C. After the incubation, beads were washed 6 times with lysis buffer, loading dye was added and beads boiled. The supernatant containing the eluted proteins was then recovered and loaded on gel. For HEK293T cells-based GFP-pulldown experiments, the protein concentration of each extract within the same experiment was measured via Bradford ensuring equal starting material in the different conditions, and each extract was then incubated with 10 µl of GFP magnetic agarose beads (Chromotek) for 1 hour at 4°C. Beads were then washed 6 times with lysis buffer, loading dye was added and beads boiled. The supernatant containing the eluted proteins was then recovered and loaded on 4-12% Bis-Tris acrylamide gel (Invitrogen).

Chromatin immunoprecipitation (ChIP)

Chromatin immunoprecipitation (ChIP) was performed as previously described [138]. Briefly, cells were lysed in lysis buffer (50 mM HEPES-KOH, pH 7.5; 150 mM NaCl; 1 mM EDTA; 1% Triton X-100; 0.1% Na-deoxycholate; 0.1% SDS) with zirconia beads using a bead beater. Chromatin was the sonicated to get fragments around 200-500 bp. Cell lysates were centrifuged at 4°C at 6150 g and diluted 1:1 with lysis buffer. 1% of the extract was taken as input sample. RPA was immunoprecipitated using an anti-RFA antibody (Agrisera) for 2 hours. Subsequently, protein A dynabeads (Invitrogen) were added to the mixture for 30 minutes. Beads were then washed with lysis buffer first, and lysis buffer with 500 mM NaCl after. An additional wash in wash buffer (10 mM Tris-HCl, pH 8.0; 0.25 M LiCl; 1 mM EDTA; 0.5% NP-40; 0.5% Na-deoxycholate) followed by a wash in TE buffer. Immunoprecipitated complexes were eluted using 1% SDS and proteins were degraded via addition of 1 µg/µl proteinase K for 3 hours at 42°C and crosslink was reversed (8 hours at 65°C). DNA was then purified using phenol-chloroform extraction. Residual phenol-chloroform was removed using phase-lock gel tubes (Quantabio) and DNA was precipitated with pure ethanol. DNA concentration was determined using Qubit 3.0 fluorometer (Invitrogen) and Qubit dsDNA HS assay kit (Invitrogen).

Strand-specific ChIP-sequencing

Strand-specific ChIP-seq was performed as previously reported [138]. Briefly, strand-specific ChIP-seq libraries were prepared starting from 1 to 3 ng of DNA using Accel-NGS-1S Plus Library Kit following manufacturer's instructions and 10-12 cycles for library amplification. For clean-up steps, SPRIselect beads were used. To assess the size distribution and the concentration of libraries, high sensitivity DNA Chip with Bioanalyzer 2100 (Agilent Genomics) was used. DNA was paired-end sequenced with 75 cycles per read on an Illumina NextSeq 500 sequencer (NGS core facility Max Planck Institute of Biochemistry).

Crosslinking Mass Spectrometry (XL-MS)

Crosslinking reaction and phosphatase treatment

For crosslinking of the DDK-Cdc5 kinase complex, 100 μg of DDK-Cdc5 purified complex were crosslinked with 100x molar excess of PhoX crosslinker (Bruker). For the crosslinking of Cdc5 alone, 60 μg of Cdc5 were crosslinked with a 75x molar excess of PhoX crosslinker (Bruker). Crosslinking was performed for 45 minutes at room temperature. To quench and avoid over-crosslinking, 100 mM Tris, pH 7.5 was added to the reaction for 15 minutes (at room temperature). Reactions were then supplemented with 2 mM $MnCl_2$ and 20000 U of λ phosphatase, and samples placed at 30˚C for 30 minutes (shaking at 1200 rpm).

Sample preparation

For denaturation of the crosslinked proteins, 4M Urea and 50 mM Tris was added and the samples were sonicated using a Bioruptor Plus sonication system (Diogenode) for 10x30 seconds at high intensity. For reduction and alkylation of the proteins, 40 mM 2-cloroacetamide (CAA, Sigma-Aldrich) and 10 mM tris(2-carboxyethyl)phosphine (TCEP; Thermo Fisher Scientific) and 100 mM Tris-HCl, pH 8.0 was added. After incubation for 20 minutes at 37 °C, the samples were diluted 1:2 with MS grade water (VWR). Proteins were digested overnight at 37 °C with 3 μg trypsin (Promega) and 2 μg LysC (Promega). After digestion, the solution was acidified with trifluoroacetic acid (TFA; Merck) to a final concentration of 1% and pH value of < 2. The peptide mixtures were purified via Sep-Pak C18 1cc vacuum cartridges (Waters). Samples were vacuum dried.

Crosslinked peptides were enriched with Fe(III)-NTA cartridges (Agilent Technologies; Santa Clara, Ca) using the AssayMAP Bravo Platform (Agilent Technologies; Santa Clara, Ca) in an automated fashion. Cartridges were primed at a flow rate of 100 µl/min with 250 µl of priming buffer (0.1% TFA, 99.9% ACN) and equilibrated at a flow-rate of 50 µl/min with 250 µl of loading buffer (0.1% TFA, 80% ACN). The flow-through was collected into a separate plate. Dried samples were dissolved in 200 µl of loading buffer and loaded at a flow-rate of 5 µl/min onto the cartridge. Cartridges were washed with 250 µl of loading buffer at a flow-rate of 20 µl/min and cross-linked peptides were eluted with 35 µl of 10% ammonia directly into 35 µl of 10% formic acid. Samples were dried down and stored at -20 °C prior to further use. Before to LC–MS/MS analysis, the samples were resuspended in 0.1% formic acid.

LC-MS/MS data acquisition

Enriched peptides were loaded onto a 30-cm column (inner diameter: 75 microns; packed in-house with ReproSil-Pur C18-AQ 1.9-micron beads, Dr. Maisch GmbH) via the autosampler of the Thermo Easy-nLC 1000 (Thermo Fisher Scientific) at 60°C. Using the nanoelectrospray interface, eluting peptides were directly sprayed onto the benchtop Orbitrap mass spectrometer Q Exactive HF (Thermo Fisher Scientific).

Peptides were loaded in buffer A (0.1% (v/v) Formic acid) at 400 nl/min and percentage of buffer B (80% acetonitril, 0.1% formic acid) was ramped from 8% to 30% over 60 minutes followed by a ramp to 60% over 5 minutes, 95% over the next 5 minutes and maintained at 95% for another 5 minutes. The mass spectrometer was operated in a data-dependent mode with survey scans from 300 to 1650 m/z (resolution of 60000 at m/z =200), and up to 15 of the top precursors were selected and fragmented using stepped higher energy collisional dissociation (HCD with a normalized collision energy of value of 19, 27, 35). The MS2 spectra were recorded at a resolution of 30000 (at m/z = 200). AGC target for MS1 and MS2 scans were set to 3E6 and 1E5 respectively within a maximum injection time of 100 and 60 ms for MS and MS2 scans respectively. Charge state z=2 was excluded from fragmentation.

Data Analysis

The acquired raw data were processed using Proteome Discoverer (version 2.4.0.388) with the XlinkX/PD nodes integrated. Cysteine carbamidomethylation was set as fixed modification. Methionine oxidation and protein N-term acetylation was set as dynamic modification. For the search of mono-links, water-quenched (C8H5O6P) and Tris-

quenched (C12H14O8PN) were set as dynamic modifications. Trypsin/P was specified as the cleavage enzyme with a minimal peptide length of six and up to two miss cleavages were allowed. Filtering at 1% false discovery rate (FDR) at the peptide level was applied through the Percolator node. For crosslinked peptides, a database search was performed against a FASTA containing the sequences of the proteins under investigation. Cysteine carbamidomethylation was set as fixed modification and methionine oxidation and protein N-term acetylation were set as dynamic modifications. Trypsin/P was specified as enzyme and up to two missed cleavages were allowed. Furthermore, identifications were only accepted with a minimal score of 40 and a minimal delta score of 4. Otherwise, standard settings were applied. Filtering at 1% false discovery rate (FDR) at peptide level was applied through the XlinkX Validator node with setting simple.

Phosphoproteomics

Cell preparation

Wild Type, *bob1-1* and *bob1-1dbf4Δ* cells were grown to log-phase and arrested in the M-phase of the cell cycle with nocodazole. 200 ODs (1 OD corresponds to around $2x10^7$ cells) of cells were then centrifuged, and the pellet washed twice in PBS 1x.

Sample preparation

The cell pellets were incubated with 6 ml of preheated SDC buffer containing 1% sodium deoxycholate (SDC, Sigma-Aldrich), 40 mM 2-cloroacetamide (CAA, Sigma-Aldrich), 10 mM tris(2-carboxyethyl)phosphine (TCEP; Thermo Fisher Scientific) and 100 mM Tris, pH 8.0. After incubation for 2 minutes at 95°C, the samples were ultrasonicated for 2 minutes with 0.5 seconds pulse (50% intensity) and 0.2 seconds pause (Sonopuls, Bandelin). Incubation and ultrasonication was repeated for a second time. After a final incubation for 2 minutes at 95°C, 1/6 of the sample was diluted 1:2 with MS grade water (VWR). Proteins were digested overnight at 37 °C with 50 µg trypsin (Promega). The solution of peptides was then acidified with trifluoroacetic acid (Merck) to a final concentration of 1%, followed by desalting via Sep-Pak C18 5cc vacuum cartridges (Waters). The cartridge was washed twice with 1 ml of 100 % methanol, twice with 1 ml of 0.1% FA in 80% ACN and twice with 1 ml of 0.1% FA in water prior to sample loading. After loading the acidified sample, the cartridge was washed twice with 1 ml of 0.1% FA in water Elution was done with 2x 1 ml of 0.1% FA in 80% ACN.

Phospho-peptide enrichment

To 1 ml of the desalted peptides, 400 µl isopropanol and 100 µl of enrichment buffer (48% TFA, 8mM K2HPO4) was added and mixed at room temperature at 1500 rpm. Then, TiO_2 beads (10 mg) in EP loading buffer (80% ACN/6% TFA) were subsequently and incubated at 37 °C for 5 minutes at 2000 rpm. Beads were subsequently pelleted by centrifugation for 1 minute at 3500 *g*, and the supernatant (containing non-phosphopeptides) was aspirated. Beads were suspended in wash buffer (60% ACN, 1% TFA) and transferred to clean vials and washed a further four times with 1 ml wash buffer. After the final wash, beads were suspended in 150 µl transfer buffer (60% isopropanol, 0.1% TFA) and transferred onto the top of a C8 StageTip, and centrifuged for 3–5 minutes at 500 *g* or until no liquid remained on StageTip. Bound phosphopeptides were eluted 2x with 30 µl elution buffer (40% ACN, 20% NH_4OH (25%, HPLC grade)), and collected by centrifugation into clean PCR tubes. Samples were concentrated in a SpeedVac for 15 minutes at 45°C.

LC MS/MS data acquisition - Peptides were loaded onto a 30-cm column (inner diameter: 75 microns; packed in-house with ReproSil-Pur C18-AQ 1.9-micron beads, Dr. Maisch GmbH) via the autosampler of the Thermo Easy-nLC 1000 (Thermo Fisher Scientific) at 60°C. Using the nanoelectrospray interface, eluting peptides were directly sprayed onto the benchtop Orbitrap mass spectrometer Q Exactive HF (Thermo Fisher Scientific).

Peptides were loaded in buffer A (0.1% (v/v) formic acid) at 250 nl/min and percentage of buffer B (80% acetonitril, 0.1% formic acid) was ramped to 30% over 120 minutes followed by a ramp to 60% over 10 minutes then 95% over the next 5 minutes and maintained at 95% for another 5 minutes.

The mass spectrometer was operated in a data-dependent mode with survey scans from 300 to 1750 m/z (resolution of 60000 at m/z =200), and up to 12 of the top precursors were selected and fragmented using higher energy collisional dissociation (HCD with a normalized collision energy of value of 28). The MS2 spectra were recorded at a resolution of 15000 (at m/z = 200). AGC target for MS and MS2 scans were set to 3E6 and 1E5 respectively within a maximum injection time of 20 ms for MS1 and 50 ms for MS2 scans. Dynamic exclusion was set to 16 ms.

Data Analysis

Raw data were processed using the MaxQuant computational platform with standard settings applied. Shortly, the peak list was searched against the reviewed Human

proteome data base with an allowed precursor mass deviation of 4.5 ppm and an allowed fragment mass deviation of 20 ppm. MaxQuant by default enables individual peptide mass tolerances, which was used in the search. Cysteine carbamidomethylation was set as static modification, and methionine oxidation, N-terminal acetylation, deamidation and phosphorylation as variable modifications.

Biochemistry methods

TCA precipitation of proteins

1 OD (1 OD corresponds to around $2x10^7$ cells) of cells was harvested and frozen in liquid nitrogen and subsequently stored at -80°C till further use. The pellet was then resuspended in 1 ml of cold water, 150 µl 1.85 M NaOH and 7.5% β-mercaptoethanol and incubated at 4°C for 15 minutes. 150 µl of 55% trichloroacetic acid (TCA) were added and samples incubated for another 10 minutes on ice. Samples were then centrifuged, and the pellet resuspended in 50 µl HU buffer (8M urea; 5% SDS; 200 mM Tris-HCl, pH 6.8; 1.5% DTT; traces of bromophenol blue) for 10 minutes at 65°C.

Gel electrophoresis

Samples were generally run on NuPAGE 4-12% Bis-Tris acrylamide gels (Invitrogen) using MOPS buffer (50 mM MOPS; 50 mM Tris base; 0.1% SDS; 1 mM EDTA) for 1 hour at 180 V. To resolve the Sae2 phosphoshift, samples were run on standard 10% acrylamide gels in SDS buffer (25 mM Tris base; 192 mM glycine; 0.1% SDS) for at least 3 hours at 170 V at 4°C. For the Sld2 phosphoshift samples were run on NuPAGE 12% Bis-Tris acrylamide gels (Invitrogen) for 3 hours with MOPS buffer 1x at 4°C.

Gel staining

After gel electrophoresis, gels were fixed for 15 minutes with fixing Solution, washed for 15 minutes with water and stained using GelCode Blue (Thermo Fisher)

Western blot

After gel electrophoresis, gels were transferred to a nitrocellulose membrane using transfer buffer (48 mM Tris base; 39 mM glycine; 0.0375% SDS; 20% methanol) at 4°C

for 90 minutes at 90 V. Membranes were then washed once for 5 minutes with western wash buffer (0.2% NP-40 in TBS) and incubated with the primary antibody of interest. After overnight incubation with the primary antibody, membranes were washed twice for 5 minutes with western wash buffer and the secondary antibody at a concentration of 1:3000 was added for 2 hours. After incubation membranes were washed 6 times for 5 minutes each and detection was achieved using Pierce ECL reagents (Thermo Fisher) and a LAS-300 CCD camera system (Fujifilm).

List of antibodies used in this study

Antibody	Catalog number/company
Anti-FLAG	A8592 (Sigma)
Anti-MYC	4A6 (Millipore)
Anti-Dbf4	sc-5705 (Santa Cruz)
Anti-Cdc5	sc-6733 (SantaCruz)
Anti-Cdc7	John Diffley
Anti-miniAID	M214-3 (MBL/biozol)
Anti-Sld2	PZ45/Philip Zegerman
Anti-RFA	AS07-214 (Agrisera)
Anti-GFP	sc-9996 (Santa Cruz)
Anti-PLK1	ab17056 (Abcam)
Anti-DBF4A (N-terminus)	ab124707 (Abcam)
Anti-DBF4A (C-terminus)	MABE338 (Millipore)
Anti-CDC7	ab113956 (Abcam)
Anti-GAPDH	ab9485 (Abcam)

Protein purifications:

Dbf4-Cdc7 (DDK) purification

For purification of DDK, YSDK8 cells were grown in 6 liters of YPR (YP supplemented with 2% raffinose) at 30°C, and overexpression of both CBP-Dbf4 and Cdc7 was induced via addition of 2% galactose for 8 hours at 30°C. Cells were then harvested and pellets washed first with sorbitol buffer (25 mM HEPES-KOH, pH 7.6; 1 M sorbitol) and then with buffer I (25 mM HEPES-KOH, pH 7.6; 0.03 mM NP-40; 5% glycerol; 400 mM NaCl). Pellets were then resuspended in 1 volume lysis Buffer (25 mM HEPES-KOH, pH 7.6; 0.03 mM

NP-40; 5% glycerol; 400 mM NaCl; 2 mM β-mercaptoethanol; protease inhibitors (400 µM PMSF; 4 µM aprotinin; 4 mM benzamidin; 400 µM leupeptin; 300 µM pepstatin A; 100 nM okadaic acid)) and drop by drop snap frozen in liquid nitrogen. Frozen pellets were then lysed using Cryo Mill (Spex SamplePrep 6870) with 6 cycles at a rate of 15 cps (cycles per second) for 2 minutes each. The thawed powder was then centrifuged at 50000 rpm for 1 hour at 4°C and the clear upper phase was recovered. 2 mM $CaCl_2$ was then added to the suspension together with 1.5 ml bed volume calmodulin affinity resin (Agilent) and the suspension with the beads was stirred for 3 hours at 4°C. Beads were then recovered and washed 5 times with 3 ml wash buffer (25 mM HEPES-KOH, pH 7.6; 0.03 mM NP-40; 5% glycerol; 400 mM NaCl; 2 mM β-mercaptoethanol; 2 mM $CaCl_2$; 0.1 mM EGTA; 0.1 mM EDTA), followed by 5 washes with 4.5 ml of ATP-wash buffer (25 mM HEPES-KOH, pH 7.6; 200 mM NaCl; 50 mM KCl; 10 mM magnesium acetate; 2 mM ATP; 5% glycerol; 0.03 mM NP-40; 2 mM β-mercaptoethanol; 0.1 mM EDTA; 0.1 mM EGTA; 2 mM $CaCl_2$) for removal of an otherwise co-purifying chaperone. After the ATP wash, beads were washed 10 times with 4.5 ml of wash buffer and eluted with 2 ml of elution buffer (25 mM HEPES-KOH, pH 7.6; 0.03 mM NP-40; 5% glycerol; 400 mM NaCl; 2 mM β-mercaptoethanol; 2 mM EGTA; 1 mM EDTA) 10 times. Fractions containing DDK were then concentrated using Amicon 50 KDa concentrator (Merck) and snap frozen in liquid nitrogen. Purified DDK was tested for being active.

Cdc5 purification

For purification of Cdc5, YLG46 cells were grown in 10 liters of YPR (YP supplemented with 2% raffinose) at 30°C, and overexpression of Cdc5-3FLAG was induced via addition of 2% galactose for 8 hours at 30°C. Cells were then harvested and pellets washed first with sorbitol buffer (25 mM HEPES-KOH, pH 7.6; 1 M sorbitol) and then with buffer I (100 mM HEPES-KOH, pH 7.6; 0.02% NP-40; 5% glycerol; 500 mM NaCl). Pellets were then resuspended in 1 volume lysis Buffer (100 mM HEPES-KOH, pH 7.6; 0.02% NP-40; 5% glycerol; 500 mM NaCl; 2 mM β-mercaptoethanol; protease inhibitors (400 µM PMSF; 4 µM aprotinin; 4 mM benzamidin; 400 µM leupeptin; 300 µM pepstatin A; 100 nM okadaic acid)) and drop by drop snap frozen in liquid nitrogen. Frozen pellets were then lysed using Cryo Mill (Spex SamplePrep 6870) with 6 cycles at a rate of 15 cps (cycles per second) for 2 minutes each. The thawed powder was then centrifuged at 50000 rpm for 1 hour at 4°C and the clear upper phase was recovered. 1 ml bed volume FLAG agarose

resin (Merck) was added to the suspension and the suspension with the beads was stirred for 2 hours at 4°C. Beads were then recovered and washed 5 times with 5 ml of lysis buffer (without protease inhibitors) and Cdc5 was eluted via incubation with 1 ml lysis buffer (without protease inhibitors) supplemented with 0.5 mg/ml 3FLAG peptide (Merck) for 30 minutes twice. Fractions containing Cdc5-3FLAG were then concentrated using Amicon 10 KDa concentrator (Merck) and snap frozen in liquid nitrogen. Purified Cdc5-3FLAG was tested for being active.

DDK-Cdc5 complex purification

For co-purification of DDK-Cdc5, YLG53 cells were grown in 10 liters of YPR (YP supplemented with 2% raffinose) at 30°C, and overexpression of CBP-Dbf4, Cdc7 and Cdc5-3FLAG was induced via addition of 2% galactose for 6 hours at 30°C. Cells were then harvested and pellets washed first with sorbitol buffer (25 mM HEPES-KOH, pH 7.6; 1 M sorbitol) and then with buffer I (50 mM HEPES-KOH, pH 7.6; 400 mM NaCl; 0.02% NP-40; 5% glycerol). Pellets were then resuspended in 1 volume lysis buffer (50 mM HEPES-KOH, pH 7.6; 0.02% NP-40; 5% glycerol; 400 mM NaCl; 2 mM β-mercaptoethanol; protease inhibitors (400 µM PMSF, 4 µM aprotinin, 4 mM benzamidin, 400 µM leupeptin, 300 µM pepstatin A; 100 nM Okadaic acid)) and drop by drop snap frozen in liquid nitrogen. Frozen pellets were then lysed using Cryo Mill (Spex SamplePrep 6870) with 6 cycles at a rate of 15 cps (cycles per second) for 2 minutes each. The thawed powder was then centrifuged at 50000 rpm for 1 hour at 4°C and the clear upper phase was recovered. 2 mM $CaCl_2$ was then added to the suspension together with 1.5 ml bed volume calmodulin affinity resin (Agilent) and the suspension with the beads was stirred for 3 hours at 4°C. Beads were then recovered and washed 5 times with 3 ml CBP-wash buffer (50 mM HEPES-KOH, pH 7.6; 0.02% NP-40; 5% glycerol; 400 mM NaCl; 2 mM β-mercaptoethanol; 2 mM $CaCl_2$; 0.1 mM EGTA; 0.1 mM EDTA). Elution was then preformed with 2 ml of CBP-elution buffer (50 mM HEPES-KOH, pH 7.6; 0.02% NP-40; 5% glycerol; 400 mM NaCl; 2 mM β-mercaptoethanol; 2 mM EGTA; 1 mM EDTA) 10 times. Fractions containing DDK-Cdc5 were then pooled together, and subjected to a FLAG pulldown via addition of 0.5 ml bed volume FLAG beads and incubated for 2 hours at 4°C. Beads were then recovered and washed 5 times with 2.5 ml of FLAG-buffer (50 mM HEPES-KOH, pH 7.6; 0.02% NP-40; 5% glycerol; 400 mM NaCl; 2 mM β-mercaptoethanol) and DDK-Cdc5

was eluted via incubation with 0.5 ml FLAG-buffer supplemented with 0.5 mg/ml 3FLAG peptide (Merck) for 30 minutes twice. Purified DDK-Cdc5 was tested for being active.

CDK purification

CDK was purified from bacterial cells carrying the pRIL plasmid as previously described [146]. Cells carrying the pRIL plasmid (chloramphenicol resistant) were transformed separately with CDK2 plasmid (Human GST-CDK2; ampicillin resistant) or with the CycA plasmid (bovine CycA-His-ΔN170; ampicillin resistant) and colonies of each were separately inoculated in LB medium (supplemented with 35 μg/ml chloramphenicol and 0.1 μg/ml ampicillin) overnight, and subsequently diluted 1/100 in 1 liter LB (supplemented with antibiotics) each. At OD_{600} around 0.8 cells were cooled down, and induction was performed via addition of 1 mM IPTG overnight at 20°C. Cells were then collected and the pellet resuspended in lysis buffer 1 (20 mM HEPES-KOH, pH 7.6, 300 mM NaCl, 5 mM β-mercaptoethanol, 0.01% NP-40, cOmplete protease inhibitor (Roche)). Resuspended cells were then lysed using an Avestin homogenizer (Avestin) with three rounds at 1000 bar, and after lysis supplemented with 1 mM PMSF. Subsequently, lysates were centrifuged at 45000 rpm for 1 hour at 4°C. The clear upper phase was recovered for each and based on gel quantification the two extracts were mixed to have a similar ratio of the two subunits of the complex and stirred at 4°C for 1 hour for CDK2-CycA complex formation. 1 ml bed volume of glutathione agarose beads was added to the mixture and incubated for 2 hours at 4°C. Beads were then washed 5 times with lysis buffer 1 and 3 times with lysis buffer 2 (as lysis buffer 1 but with 150 mM NaCl instead of 300 mM) and CDK-CycA was eluted incubating the beads with 250 U GST-PreScission protease. Eluate was then supplemented with 6 mM imidazole and NaCl concentration brought back to 300 mM and incubated with Ni-NTA agarose beads (Qiagen). Elution was then achieved with 8 elution steps using 1 ml of elution buffer (150 mM NaCl, 20 mM HEPES-KOH, pH 7.6, 5 mM β-mercaptoethanol, 0.01% NP-40, 250 mM imidazole, 5% glycerol). Aliquots of the fraction containing CDK were then prepared and snap frozen in liquid nitrogen. Purified CDK was tested for being active.

Mus81-Mms4 purification

For co-purification of Mus81-Mms4, YLG47 cells were grown in 10 liters of YPR (YP supplemented with 2% raffinose) at 30°C, and overexpression of Mus81-9Myc and Mms4-3FLAG was induced via addition of 2% galactose for 4 hours at 30°C. Cells were then harvested and pellets washed first with sorbitol buffer (25 mM HEPES-KOH, pH 7.6; 1 M sorbitol) and then with buffer I (500 mM NaCl; 40 mM Tris-HCl, pH 7.5; 0.05% NP-40; 10% glycerol). Pellets were then resuspended in 1 volume lysis buffer (500 mM NaCl; 40 mM Tris-HCl, pH 7.5; 0.05% NP-40; 10% glycerol; 1 mM DTT; protease inhibitors (400 µM PMSF; 4 µM aprotinin; 4 mM benzamidin; 400 µM leupeptin; 300 µM pepstatin A; 100 nM okadaic acid)) and drop by drop snap frozen in liquid nitrogen. Frozen pellets were then lysed using Cryo Mill (Spex SamplePrep 6870) with 6 cycles at a rate of 15 cps (cycles per second) for 2 minutes each. The thawed powder was then centrifuged at 50000 rpm for 1 hour at 4°C and the clear upper phase was recovered. Subsequently, 1 ml bed volume FLAG agarose resin (Merck) was added to the suspension and the suspension with the beads was stirred for 2 hours at 4°C. Beads were then recovered, washed 5 times with 5 ml of lysis buffer (without protease inhibitors) and resuspended in 5 ml lysis buffer (without protease inhibitors) supplemented with 2 mM $MnCl_2$ and 5000 U λ phosphatase (NEB) and stirred for 1 hour at 4°C. Beads were then washed 5 times with 5 ml of lysis buffer and Mus81-Mms4 was eluted via incubation with 1 ml lysis buffer (without protease inhibitors) supplemented with 0.5 mg/ml 3FLAG peptide (Merck) for 30 minutes twice. Eluted fractions 1 and 2 were pooled together, concentrated up to a volume of 500 µl using an Amicon 10 KDa concentrator (Merck) and loaded on a Superdex200 10/300 (GE) equilibrated with SEC buffer (500 mM NaCl; 40 mM Tris-HCl, pH 7.5; 0.02% NP-40; 10% glycerol; 1 mM DTT). Fractions containing Mus81-Mms4 were pooled together, concentrated using an Amicon 10 KDa concentrator (Merck) and snap frozen in liquid nitrogen.

Xrs2-FHA$^{(1-117)}$ purification

A construct spanning amino acids 1 to 117 of Xrs2 was purified from bacterial cells carrying the pRIL plasmid (chloramphenicol resistant). Cells were transformed with a plasmid carrying the Xrs2-FHA$^{(1-117)}$ construct with a N-terminal twin-strep tag and a single colony was inoculated in LB medium (supplemented with 35 µg/ml chloramphenicol and 30 µg/ml kanamycin) overnight, and subsequently diluted 1/100

in 1 liter LB medium (with antibiotics). At OD_{600} around 0.8 cells were cooled down, and induction was performed via addition of 1 mM IPTG overnight at 18°C. Cells were then collected and the pellet resuspended in lysis buffer 1 (500 mM NaCl; 50 mM Tris-HCl pH 7.5; 10% glycerol; 0.02% NP-40; 2 mM β-mercaptoethanol; cOmplete protease inhibitor (Roche)). Resuspended cells were then lysed using an Avestin homogenizer (Avestin) with three rounds at 1000 bar, and after lysis supplemented with 1 mM PMSF. Subsequently, lysates were centrifuged at 40000 rpm for 1 hour at 4°C. The clear upper phase was recovered and incubated with 1 ml bed volume strep-tactin sepharose resin (IBA) for 2 hours at 4°C. The resin was then washed 5 times with 5 ml of lysis buffer 1. Elution was achieved with addition of 1 ml of elution buffer (500 mM NaCl; 50 mM Tris-HCl pH 7.5; 10% glycerol; 0.02% NP-40; 2 mM β-mercaptoethanol; 5 mM desthiobiotin) followed by incubation for 5 minutes and collection. A total of 10 elutions were performed as described. Fractions containing Xrs2-FHA$^{(1-117)}$ were then pooled together, concentrated using an Amicon 3 KDa concentrator (Merck) and loaded on a Superdex200 10/300 (GE) equilibrated with SEC buffer (150 mM NaCl; 50 mM Tris pH 7.5; 10% glycerol; 0.02% NP-40; 2 mM β-mercaptoethanol). Fractions containing Xrs2-FHA$^{(1-117)}$ in a size range that would fit with a molecular weight around 20 KDa (based on molecular weight standards) were pooled together and concentrated. Aliquots were then prepared and snap frozen in liquid nitrogen for storage at -80°C.

MRX purification

The MRX complex was purified as previously described ([147]). Briefly, MRX was purified from Sf9 insect cells with Mre11 and Xrs2 carrying a C-terminal His and FLAG-tag, respectively, via affinity chromatography. First the soluble fraction of the extracts was subjected to Ni-NTA affinity chromatography using Ni-NTA resin (Qiagen) and eluted with 400 mM imidazole. Eluted fractions were then incubated with M2-anti FLAG resin (Sigma) and eluted using 0.2 mg/ml FLAG peptide (Sigma).

Sae2 purification

Sae2 was purified as previously described [120]. Briefly, Sae2 was purified from Sf9 insect cells. Sae2 carries a MBP-tag at its N-terminus and a His-tag at its C-terminus. Affinity chromatography using amylose resin (NEB) was used for the first purification step.

Eluted Sae2 was treated with PreScission protease to cleave the MBP-tag. Sae2 was then subjected to Ni-NTA affinity chromatography using Ni-NTA resin (Qiagen). Sae2 obtained with this protocol would retain the cellular phosphorylation. To obtain dephosphorylated Sae2 a treatment with λ phosphatase (NEB) was included after elution from amylose resin, before PreScission mediated cleavage of MBP-tag.

DNA end resection assays

In vitro DNA end resection assays to monitor the endonucleolytic activity of the Sae2-MRX complex on a template DNA were performed as previously described [120].

***In vitro* kinase assays**

For the *in vitro* kinase assays 2 pmol of each kinase were used. The kinases used in the assays were first treated with 100 U λ phosphatase (NEB) in the presence of 2 mM manganese chloride ($MnCl_2$) to remove possible inhibitory phosphorylation derived from cells. 10 pmol of substrate of interest were then added to the kinase(s) in reaction buffer (100 mM NaCl; 50 mM HEPES-KOH, pH 7.6; 5% glycerol; 10 mM magnesium acetate; 10 mM magnesium chloride; 0.02% NP-40; 50 mM β-glycerophosphate; 10 mM sodium orthovanadate; 50 mM sodium fluoride; 2 mM β-mercaptoethanol; 5 μg bovine serum albumin) supplemented with a mixture of cold ATP (at a final concentration of 2 mM) and 5 μci ATP γ-32P (Perkin Elmer) for 30 minutes at 30°C. Samples were then resolved on 4-12% Bis-Tris acrylamide gel (Invitrogen) and analyzed by autoradiography using a Typhoon FLA 9500 imager (GE).

Sae2 oligomeric state

Cells YLG211 and YLG214 were grown in YPD and arrested in M with nocodazole. 800 ODs (1 OD corresponds to around $2x10^7$ cells) of cells were collected and washed twice with sorbitol buffer (25 mM HEPES-KOH, pH 7.6; 1 M sorbitol). Pellets were then resuspended in 1 volume lysis buffer (150 mM NaCl; 50 mM Tris-HCl, pH 7.5; 0.05% NP-40; 10% glycerol; 2 mM β-mercaptoethanol; 10 mM sodium fluoride; 20 mM β-glycerophosphate; protease inhibitors (400 μM PMSF, 4 μM aprotinin, 4 mM benzamidin, 400 μM leupeptin, 300 μM pepstatin A; 100 nM okadaic acid)) and drop by drop snap frozen in liquid nitrogen. Frozen pellets were then lysed using Cryo Mill (Spex

SamplePrep 6870) with 6 cycles at a rate of 15 cps (cycles per second) for 2 minutes each. Thawed extracts were then spun at 50000 rpm for 1 hour at 4°C and the supernatant was recovered and supplemented with 250 µl bed volume of FLAG agarose resin (to pulldown Sae2-3FLAG) and incubated at 4°C for 2 hours. Beads were then recovered and washed 5 times with 1 ml of lysis buffer and Sae2-FLAG was eluted via incubation with 1 ml lysis buffer supplemented with 0.5 mg/ml 3FLAG peptide (Merck) for 30 minutes twice. Elutions were pooled together and spun at 20000 g for 20 minutes at 4°C and subjected to size exclusion chromatography on a Superdex200 10/300 (GE) pre equilibrated in SEC-buffer (150 mM NaCl; 50mM Tris HCl, pH 7.5; 0.02% NP-40; 10% glycerol; 2 mM β-mercaptoethanol; 10 mM sodium fluoride; 20 mM β-glycerophosphate). To increase protein concentrations before loading on gel, fractions were then supplemented with 1/10 volume of TCA 55% and after 10 minutes on ice spun down. The pellet containing precipitated proteins was the resuspended in 25 µl of HU buffer and fractions were loaded on 4-12% Bis-Tris acrylamide gels to monitor their elution profile.

In vitro pulldown

40 pmol of Sae2 were either mock treated (no addition of the kinase) or treated with 5 pmol of DDK in the presence of 5 mM ATP for 30 minutes at 30°C in reaction buffer (100 mM NaCl; 50 mM Tris-HCl pH 7.5; 5% glycerol; 10 mM magnesium acetate; 10 mM magnesium chloride; 0.02% NP-40; 50 mM β-glycerophosphate; 2 mM β-mercaptoethanol). After the mock/kinase reaction, 16 pmol of strep-Xrs2-FHA$^{(1-117)}$ were added to each reaction (a reaction containing only Sae2 mock treated without addition of strep-Xrs2-FHA$^{(1-117)}$ was also performed as control of possible unspecific binding to the beads) and incubated for 30 minutes at 30°C. 2 µl bed volume of magnetic strep-beads (MagStrep-Type3-XT beads; IBA) were added to each reaction and incubated for 30 minutes at 30°C. Beads were then collected, washed with reaction buffer 5 times and eluted via boiling at 95°C for 2 minutes in loading dye. Samples were then run on 4-12% Bis-Tris acrylamide gel (Invitrogen) and stained with GelCode Blue (Thermo Fisher).

Appendix

List of abbreviations

AID	auxin inducible degron
Alt-ej	alternative-end joining
ATP	adenosine triphosphate
BIR	break induced replication
BSA	bovine serum albumin
CDK	cyclin-dependent kinase
CHX	Cycloheximide
CPT	camptotechin
DDK	dbf4-dependent kinase
DMSO	dimethyl sulfoxide
DNA	deoxyribonucleic acid
DSB	double-strand break
(d)HJ	double holliday junction
dsDNA	double stranded DNA
FACS	fluorescence-activated cell sorting
FHA	forkhead-associated
GAL	galactose
GFP	green fluorescent protein
GST	glutathione S-transferase
HR	homologous recombination
IAA	indole-3 acetic acid
IP	immunoprecipitation
MMEJ	microhomology-mediated end joining
MS	mass spectrometry
MRX	Mre11-Rad50-Xrs2
MRN	Mre11-Rad50-Nbs1
NAA	1-napthylacetic aicd
NHEJ	non homologous end joining
PBD	polo box domain
PCR	polymerase chain reaction
PTM	post translationl modification
RPA	replication protein A
SDSA	synthesys-dependent strand annealing
SSA	single strand annealing
ssDNA	single stranded DNA
TMEJ	Theta-mediated end joining

References

1. Sefton, B. M. & Shenolikar, S. Overview of protein phosphorylation. *Curr Protoc Protein Sci* Chapter 13, Unit13.1–13.1.5 (2001).
2. Malumbres, M. Cyclin-dependent kinases. *Genome Biol.* 15, 122–10 (2014).
3. Bloom, J. & Cross, F. R. Multiple levels of cyclin specificity in cell-cycle control. *Nat Rev Mol Cell Biol* 8, 149–160 (2007).
4. Tanaka, S. *et al.* CDK-dependent phosphorylation of Sld2 and Sld3 initiates DNA replication in budding yeast. *Nature* 445, 328–332 (2007).
5. Zegerman, P. & Diffley, J. F. X. Phosphorylation of Sld2 and Sld3 by cyclin-dependent kinases promotes DNA replication in budding yeast. *Nature* 445, 281–285 (2007).
6. Bell, S. P. & Labib, K. Chromosome Duplication in Saccharomyces cerevisiae. *Genetics* 203, 1027–1067 (2016).
7. Nguyen, V. Q., Co, C. & Li, J. J. Cyclin-dependent kinases prevent DNA re-replication through multiple mechanisms. *Nature* 411, 1068–1073 (2001).
8. Reusswig, K.-U., Zimmermann, F., Galanti, L. & Pfander, B. Robust Replication Control Is Generated by Temporal Gaps between Licensing and Firing Phases and Depends on Degradation of Firing Factor Sld2. *Cell Rep* 17, 556–569 (2016).
9. Huertas, P., Cortés-Ledesma, F., Sartori, A. A., Aguilera, A. & Jackson, S. P. CDK targets Sae2 to control DNA-end resection and homologous recombination. *Nature* 455, 689–692 (2008).
10. Chen, X. *et al.* Cell cycle regulation of DNA double-strand break end resection by Cdk1-dependent Dna2 phosphorylation. *Nat. Struct. Mol. Biol.* 18, 1015–1019 (2011).
11. Bantele, S. C., Ferreira, P., Gritenaite, D., Boos, D. & Pfander, B. Targeting of the Fun30 nucleosome remodeller by the Dpb11 scaffold facilitates cell cycle-regulated DNA end resection. *Elife* 6, 836 (2017).
12. Matos, J., Blanco, M. G. & West, S. C. Cell-cycle kinases coordinate the resolution of recombination intermediates with chromosome segregation. *Cell Rep* 4, 76–86 (2013).
13. Princz, L. N. *et al.* Dbf4-dependent kinase and the Rtt107 scaffold promote Mus81-Mms4 resolvase activation during mitosis. *EMBO J.* 36, 664–678 (2017).
14. Wan, L. *et al.* Cdc28-Clb5 (CDK-S) and Cdc7-Dbf4 (DDK) collaborate to initiate meiotic recombination in yeast. *Genes Dev.* 22, 386–397 (2008).
15. Jackson, A. L., Pahl, P. M., Harrison, K., Rosamond, J. & Sclafani, R. A. Cell cycle regulation of the yeast Cdc7 protein kinase by association with the Dbf4 protein. *Mol. Cell. Biol.* 13, 2899–2908 (1993).
16. Nougarède, R., Seta, Della, F., Zarzov, P. & Schwob, E. Hierarchy of S-phase-promoting factors: yeast Dbf4-Cdc7 kinase requires prior S-phase cyclin-dependent kinase activation. *Mol. Cell. Biol.* 20, 3795–3806 (2000).
17. Ferreira, M. F., Santocanale, C., Drury, L. S. & Diffley, J. F. Dbf4p, an essential S phase-promoting factor, is targeted for degradation by the anaphase-promoting complex. *Mol. Cell. Biol.* 20, 242–248 (2000).
18. Oshiro, G., Owens, J. C., Shellman, Y., Sclafani, R. A. & Li, J. J. Cell cycle control of Cdc7p kinase activity through regulation of Dbf4p stability. *Mol. Cell. Biol.* 19, 4888–4896 (1999).
19. Bousset, K. & Diffley, J. F. The Cdc7 protein kinase is required for origin firing during S phase. *Genes Dev.* 12, 480–490 (1998).

20. Donaldson, A. D., Fangman, W. L. & Brewer, B. J. Cdc7 is required throughout the yeast S phase to activate replication origins. *Genes Dev.* 12, 491–501 (1998).
21. Sheu, Y.-J. & Stillman, B. The Dbf4-Cdc7 kinase promotes S phase by alleviating an inhibitory activity in Mcm4. *Nature* 463, 113–117 (2010).
22. Hiraga, S.-I. *et al.* Rif1 controls DNA replication by directing Protein Phosphatase 1 to reverse Cdc7-mediated phosphorylation of the MCM complex. *Genes Dev.* 28, 372–383 (2014).
23. Natsume, T. *et al.* Kinetochores coordinate pericentromeric cohesion and early DNA replication by Cdc7-Dbf4 kinase recruitment. *Mol. Cell* 50, 661–674 (2013).
24. Matos, J. *et al.* Dbf4-dependent CDC7 kinase links DNA replication to the segregation of homologous chromosomes in meiosis I. *Cell* 135, 662–678 (2008).
25. Argunhan, B. *et al.* Fundamental cell cycle kinases collaborate to ensure timely destruction of the synaptonemal complex during meiosis. *EMBO J.* 36, 2488–2509 (2017).
26. Sasanuma, H. *et al.* Cdc7-dependent phosphorylation of Mer2 facilitates initiation of yeast meiotic recombination. *Genes Dev.* 22, 398–410 (2008).
27. Katis, V. L. *et al.* Rec8 phosphorylation by casein kinase 1 and Cdc7-Dbf4 kinase regulates cohesin cleavage by separase during meiosis. *Dev. Cell* 18, 397–409 (2010).
28. Lee, S.-Y., Jang, C. & Lee, K.-A. Polo-like kinases (plks), a key regulator of cell cycle and new potential target for cancer therapy. *Dev Reprod* 18, 65–71 (2014).
29. Elia, A. E. H. *et al.* The molecular basis for phosphodependent substrate targeting and regulation of Plks by the Polo-box domain. *Cell* 115, 83–95 (2003).
30. Endicott, J. A., Noble, M. E. M. & Johnson, L. N. The structural basis for control of eukaryotic protein kinases. *Annu. Rev. Biochem.* 81, 587–613 (2012).
31. Cheng, L., Hunke, L. & Hardy, C. F. Cell cycle regulation of the Saccharomyces cerevisiae polo-like kinase cdc5p. *Mol. Cell. Biol.* 18, 7360–7370 (1998).
32. Darieva, Z. *et al.* Polo kinase controls cell-cycle-dependent transcription by targeting a coactivator protein. *Nature* 444, 494–498 (2006).
33. Asano, S. *et al.* Concerted mechanism of Swe1/Wee1 regulation by multiple kinases in budding yeast. *EMBO J.* 24, 2194–2204 (2005).
34. Alexandru, G., Uhlmann, F., Mechtler, K., Poupart, M. A. & Nasmyth, K. Phosphorylation of the cohesin subunit Scc1 by Polo/Cdc5 kinase regulates sister chromatid separation in yeast. *Cell* 105, 459–472 (2001).
35. Stegmeier, F. & Amon, A. Closing mitosis: the functions of the Cdc14 phosphatase and its regulation. *Annu Rev Genet* 38, 203–232 (2004).
36. Botchkarev, V. V. & Haber, J. E. Functions and regulation of the Polo-like kinase Cdc5 in the absence and presence of DNA damage. *Curr Genet* 64, 87–96 (2018).
37. Gallo-Fernández, M., Saugar, I., Ortiz-Bazán, M. Á., Vázquez, M. V. & Tercero, J. A. Cell cycle-dependent regulation of the nuclease activity of Mus81-Eme1/Mms4. *Nucleic Acids Res.* 40, 8325–8335 (2012).
38. Attner, M. A., Miller, M. P., Ee, L.-S., Elkin, S. K. & Amon, A. Polo kinase Cdc5 is a central regulator of meiosis I. *Proc. Natl. Acad. Sci. U.S.A.* 110, 14278–14283 (2013).
39. Deegan, T. D., Yeeles, J. T. & Diffley, J. F. Phosphopeptide binding by Sld3 links Dbf4-dependent kinase to MCM replicative helicase activation. *EMBO J.* 35, 961–973 (2016).

40. Cho, W.-H., Lee, Y.-J., Kong, S.-I., Hurwitz, J. & Lee, J.-K. CDC7 kinase phosphorylates serine residues adjacent to acidic amino acids in the minichromosome maintenance 2 protein. *Proc. Natl. Acad. Sci. U.S.A.* 103, 11521–11526 (2006).
41. Charych, D. H. *et al.* Inhibition of Cdc7/Dbf4 kinase activity affects specific phosphorylation sites on MCM2 in cancer cells. *J Cell Biochem* 104, 1075–1086 (2008).
42. Montagnoli, A. *et al.* Identification of Mcm2 phosphorylation sites by S-phase-regulating kinases. *J. Biol. Chem.* 281, 10281–10290 (2006).
43. Hardy, C. F. & Pautz, A. A novel role for Cdc5p in DNA replication. *Mol. Cell. Biol.* 16, 6775–6782 (1996).
44. Miller, C. T., Gabrielse, C., Chen, Y.-C. & Weinreich, M. Cdc7p-Dbf4p regulates mitotic exit by inhibiting Polo kinase. *PLoS Genet.* 5, e1000498 (2009).
45. Chen, Y.-C. & Weinreich, M. Dbf4 regulates the Cdc5 Polo-like kinase through a distinct non-canonical binding interaction. *J. Biol. Chem.* 285, 41244–41254 (2010).
46. Ciccia, A. & Elledge, S. J. The DNA damage response: making it safe to play with knives. *Mol. Cell* 40, 179–204 (2010).
47. Vilenchik, M. M. & Knudson, A. G. Endogenous DNA double-strand breaks: production, fidelity of repair, and induction of cancer. *Proc. Natl. Acad. Sci. U.S.A.* 100, 12871–12876 (2003).
48. Chang, H. H. Y., Pannunzio, N. R., Adachi, N. & Lieber, M. R. Non-homologous DNA end joining and alternative pathways to double-strand break repair. *Nat Rev Mol Cell Biol* 18, 495–506 (2017).
49. Daley, J. M., Palmbos, P. L., Wu, D. & Wilson, T. E. Nonhomologous end joining in yeast. *Annu Rev Genet* 39, 431–451 (2005).
50. Daley, J. M. & Wilson, T. E. Rejoining of DNA double-strand breaks as a function of overhang length. *Mol. Cell. Biol.* 25, 896–906 (2005).
51. Gottlieb, T. M. & Jackson, S. P. The DNA-dependent protein kinase: requirement for DNA ends and association with Ku antigen. *Cell* 72, 131–142 (1993).
52. Ramsden, D. A. & Gellert, M. Ku protein stimulates DNA end joining by mammalian DNA ligases: a direct role for Ku in repair of DNA double-strand breaks. *EMBO J.* 17, 609–614 (1998).
53. Wilson, T. E., Grawunder, U. & Lieber, M. R. Yeast DNA ligase IV mediates non-homologous DNA end joining. *Nature* 388, 495–498 (1997).
54. Seol, J.-H., Shim, E. Y. & Lee, S. E. Microhomology-mediated end joining: Good, bad and ugly. *Mutat Res* 809, 81–87 (2018).
55. Sfeir, A. & Symington, L. S. Microhomology-Mediated End Joining: A Back-up Survival Mechanism or Dedicated Pathway? *Trends Biochem Sci* 40, 701–714 (2015).
56. Audebert, M., Salles, B. & Calsou, P. Involvement of poly(ADP-ribose) polymerase-1 and XRCC1/DNA ligase III in an alternative route for DNA double-strand breaks rejoining. *J. Biol. Chem.* 279, 55117–55126 (2004).
57. Simsek, D. *et al.* DNA ligase III promotes alternative nonhomologous end-joining during chromosomal translocation formation. *PLoS Genet.* 7, e1002080 (2011).
58. Bennardo, N., Cheng, A., Huang, N. & Stark, J. M. Alternative-NHEJ is a mechanistically distinct pathway of mammalian chromosome break repair. *PLoS Genet.* 4, e1000110 (2008).

59. Mateos-Gomez, P. A. *et al.* Mammalian polymerase θ promotes alternative NHEJ and suppresses recombination. *Nature* 518, 254–257 (2015).
60. Mateos-Gomez, P. A. *et al.* The helicase domain of Polθ counteracts RPA to promote alt-NHEJ. *Nat. Struct. Mol. Biol.* 24, 1116–1123 (2017).
61. Ranjha, L., Howard, S. M. & Cejka, P. Main steps in DNA double-strand break repair: an introduction to homologous recombination and related processes. *Chromosoma* 127, 187–214 (2018).
62. Brambati, A., Barry, R. M. & Sfeir, A. DNA polymerase theta (Polθ) - an error-prone polymerase necessary for genome stability. *Curr Opin Genet Dev* 60, 119–126 (2020).
63. Wyatt, D. W. *et al.* Essential Roles for Polymerase θ-Mediated End Joining in the Repair of Chromosome Breaks. *Mol. Cell* 63, 662–673 (2016).
64. Cejka, P. DNA End Resection: Nucleases Team Up with the Right Partners to Initiate Homologous Recombination. *J. Biol. Chem.* 290, 22931–22938 (2015).
65. Reginato, G. & Cejka, P. The MRE11 complex: A versatile toolkit for the repair of broken DNA. *DNA Repair (Amst)* 91-92, 102869 (2020).
66. Symington, L. S. Mechanism and regulation of DNA end resection in eukaryotes. *Crit. Rev. Biochem. Mol. Biol.* 51, 195–212 (2016).
67. Symington, L. S. & Gautier, J. Double-strand break end resection and repair pathway choice. *Annu Rev Genet* 45, 247–271 (2011).
68. Johzuka, K. & Ogawa, H. Interaction of Mre11 and Rad50: two proteins required for DNA repair and meiosis-specific double-strand break formation in Saccharomyces cerevisiae. *Genetics* 139, 1521–1532 (1995).
69. Keeney, S. & Kleckner, N. Covalent protein-DNA complexes at the 5' strand termini of meiosis-specific double-strand breaks in yeast. *Proc. Natl. Acad. Sci. U.S.A.* 92, 11274–11278 (1995).
70. Sartori, A. A. *et al.* Human CtIP promotes DNA end resection. *Nature* 450, 509–514 (2007).
71. Cannavo, E. & Cejka, P. Sae2 promotes dsDNA endonuclease activity within Mre11-Rad50-Xrs2 to resect DNA breaks. *Nature* 514, 122–125 (2014).
72. Reginato, G., Cannavo, E. & Cejka, P. Physiological protein blocks direct the Mre11-Rad50-Xrs2 and Sae2 nuclease complex to initiate DNA end resection. *Genes Dev.* 31, 2325–2330 (2017).
73. Anand, R., Ranjha, L., Cannavo, E. & Cejka, P. Phosphorylated CtIP Functions as a Co-factor of the MRE11-RAD50-NBS1 Endonuclease in DNA End Resection. *Mol. Cell* 64, 940–950 (2016).
74. Neale, M. J., Pan, J. & Keeney, S. Endonucleolytic processing of covalent protein-linked DNA double-strand breaks. *Nature* 436, 1053–1057 (2005).
75. Shibata, A. *et al.* DNA double-strand break repair pathway choice is directed by distinct MRE11 nuclease activities. *Mol. Cell* 53, 7–18 (2014).
76. Garcia, V., Phelps, S. E. L., Gray, S. & Neale, M. J. Bidirectional resection of DNA double-strand breaks by Mre11 and Exo1. *Nature* 479, 241–244 (2011).
77. Deshpande, R. A., Lee, J.-H. & Paull, T. T. Rad50 ATPase activity is regulated by DNA ends and requires coordination of both active sites. *Nucleic Acids Res.* 45, 5255–5268 (2017).
78. Oh, J., Al-Zain, A., Cannavo, E., Cejka, P. & Symington, L. S. Xrs2 Dependent and Independent Functions of the Mre11-Rad50 Complex. *Mol. Cell* 64, 405–415 (2016).

79. Anand, R. *et al.* NBS1 promotes the endonuclease activity of the MRE11-RAD50 complex by sensing CtIP phosphorylation. *EMBO J.* 38, e101005 (2019).
80. Wang, W., Daley, J. M., Kwon, Y., Krasner, D. S. & Sung, P. Plasticity of the Mre11-Rad50-Xrs2-Sae2 nuclease ensemble in the processing of DNA-bound obstacles. *Genes Dev.* 31, 2331–2336 (2017).
81. Bonetti, D., Clerici, M., Manfrini, N., Lucchini, G. & Longhese, M. P. The MRX complex plays multiple functions in resection of Yku- and Rif2-protected DNA ends. *PLoS One* 5, e14142 (2010).
82. Keeney, S., Giroux, C. N. & Kleckner, N. Meiosis-specific DNA double-strand breaks are catalyzed by Spo11, a member of a widely conserved protein family. *Cell* 88, 375–384 (1997).
83. Langerak, P., Mejia-Ramirez, E., Limbo, O. & Russell, P. Release of Ku and MRN from DNA ends by Mre11 nuclease activity and Ctp1 is required for homologous recombination repair of double-strand breaks. *PLoS Genet.* 7, e1002271 (2011).
84. Chanut, P., Britton, S., Coates, J., Jackson, S. P. & Calsou, P. Coordinated nuclease activities counteract Ku at single-ended DNA double-strand breaks. *Nat Commun* 7, 12889 (2016).
85. Mimitou, E. P. & Symington, L. S. Ku prevents Exo1 and Sgs1-dependent resection of DNA ends in the absence of a functional MRX complex or Sae2. *EMBO J.* 29, 3358–3369 (2010).
86. Symington, L. S. End resection at double-strand breaks: mechanism and regulation. *Cold Spring Harb Perspect Biol* 6, a016436–a016436 (2014).
87. Tran, P. T., Erdeniz, N., Dudley, S. & Liskay, R. M. Characterization of nuclease-dependent functions of Exo1p in Saccharomyces cerevisiae. *DNA Repair (Amst)* 1, 895–912 (2002).
88. Bae, S. H. *et al.* Dna2 of Saccharomyces cerevisiae possesses a single-stranded DNA-specific endonuclease activity that is able to act on double-stranded DNA in the presence of ATP. *J. Biol. Chem.* 273, 26880–26890 (1998).
89. Zhu, Z., Chung, W.-H., Shim, E. Y., Lee, S. E. & Ira, G. Sgs1 helicase and two nucleases Dna2 and Exo1 resect DNA double-strand break ends. *Cell* 134, 981–994 (2008).
90. Levikova, M., Klaue, D., Seidel, R. & Cejka, P. Nuclease activity of Saccharomyces cerevisiae Dna2 inhibits its potent DNA helicase activity. *Proc. Natl. Acad. Sci. U.S.A.* 110, E1992–2001 (2013).
91. Levikova, M., Pinto, C. & Cejka, P. The motor activity of DNA2 functions as an ssDNA translocase to promote DNA end resection. *Genes Dev.* 31, 493–502 (2017).
92. Miller, A. S. *et al.* A novel role of the Dna2 translocase function in DNA break resection. *Genes Dev.* 31, 503–510 (2017).
93. Lee, C.-S. *et al.* Chromosome position determines the success of double-strand break repair. *Proc. Natl. Acad. Sci. U.S.A.* 113, E146–54 (2016).
94. Wold, M. S. Replication protein A: a heterotrimeric, single-stranded DNA-binding protein required for eukaryotic DNA metabolism. *Annu. Rev. Biochem.* 66, 61–92 (1997).
95. Song, B. & Sung, P. Functional interactions among yeast Rad51 recombinase, Rad52 mediator, and replication protein A in DNA strand exchange. *J. Biol. Chem.* 275, 15895–15904 (2000).
96. Zelensky, A., Kanaar, R. & Wyman, C. Mediators of homologous DNA pairing. *Cold Spring Harb Perspect Biol* 6, a016451 (2014).

97. Prakash, R., Zhang, Y., Feng, W. & Jasin, M. Homologous recombination and human health: the roles of BRCA1, BRCA2, and associated proteins. *Cold Spring Harb Perspect Biol* 7, a016600 (2015).
98. San Filippo, J., Sung, P. & Klein, H. Mechanism of eukaryotic homologous recombination. *Annu. Rev. Biochem.* 77, 229–257 (2008).
99. Wilson, M. A. *et al.* Pif1 helicase and Polδ promote recombination-coupled DNA synthesis via bubble migration. *Nature* 502, 393–396 (2013).
100. Li, X., Stith, C. M., Burgers, P. M. & Heyer, W.-D. PCNA is required for initiation of recombination-associated DNA synthesis by DNA polymerase delta. *Mol. Cell* 36, 704–713 (2009).
101. Duckett, D. R. *et al.* The structure of the Holliday junction, and its resolution. *Cell* 55, 79–89 (1988).
102. Cejka, P., Plank, J. L., Bachrati, C. Z., Hickson, I. D. & Kowalczykowski, S. C. Rmi1 stimulates decatenation of double Holliday junctions during dissolution by Sgs1-Top3. *Nat. Struct. Mol. Biol.* 17, 1377–1382 (2010).
103. Chen, S. H., Plank, J. L., Willcox, S., Griffith, J. D. & Hsieh, T.-S. Top3α is required during the convergent migration step of double Holliday junction dissolution. *PLoS One* 9, e83582 (2014).
104. Bizard, A. H. & Hickson, I. D. The dissolution of double Holliday junctions. *Cold Spring Harb Perspect Biol* 6, a016477 (2014).
105. Matos, J. & West, S. C. Holliday junction resolution: regulation in space and time. *DNA Repair (Amst)* 19, 176–181 (2014).
106. Blanco, M. G. & Matos, J. Hold your horSSEs: controlling structure-selective endonucleases MUS81 and Yen1/GEN1. *Front Genet* 6, 253 (2015).
107. Kaliraman, V., Mullen, J. R., Fricke, W. M., Bastin-Shanower, S. A. & Brill, S. J. Functional overlap between Sgs1-Top3 and the Mms4-Mus81 endonuclease. *Genes Dev.* 15, 2730–2740 (2001).
108. Oh, S. D., Lao, J. P., Taylor, A. F., Smith, G. R. & Hunter, N. RecQ helicase, Sgs1, and XPF family endonuclease, Mus81-Mms4, resolve aberrant joint molecules during meiotic recombination. *Mol. Cell* 31, 324–336 (2008).
109. Bastin-Shanower, S. A., Fricke, W. M., Mullen, J. R. & Brill, S. J. The mechanism of Mus81-Mms4 cleavage site selection distinguishes it from the homologous endonuclease Rad1-Rad10. *Mol. Cell. Biol.* 23, 3487–3496 (2003).
110. Ehmsen, K. T. & Heyer, W.-D. Saccharomyces cerevisiae Mus81-Mms4 is a catalytic, DNA structure-selective endonuclease. *Nucleic Acids Res.* 36, 2182–2195 (2008).
111. Ip, S. C. Y. *et al.* Identification of Holliday junction resolvases from humans and yeast. *Nature* 456, 357–361 (2008).
112. Jessop, L. & Lichten, M. Mus81/Mms4 endonuclease and Sgs1 helicase collaborate to ensure proper recombination intermediate metabolism during meiosis. *Mol. Cell* 31, 313–323 (2008).
113. Kowalczykowski, S. C. An Overview of the Molecular Mechanisms of Recombinational DNA Repair. *Cold Spring Harb Perspect Biol* 7, a016410 (2015).
114. Bhargava, R., Onyango, D. O. & Stark, J. M. Regulation of Single-Strand Annealing and its Role in Genome Maintenance. *Trends Genet* 32, 566–575 (2016).
115. Llorente, B., Smith, C. E. & Symington, L. S. Break-induced replication: what is it and what is it for? *Cell Cycle* 7, 859–864 (2008).

116. Sakofsky, C. J. & Malkova, A. Break induced replication in eukaryotes: mechanisms, functions, and consequences. *Crit. Rev. Biochem. Mol. Biol.* 52, 395–413 (2017).
117. Mathiasen, D. P. & Lisby, M. Cell cycle regulation of homologous recombination in Saccharomyces cerevisiae. *FEMS Microbiol Rev* 38, 172–184 (2014).
118. Ira, G. *et al.* DNA end resection, homologous recombination and DNA damage checkpoint activation require CDK1. *Nature* 431, 1011–1017 (2004).
119. Aylon, Y., Liefshitz, B. & Kupiec, M. The CDK regulates repair of double-strand breaks by homologous recombination during the cell cycle. *EMBO J.* 23, 4868–4875 (2004).
120. Cannavo, E. *et al.* Regulatory control of DNA end resection by Sae2 phosphorylation. *Nat Commun* 9, 4016–14 (2018).
121. Huertas, P. & Jackson, S. P. Human CtIP mediates cell cycle control of DNA end resection and double strand break repair. *J. Biol. Chem.* 284, 9558–9565 (2009).
122. Tomimatsu, N. *et al.* Phosphorylation of EXO1 by CDKs 1 and 2 regulates DNA end resection and repair pathway choice. *Nat Commun* 5, 3561–10 (2014).
123. Chen, X. *et al.* Enrichment of Cdk1-cyclins at DNA double-strand breaks stimulates Fun30 phosphorylation and DNA end resection. *Nucleic Acids Res.* 44, 2742–2753 (2016).
124. Baroni, E., Viscardi, V., Cartagena-Lirola, H., Lucchini, G. & Longhese, M. P. The functions of budding yeast Sae2 in the DNA damage response require Mec1- and Tel1-dependent phosphorylation. *Mol. Cell. Biol.* 24, 4151–4165 (2004).
125. Kim, H.-S. *et al.* Functional interactions between Sae2 and the Mre11 complex. *Genetics* 178, 711–723 (2008).
126. Fu, Q. *et al.* Phosphorylation-regulated transitions in an oligomeric state control the activity of the Sae2 DNA repair enzyme. *Mol. Cell. Biol.* 34, 778–793 (2014).
127. Yu, T.-Y., Garcia, V. E. & Symington, L. S. CDK and Mec1/Tel1-catalyzed phosphorylation of Sae2 regulate different responses to DNA damage. *Nucleic Acids Res.* 47, 11238–11249 (2019).
128. Liang, J., Suhandynata, R. T. & Zhou, H. Phosphorylation of Sae2 Mediates Forkhead-associated (FHA) Domain-specific Interaction and Regulates Its DNA Repair Function. *J. Biol. Chem.* 290, 10751–10763 (2015).
129. Wang, H. *et al.* The interaction of CtIP and Nbs1 connects CDK and ATM to regulate HR-mediated double-strand break repair. *PLoS Genet.* 9, e1003277 (2013).
130. Zdravković, A. *et al.* A conserved Ctp1/CtIP C-terminal peptide stimulates Mre11 endonuclease activity. *Proc. Natl. Acad. Sci. U.S.A.* 118, (2021).
131. Hardy, C. F., Dryga, O., Seematter, S., Pahl, P. M. & Sclafani, R. A. mcm5/cdc46-bob1 bypasses the requirement for the S phase activator Cdc7p. *Proc. Natl. Acad. Sci. U.S.A.* 94, 3151–3155 (1997).
132. Tyanova, S. *et al.* The Perseus computational platform for comprehensive analysis of (prote)omics data. *Nat Methods* 13, 731–740 (2016).
133. Lanz, M. C. *et al.* In-depth and 3-dimensional exploration of the budding yeast phosphoproteome. *EMBO Rep.* 22, e51121 (2021).
134. Shim, E. Y. *et al.* RSC mobilizes nucleosomes to improve accessibility of repair machinery to the damaged chromatin. *Mol. Cell. Biol.* 27, 1602–1613 (2007).
135. Kent, N. A., Chambers, A. L. & Downs, J. A. Dual chromatin remodeling roles for RSC during DNA double strand break induction and repair at the yeast MAT locus. *J. Biol. Chem.* 282, 27693–27701 (2007).

136. van Attikum, H., Fritsch, O. & Gasser, S. M. Distinct roles for SWR1 and INO80 chromatin remodeling complexes at chromosomal double-strand breaks. *EMBO J.* 26, 4113–4125 (2007).
137. Lademann, C. A., Renkawitz, J., Pfander, B. & Jentsch, S. The INO80 Complex Removes H2A.Z to Promote Presynaptic Filament Formation during Homologous Recombination. *Cell Rep* 19, 1294–1303 (2017).
138. Peritore, M., Reusswig, K.-U., Bantele, S. C. S., Straub, T. & Pfander, B. Strand-specific ChIP-seq at DNA breaks distinguishes ssDNA versus dsDNA binding and refutes single-stranded nucleosomes. *Mol. Cell* 81, 1841–1853.e4 (2021).
139. Hertzberg, R. P., Caranfa, M. J. & Hecht, S. M. On the mechanism of topoisomerase I inhibition by camptothecin: evidence for binding to an enzyme-DNA complex. *Biochemistry* 28, 4629–4638 (1989).
140. Eng, W. K., Faucette, L., Johnson, R. K. & Sternglanz, R. Evidence that DNA topoisomerase I is necessary for the cytotoxic effects of camptothecin. *Mol Pharmacol* 34, 755–760 (1988).
141. Vaze, M. B. *et al.* Recovery from checkpoint-mediated arrest after repair of a double-strand break requires Srs2 helicase. *Mol. Cell* 10, 373–385 (2002).
142. Nishimura, K., Fukagawa, T., Takisawa, H., Kakimoto, T. & Kanemaki, M. An auxin-based degron system for the rapid depletion of proteins in nonplant cells. *Nat Methods* 6, 917–922 (2009).
143. Morawska, M. & Ulrich, H. D. An expanded tool kit for the auxin-inducible degron system in budding yeast. *Yeast* 30, 341–351 (2013).
144. Bishop, A. C. *et al.* A chemical switch for inhibitor-sensitive alleles of any protein kinase. *Nature* 407, 395–401 (2000).
145. Pinto, C., Anand, R. & Cejka, P. Methods to Study DNA End Resection II: Biochemical Reconstitution Assays. *Meth. Enzymol.* 600, 67–106 (2018).
146. Brown, N. R. *et al.* The crystal structure of cyclin A. *Structure* 3, 1235–1247 (1995).
147. Cannavo, E., Cejka, P. & Kowalczykowski, S. C. Relationship of DNA degradation by Saccharomyces cerevisiae exonuclease 1 and its stimulation by RPA and Mre11-Rad50-Xrs2 to DNA end resection. *Proc. Natl. Acad. Sci. U.S.A.* 110, E1661–8 (2013).
148. Williams, R. S. *et al.* Nbs1 flexibly tethers Ctp1 and Mre11-Rad50 to coordinate DNA double-strand break processing and repair. *Cell* 139, 87–99 (2009).
149. Clerici, M., Mantiero, D., Guerini, I., Lucchini, G. & Longhese, M. P. The Yku70-Yku80 complex contributes to regulate double-strand break processing and checkpoint activation during the cell cycle. *EMBO Rep.* 9, 810–818 (2008).
150. Piersimoni, L. & Sinz, A. Cross-linking/mass spectrometry at the crossroads. *Anal Bioanal Chem* 412, 5981–5987 (2020).
151. Merkley, E. D. *et al.* Distance restraints from crosslinking mass spectrometry: mining a molecular dynamics simulation database to evaluate lysine-lysine distances. *Protein Sci* 23, 747–759 (2014).
152. Steigenberger, B., Pieters, R. J., Heck, A. J. R. & Scheltema, R. A. PhoX: An IMAC-Enrichable Cross-Linking Reagent. *ACS Cent Sci* 5, 1514–1522 (2019).
153. Almawi, A. W. *et al.* Distinct surfaces on Cdc5/PLK Polo-box domain orchestrate combinatorial substrate recognition during cell division. *Sci Rep* 10, 3379–13 (2020).

154. Sanchez, A. *et al.* Exo1 recruits Cdc5 polo kinase to MutLγ to ensure efficient meiotic crossover formation. *Proc. Natl. Acad. Sci. U.S.A.* 117, 30577–30588 (2020).
155. Xu, J., Shen, C., Wang, T. & Quan, J. Structural basis for the inhibition of Polo-like kinase 1. *Nat. Struct. Mol. Biol.* 20, 1047–1053 (2013).
156. Sefton, B. M. & Shenolikar, S. Overview of protein phosphorylation. *Curr Protoc Mol Biol* Chapter 18, Unit 18.1–18.1.5 (2001).
157. Reusswig, K.-U. & Pfander, B. Control of Eukaryotic DNA Replication Initiation-Mechanisms to Ensure Smooth Transitions. *Genes (Basel)* 10, 99 (2019).
158. Bonte, D. *et al.* Cdc7-Dbf4 kinase overexpression in multiple cancers and tumor cell lines is correlated with p53 inactivation. *Neoplasia* 10, 920–931 (2008).
159. Ghatalia, P. *et al.* Kinase Gene Expression Profiling of Metastatic Clear Cell Renal Cell Carcinoma Tissue Identifies Potential New Therapeutic Targets. *PLoS One* 11, e0160924 (2016).
160. Nambiar, S. *et al.* Identification and functional characterization of ASK/Dbf4, a novel cell survival gene in cutaneous melanoma with prognostic relevance. *Carcinogenesis* 28, 2501–2510 (2007).
161. Cheng, A. N. *et al.* Increased Cdc7 expression is a marker of oral squamous cell carcinoma and overexpression of Cdc7 contributes to the resistance to DNA-damaging agents. *Cancer Lett* 337, 218–225 (2013).
162. Clarke, L. E. *et al.* Cdc7 expression in melanomas, Spitz tumors and melanocytic nevi. *J Cutan Pathol* 36, 433–438 (2009).
163. Doudna, J. A. The promise and challenge of therapeutic genome editing. *Nature* 578, 229–236 (2020).
164. Yang, Y., Xu, J., Ge, S. & Lai, L. CRISPR/Cas: Advances, Limitations, and Applications for Precision Cancer Research. *Front Med (Lausanne)* 8, 649896 (2021).
165. Iwai, K. *et al.* A CDC7 inhibitor sensitizes DNA-damaging chemotherapies by suppressing homologous recombination repair to delay DNA damage recovery. *Sci Adv* 7, eabf0197 (2021).
166. Weinstock, D. M., Nakanishi, K., Helgadottir, H. R. & Jasin, M. Assaying double-strand break repair pathway choice in mammalian cells using a targeted endonuclease or the RAG recombinase. *Meth. Enzymol.* 409, 524–540 (2006).
167. Moynahan, M. E., Pierce, A. J. & Jasin, M. BRCA2 is required for homology-directed repair of chromosomal breaks. *Mol. Cell* 7, 263–272 (2001).
168. Sasi, N. K. *et al.* DDK Has a Primary Role in Processing Stalled Replication Forks to Initiate Downstream Checkpoint Signaling. *Neoplasia* 20, 985–995 (2018).
169. Rainey, M. D. *et al.* CDC7 kinase promotes MRE11 fork processing, modulating fork speed and chromosomal breakage. *EMBO Rep.* 21, e48920 (2020).
170. Neelsen, K. J. & Lopes, M. Replication fork reversal in eukaryotes: from dead end to dynamic response. *Nat Rev Mol Cell Biol* 16, 207–220 (2015).
171. Jones, M. J. K. *et al.* Human DDK rescues stalled forks and counteracts checkpoint inhibition at unfired origins to complete DNA replication. *Mol. Cell* 81, 426–441.e8 (2021).
172. Gaj, T., Gersbach, C. A. & Barbas, C. F. ZFN, TALEN, and CRISPR/Cas-based methods for genome engineering. *Trends Biotechnol* 31, 397–405 (2013).
173. Doudna, J. A. & Charpentier, E. Genome editing. The new frontier of genome engineering with CRISPR-Cas9. *Science* 346, 1258096 (2014).

174. Miura, H., Gurumurthy, C. B., Sato, T., Sato, M. & Ohtsuka, M. CRISPR/Cas9-based generation of knockdown mice by intronic insertion of artificial microRNA using longer single-stranded DNA. *Sci Rep* 5, 12799–11 (2015).
175. Yoshimi, K. *et al.* ssODN-mediated knock-in with CRISPR-Cas for large genomic regions in zygotes. *Nat Commun* 7, 10431–10 (2016).
176. Daley, J. M., Niu, H., Miller, A. S. & Sung, P. Biochemical mechanism of DSB end resection and its regulation. *DNA Repair (Amst)* 32, 66–74 (2015).
177. Lieber, M. R. The mechanism of double-strand DNA break repair by the nonhomologous DNA end-joining pathway. *Annu. Rev. Biochem.* 79, 181–211 (2010).
178. Nambiar, T. S. *et al.* Stimulation of CRISPR-mediated homology-directed repair by an engineered RAD18 variant. *Nat Commun* 10, 3395–13 (2019).
179. Chu, V. T. *et al.* Increasing the efficiency of homology-directed repair for CRISPR-Cas9-induced precise gene editing in mammalian cells. *Nat Biotechnol* 33, 543–548 (2015).
180. Gutschner, T., Haemmerle, M., Genovese, G., Draetta, G. F. & Chin, L. Post-translational Regulation of Cas9 during G1 Enhances Homology-Directed Repair. *Cell Rep* 14, 1555–1566 (2016).
181. Matsumoto, D., Tamamura, H. & Nomura, W. A cell cycle-dependent CRISPR-Cas9 activation system based on an anti-CRISPR protein shows improved genome editing accuracy. *Commun Biol* 3, 601–10 (2020).
182. Eapen, V. V., Sugawara, N., Tsabar, M., Wu, W.-H. & Haber, J. E. The Saccharomyces cerevisiae chromatin remodeler Fun30 regulates DNA end resection and checkpoint deactivation. *Mol. Cell. Biol.* 32, 4727–4740 (2012).
183. Chen, X. *et al.* The Fun30 nucleosome remodeller promotes resection of DNA double-strand break ends. *Nature* 489, 576–580 (2012).
184. Orthwein, A. *et al.* A mechanism for the suppression of homologous recombination in G1 cells. *Nature* 528, 422–426 (2015).
185. Wienert, B. *et al.* Timed inhibition of CDC7 increases CRISPR-Cas9 mediated templated repair. *Nat Commun* 11, 2109–15 (2020).
186. Saito, Y., Kobayashi, J., Kanemaki, M. T. & Komatsu, K. RIF1 controls replication initiation and homologous recombination repair in a radiation dose-dependent manner. *J Cell Sci* 133, jcs240036 (2020).
187. Hentges, P., Waller, H., Reis, C. C., Ferreira, M. G. & Doherty, A. J. Cdk1 restrains NHEJ through phosphorylation of XRCC4-like factor Xlf1. *Cell Rep* 9, 2011–2017 (2014).
188. Sorenson, K. S., Mahaney, B. L., Lees-Miller, S. P. & Cobb, J. A. The non-homologous end-joining factor Nej1 inhibits resection mediated by Dna2-Sgs1 nuclease-helicase at DNA double strand breaks. *J. Biol. Chem.* 292, 14576–14586 (2017).
189. Mojumdar, A. *et al.* Nej1 Interacts with Mre11 to Regulate Tethering and Dna2 Binding at DNA Double-Strand Breaks. *Cell Rep* 28, 1564–1573.e3 (2019).
190. Liu, Z., Sun, Q. & Wang, X. PLK1, A Potential Target for Cancer Therapy. *Transl Oncol* 10, 22–32 (2017).
191. Takahashi, T. S. & Walter, J. C. Cdc7-Drf1 is a developmentally regulated protein kinase required for the initiation of vertebrate DNA replication. *Genes Dev.* 19, 2295–2300 (2005).
192. Rothstein, R. J. One-step gene disruption in yeast. *Meth. Enzymol.* 101, 202–211 (1983).

193. Szklarczyk, D. *et al.* STRING v11: protein-protein association networks with increased coverage, supporting functional discovery in genome-wide experimental datasets. *Nucleic Acids Res.* **47,** D607–D613 (2019).

Acknowledgments

First, I would like to thank my supervisor and mentor Dr. Boris Pfander. Thank you for being a fundamental part of my scientific development through your guidance, always welcoming new ideas and being available for discussion and to provide feedback. Also, a big thanks for being always supportive throughout the all adventure. Meant a lot to me.
I would also like to thank Stefan Jentsch, and all the members of the MCB department. It was really exciting to be part of such a great department.
A big thank you also to Prof. Peter Becker for being my Doktorvater, and to my TAC committee. Thank you, Prof. Aloys Schepers, Prof. Dominik Boos and Prof. Karl Duderstadt.
Thank you to the IMPRS coordination office, for being always available and for providing an exciting environment with a lot of activities.
Big acknowledgment also to Barbara Steigenberger for the support and huge help with the Mass Spec, and to Elda Cannavo and Petr Cejka for the invaluable contributions to our project.
A big thank you goes also to all the members of the Pfander lab. It was really great to share this experience with you, and I am grateful that we could have such nice time in the lab. Thank you Uschi for all your help and for keeping the lab organized. Thank you, Giulia and Lissa, for welcoming me in the lab. Thank you Kalle. It was really nice to embark, for some time, on the study of replication control with you. Also, thanks for being always available for some nice scientific discussion, at any time of the day. You definitely are a key player of the lab (not only for our volleyball team). It was really nice to have a companion for the late times in the lab, always up for a nice chat. Susi, thanks for sharing your passion for science, and for all the nice stories you entertained us with. Thank you, Julia. Having started together always felt like were “classmates”. Thank you for keeping the lab well organized, for being always supportive and kind (well, most of the time). It was a lot of fun to work together. Also, thanks for providing me with some sweets/cake on my birthday. Was highly appreciated (guess appreciated by the whole lab as well!). Thank you, Martina, for providing the lab with many cakes and for our nice discussions. It was fun to share the lab with you, since our time in Pavia. And of course, big thank you for being our volleyball-motivator. Thank you, Leo, for being the biochemistry buddy. It was great to have you in the lab, and to share the joyful events during this time. Also,

thanks for helping with sample submissions from time to time. Simone, I really enjoyed working with you and thank you for all your help. Also thank you to all the students I had the pleasure to work with: Julian, Konstantin, Franziska and Matthias.
Thank you also to all the junior groups in the LM wing. It was really nice to share the department together and thanks for all your help during the move of the lab. Big thank you to Bianca, for being always available and helping us with anything, and to Massimo and Beate for providing us with media and stocks, making our life much easier.
Just few meters apart, a big thank you to Giulia. Thanks for being always available for a chat and for your support. I am glad to have you as a friend. And of course, a big thank you to Franz as well!!!
Lastly, a big thank you to my family. Mamma, Papa', Filippo and Emma. Your support and love are invaluable. Thank you.

Curriculum Vitae

Lorenzo Galanti

Higher Education

09/2015-present PhD in Biology
DNA Replication and Genome Integrity Laboratory, Dr. Boris Pfander
Max Planck Institute of Biochemistry, Martinsried, Germany

10/2013-07/2015 Master degree in Molecular Biology and Genetics
University of Pavia, Pavia, Italy

10/2010-10/2013 Bachelor degree in Biotechnology
University of Verona, Verona, Italy

Publications

Bittmann, J., Grigaitis, R., **Galanti, L.**, Amarell, S., Wilfling, F., Matos, J. and Pfander, B. (2020) 'An advanced cell cycle tag toolbox reveals principles underlying temporal control of structure-selective nucleases.', *eLife*. eLife Sciences Publications Limited, 9, p. 1. doi: 10.7554/eLife.52459.

Galanti, L. and Pfander, B. (2018) 'Right time, right place-DNA damage and DNA replication checkpoints collectively safeguard S phase.', *The EMBO journal*. John Wiley & Sons, Ltd, 37(21), p. e100681. doi: 10.15252/embj.2018100681.

Brambati, A., Zardoni, L., Achar, Y. J., Piccini, D., **Galanti, L.**, Colosio, A., Foiani, M. and Liberi, G. (2018) 'Dormant origins and fork protection mechanisms rescue sister forks arrested by transcription.', *Nucleic acids research*, 46(3), pp. 1227–1239. doi: 10.1093/nar/gkx945.

Reusswig, K.-U., Zimmermann, F., **Galanti, L.** and Pfander, B. (2016) 'Robust Replication Control Is Generated by Temporal Gaps between Licensing and Firing Phases and Depends on Degradation of Firing Factor Sld2.', *Cell reports*, 17(2), pp. 556–569. doi: 10.1016/j.celrep.2016.09.013.

Brambati, A., Colosio, A., Zardoni, L., **Galanti, L.** and Liberi, G. (2015) 'Replication and transcription on a collision course: eukaryotic regulation mechanisms and implications for DNA stability.', *Frontiers in genetics*. Frontiers, 6, p. 166. doi: 10.3389/fgene.2015.00166.

Awards

DGDR FLASH-talk price at 5th German-French DNA Repair Meeting (out of three available awards)
November 12-13, online meeting